

+

Key Words:
Wall sampler
End effector
Waste tank
Residual activity
Tank closure
Nuclear waste

Retention:
Permanent

TANK 18 AND TANK 19 WALL SAMPLER PERFORMANCE

Robert A. Leishear
Mark D. Fowley

1/12/2010

Savannah River National Laboratory
Savannah River Nuclear Solutions
Aiken, SC 29808

**Prepared for the U.S. Department of Energy Under
Contract Number DE-AC09-08SR22470**



DISCLAIMER

This work was prepared under an agreement with and funded by the U.S. Government. Neither the U. S. Government or its employees, nor any of its contractors, subcontractors or their employees, makes any express or implied:

- 1. warranty or assumes any legal liability for the accuracy, completeness, or for the use or results of such use of any information, product, or process disclosed; or**
- 2. representation that such use or results of such use would not infringe privately owned rights; or**
- 3. endorsement or recommendation of any specifically identified commercial product, process, or service.**

Any views and opinions of authors expressed in this work do not necessarily state or reflect those of the United States Government, or its contractors, or subcontractors.

Printed in the United States of America

**Prepared for
U.S. Department of Energy**

REVIEWS AND APPROVALS

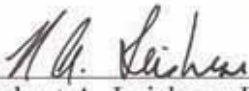
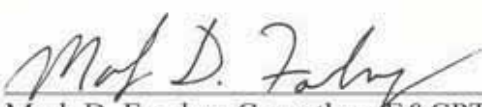

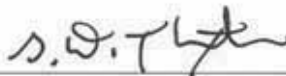

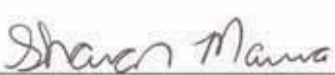
	1/12/10
Robert A. Leishear, E&CPT	Date
	1/14/10
Mark D. Fowley, Co-author, E&CPT	Date
	1/19/2010
Zafar Qureshi, Peer Reviewer, E&CPT	Date
	1/20/2010
George D. Thaxton, SRR	Date
	1/22/10
Billy Giddings, EDL Manager, E&CPT	Date
	1/26/10
Sharon Marra, Research Programs, E&CPT	Date

TABLE OF CONTENTS

LIST OF FIGURES	3
LIST OF TABLES	5
LIST OF ACRONYMS	6
1.0 EXECUTIVE SUMMARY	8
1.1 Tank 18 and Tank 19 Wall Sampling.....	8
1.1.1 SRNL Sampler Fabrication and Evaluation.....	8
1.1.2 SRR Mast Assembly and Tank Sampling.....	8
1.1.3 Project Objectives	9
2.0 INTRODUCTION.....	9
2.1 Test Requirements.....	9
2.2 Sampler Description.....	10
2.3 Sample Requirements.....	13
2.4 Waste Tank Surfaces.....	13
2.5 Analysis.....	16
3.0 SRNL SAMPLER DESIGN AND OPERATION	17
3.1 SRNL Equipment Description.....	17
3.1.1 SRNL Sampler Assembly	20
3.1.1.1 Final Sampler Design.....	21
3.1.1.2 Electromagnets and Springs	24
3.1.1.3 Operating Parameters	24
3.1.1.4 Drill Motor.....	26
3.1.1.5 Drill Bit Design.....	26
3.1.1.6 Linear Drive Motor and Spring Control	28
3.1.1.7 Vacuum Eductor	29
3.1.1.8 Sampler Heads	30
3.1.1.9 Filters	34
3.1.1.10 Sampler Controls	35
3.1.1.11 Drill Advancement.....	38
3.1.2 EDL Sampler Evaluation.....	40
3.1.3 Sample Coupons	42
3.1.4 Waste Characteristics and Test Samples.	44
4.0 EDL TESTING	45
4.1 Sampler Collection Efficiencies.....	45
4.2 Test Preparation	46
4.2.1 Test Specifications	46
4.2.2 Test Procedure.....	46
4.2.3 Mass of Material Collected by the Sampler Head.....	47
4.2.4 Mass of Material Removed from Steel Sample Coupons	49
4.2.5 Mass of Material Removed from Salt Sample Coupons.....	51
4.3 EDL Test Results	56
4.3.1 Sampler Operation and Testing at EDL	57
4.3.1.1 Sampler Material Removal.....	57
4.3.1.2 Operating Times for the Sampler.....	57

4.3.1.3 Drilling	57
4.3.2 Calculated Collection Efficiencies.....	58
5.0 SRR MAST DESIGN AND INSTALLATION	61
5.1 Mast and Sampler Components	61
5.2 Mast and Sampler Evaluation in T-Area	63
5.2.1 Rust Concern in T-Area	64
5.2.2 Resolution of for Sampler Resonance Failure Mechanism	64
5.3 Mast and Sampler Installation in FTF	71
6.0 FTF SAMPLING RESULTS	75
6.1 FTF Sampling	75
6.1.1 Tank 18 Samples.....	79
6.1.2 Tank 19 Samples.....	79
6.2 Surface Area Estimates for Tank 18 and Tank 19 Wall Samples.....	80
6.2.1 Tank 18 Wall Samples	80
6.2.1.1 Tank 18 Upper Wall Samples	81
6.2.1.2 Tank 18 Lower Wall Samples.....	83
6.2.2 Tank 19 Wall Samples	87
6.3 Sampler Material Collection for Tanks 18 and 19	89
6.4 Summary of Design Improvements.....	98
6.5 Summary of Tank 18 and Tank 19 Wall Sampling.....	99
7.0 CONCLUSIONS	101
7.1 Tank 18 and 19 Wall Samples	101
7.1.1 Wall Sampler Design.....	101
7.1.1.1 Wall Sampler Improvements.....	101
7.1.1.2 EDL Sampler Operation	102
7.1.1.3 T-Area Sampler Operation	102
7.1.2 EDL Sample Results.....	102
7.1.3 FTF Sample Results	102
7.1.3.1 Tank 18 Sampler Operation	103
7.1.3.2 Tank 18 Sample Results	103
7.1.3.3 Tank 19 Sampler Operation and Results	103
8.0 REFERENCES.....	104
APPENDIX A. Oak Ridge National Laboratory, Initial Design of Wall Sampler	105
APPENDIX B. Uncertainty Analysis for Test Data.....	112
APPENDIX C. Salt Sample Processing	118
APPENDIX D: Vibration Data for Sampler Assembly	121
APPENDIX E: Resonance in Structures	124
APPENDIX F: Flow Rate Conversion Factors	134

LIST OF FIGURES

Figure 1: Construction and Elevation View of Mast Installation in Tanks 18 and 19.....	10
Figure 2: SRNL Sampler Assembly (unmodified)	11
Figure 3: Elevation View of Mast Installation in Tanks 18 and 19	12
Figure 4: Tanks 18 and 19	13
Figure 5: Tank 18 Wall and Tank Bottom.....	14
Figure 6: Tank 18 Wall Details.....	15
Figure 7: Tank 19 Wall and Tank Bottom.....	16
Figure 8: Sampler Head Delivered from FTF to SRNL	17
Figure 9: EDL Test Setup and Sampler Components	19
Figure 10: Sampler Assembly Installed for Testing (modified)	20
Figure 11: Sampler Assembly with Sampler Head Removed, Front View	21
Figure 12: Sampler Assembly with Sampler Head Removed, Side View.....	22
Figure 13: Sampler Assembly with Sampler Head Installed.....	22
Figure 14: Delivered Sampler Assembly.....	23
Figure 15: Delivered Sampler Assembly Without Sampler Head.....	23
Figure 16: EDL Sampler Controls	25
Figure 17: Drill Bit Terminology.....	27
Figure 18: Typical Eductor Design.....	29
Figure 19: White Tape Used to Collect Chips Falling From the Drill Bit.....	30
Figure 20: Chips from Drill Bit Following Drilling of Three Holes	30
Figure 21: Flow Path Through the Sampler Head	31
Figure 22: Test Sample Prior to Initial SRR Delivery, One 0.060” Deep Hole	32
Figure 23: Sampler Head and Filter Housing	32
Figure 24: Sampler Head Drill Bit Shroud	33
Figure 25: Sampler Head Drill Bit.....	33
Figure 26: Unacceptable HEPA Filter Design.....	35
Figure 27: EDL Sampler Controls, P&ID.....	36
Figure 28: Sampler in the Fully Retracted Position.....	37
Figure 29: SRNL Linear Motor, Fully Retracted.....	37
Figure 30: SRNL Linear Motor, Advancing.....	38
Figure 31: SRNL Linear Motor, Fully Advanced.....	39
Figure 32: SRNL Linear Motor, Retracting.....	39
Figure 33: EDL Sample Setup	41
Figure 34: EDL Test Plate	42
Figure 35: Prepared Test Coupons.....	43
Figure 36: Typical Sample with Salt Deposition.....	44
Figure 37: Material Coating the Sampler Surfaces Following Steel Sampling.....	48
Figure 38: Large Chips Clogged in Drill Cavity	49
Figure 39: Typical Drilled Steel Sample Coupon.....	50
Figure 40: Collected Steel Sample Removed From Sampler	51
Figure 41: Liquefying Salt Sample	52
Figure 42: Salt + Rust Sample Coupon with Portion of Salt Cake Detached.....	52

Figure 43: Undamaged Salt Sample	53
Figure 44: Collected Salt Sample	53
Figure 45: Collection Tray Mounted on EDL Test Plate.....	54
Figure 46: Sampler Weighing Station.....	55
Figure 47: Sampler Weighing with Installed Dessicant	56
Figure 48: Hole Depths of Samples	58
Figure 49: Collection Efficiencies	59
Figure 50: Installation Procedure for Tank 18.....	62
Figure 51: Installation Procedure for Tank 19.....	63
Figure 52: Motor Vibration Before Spring Change.....	65
Figure 53: Sampler Resonance	66
Figure 54: Sampler Lowering into a Simulated Riser Opening.....	67
Figure 55: Sampler Passing Through a Simulated Riser Opening	68
Figure 56: Plan View of Installed Sampler in T-Area	68
Figure 57: Mounting Plate and Mast in T-Area.....	69
Figure 58: Mast Arm in Vertical Position.....	69
Figure 59: Mast Arm in Leveled Position.....	70
Figure 60: Sampler Attached to Wall in T-Area.....	70
Figure 61: Samples at T-Area on an Unrusted Surface	71
Figure 62: Mast and Sampler Installation in Tank 19.....	72
Figure 63: Mast and Sampler Installation in Tank 19.....	73
Figure 64: Sampler Installed in Tank 18, Upper Sample.....	74
Figure 65: Close-up of Sampler Installed in Tank 18.....	75
Figure 66: Tank 18 Wall Sampling Results.....	77
Figure 67: Tank 19 Wall Sampling Results.....	78
Figure 68: Tank 18 Upper Sample, Steel Removed from the Wall.....	82
Figure 69: Tank 18 Lower Sample, Small Chip of Waste Removed from the Wall	83
Figure 70: Sampler Head and Tank 18 Lower Sample Area.....	84
Figure 71: Tank 18 Lower Sample Area.....	85
Figure 72: Partially Drilled Hole at Upper Level in Tank 18	86
Figure 73: Dimensioned Tank 18 Lower Sample Area	87
Figure 74: Typical Drilled Hole in Tank 19	88
Figure 75: All Four Drilled Holes in Tank 19	89
Figure 76: Delivered Sampler Head	90
Figure 77: Sampler Head Disassembly.....	91
Figure 78: Disassembled Drill Collar	91
Figure 79: Filter Cavity, Tank 18 Scale Sample, TK 18-2	92
Figure 80: Collected Material, Tank 18 Scale Sample, TK 18-2.....	92
Figure 81: Drill Cavity, Tank 18 Scale Sample, TK 18-2	93
Figure 82: Collected Sample, Second Tank 18 Sample Attempt, SP3	93
Figure 83: Drill Cavity, Second Tank 18 Sample Attempt, SP3	94
Figure 84: Collected Sample, Final Tank 18 Upper Sample, TK 18-1.....	94
Figure 85: Filter Cavity, Final Tank 18 Upper Sample, TK 18-1.....	95
Figure 86: Filter Plate, Final Tank 18 Upper Sample, TK 18-1	95
Figure 87: Filter Cavity, Final Tank 18 Lower Sample, SP 4	96
Figure 88: Drill, Cavity, Final Tank 18 Lower Sample, SP 4	96

Figure 89: Collected Sample, Final Tank 18 Lower Sample, SP 4	97
Figure 90: Collected Sample, Final Lower Sample, Tank 19, TK 19-2 (Upper Sample showed similar results).....	97
Figure 91: Filter Cavity, Final Lower Sample, Tank 19, TK 19-2	98
Figure 92: Oak Ridge and West Valley Wall Sampler Design.....	99

LIST OF TABLES

Table 1: Test Specifications.....	46
Table 2: Collection Efficiency Test Results from EDL.....	60
Table 3: Elevation Requirements for Tank Samples	71
Table 4: Tank 18 and Tank 19 Test Summary.....	76
Table 5: Test Instrumentation	117

LIST OF ACRONYMS

Acronyms

CE	collection efficiency
DM	drill motor
DM flow	flow rate, drill motor
EDL	Engineering Development Laboratory, SRNL
f, f _i , f ₁ , f ₂	frequency, 1/second
F	force, pounds
FS	full scale
FTF	F Area Tank Farm
g	gram
ID	inner diameter
K	spring constant
LM	linear motor
LM flow	flow rate, linear motor
M or m	mass, pound mass
M&TE	measurement and test equipment
mg	milligram
ORNL	Oak Ridge National Laboratory
P	pressure
P DM	pressure, drill motor
P LM	pressure, linear motor
P V	pressure, vacuum
PID	process and instrumentation diagram
RDG	reading
RSS	root-sum-square
TR	transmissibility
SD	standard deviation
sg	specific gravity
SRNL	Savannah River National Laboratory
SRR	Savannah River Remediation, LLC
SRS	Savannah River Site
T	student T-factor
V	vacuum
V flow	flow rate, vacuum
x	distance, feet

Symbols

∂	partial differential
σ	uncertainty

Subscripts

A	average (of CE)
---	-----------------

a	first coupon of a sample pair
b	second coupon of a sample pair
C	coupon
CE	collection efficiency
F	filter
H	sampler head
M	mass, grams, milligrams
P	polished coupons
R	coupons with salt residue
S	sampler
T	collection tray, weighing tray, or test
x	first or second coupon of a sample pair
1	pre-test
2	post-test

1.0 EXECUTIVE SUMMARY

1.1 TANK 18 AND TANK 19 WALL SAMPLING

Wall samples were successfully machined from Tanks 18 and 19 in FTF (F-Area Tank Farm), Savannah River Site (SRS). Samples were required to establish the residual activity (μ Curies) prior to permanent closure of these two 85 feet diameter, 1.3 million gallon, steel wall, radioactive waste storage tanks. To collect samples, an improved Oak Ridge and West Valley design was used, which was attached to a complex robotic arm assembly. Based on their work, SRS developed a simplified and improved design. A significant cost savings was realized by SRS from the novel design changes, provided through a joint effort between SRNL and SRR.

1.1.1 SRNL Sampler Fabrication and Evaluation

Savannah River National Laboratory (SRNL) was contracted by Savannah River Remediation (SRR) to fabricate and test a sampling device to obtain the wall samples. A sampling device was adapted for SRS use, which was previously designed by Oak Ridge National Laboratory (ORNL) and used on concrete tanks. That sampler design was modified for use at West Valley to sample steel walled tanks. To perform Tank 18 and Tank 19 sampling, the West Valley design was further modified by SRNL.

SRNL provided the initial design concept for the sampling process, and a joint effort between SRR and SRNL resulted in the invention of the final sampler and mast assembly. SRNL modified the ORNL sampler design to ensure success in SRS waste tanks, and then tested the sampler and evaluated performance. Modifications included an innovative identification and correction of equipment resonance problems, which would have caused failure of the sampler in SRS tanks.

1.1.2 SRR Mast Assembly and Tank Sampling

SRR Site Construction services designed the mast assembly to mount the sampler, and then built, tested, and installed the mast and sampler assembly in the waste tanks. One of two fabricated samplers was attached to a cantilevered arm controlled by a cable and winch, which lowered a hinged arm from a vertical mast to drill wall samples. After testing the sampler at EDL (Engineering Development Laboratory), the sampler was attached to the mast assembly by SRR. The fully assembled sampler and mast assembly were then installed by crane and tested at the non-radioactive Full Tank Facility in T-Area, which is an 85 feet diameter tank with overhead structural steel platforms. Once testing was complete in the Full Tank, the sampler and mast assembly were transported to FTF, and samples were taken from the Tank 18 and Tank 19 walls at two different elevation ranges in each tank. In tank 18, waste was observed on the walls, while waste was not observed on the Tank 19 wall. EDL provided technical support throughout SRR activities.

1.1.3 Project Objectives

This report provides a description of sampler fabrication, testing, and evaluation as well as a description of sampling in Tanks 18 and 19. The primary outputs of this report are determinations of sampler collection efficiencies and estimates of the surface areas of the samples taken in Tanks 18 and 19. Collection efficiencies were determined for steel and salt coated samples, but efficiencies were not determined for rust only, thin salt layers, or waste. Surface areas were conservatively estimated to be less than the actual surface areas, where the actual surface area of collected material may exceed the calculated surface area by as much as 75% or more. Surface areas were estimated to determine the activity (μ Curies) per unit area for the sample areas only. Additional analysis will be provided by SRNL to quantify the total activity and radionuclides in the collected samples, which were transported to SRNL. Those test results will be identified in a separate report.

2.0 INTRODUCTION

2.1 TEST REQUIREMENTS

The primary purpose of sampling was to provide data to SRR to evaluate existing calculations with respect to contamination levels in the waste tanks. Wall samples were required from two, FTF, Type IV tanks to evaluate potential contamination contained in the corrosion layer on the waste tank wall surfaces. The Type IV waste tanks have a single, 3/8 inch thick, 85 foot diameter, steel wall construction, as shown in Figure 1. The steel walls are encased by a concrete wall, and the walls are below ground level.

As specified by SRR (Ref. [1]), samples were obtained for at least two different locations at each of two different elevation ranges in each tank to provide representative samples for analysis. At least two samples were required at a time in a common sampler head, which contains samples for transport to SRNL for analysis. Five sampler heads were actually required for sample collection in Tanks 18 and 19. Sample location requirements are summarized in Figure 1. The five samples for activity analysis are referred to in this report as: Tank 18 scale sample, Tank 18 upper sample, Tank 18 lower sample, Tank 19 upper sample, and Tank 19 lower sample. The latter four samples collected material from the corrosion layer, while the scale sample collected waste from the wall.

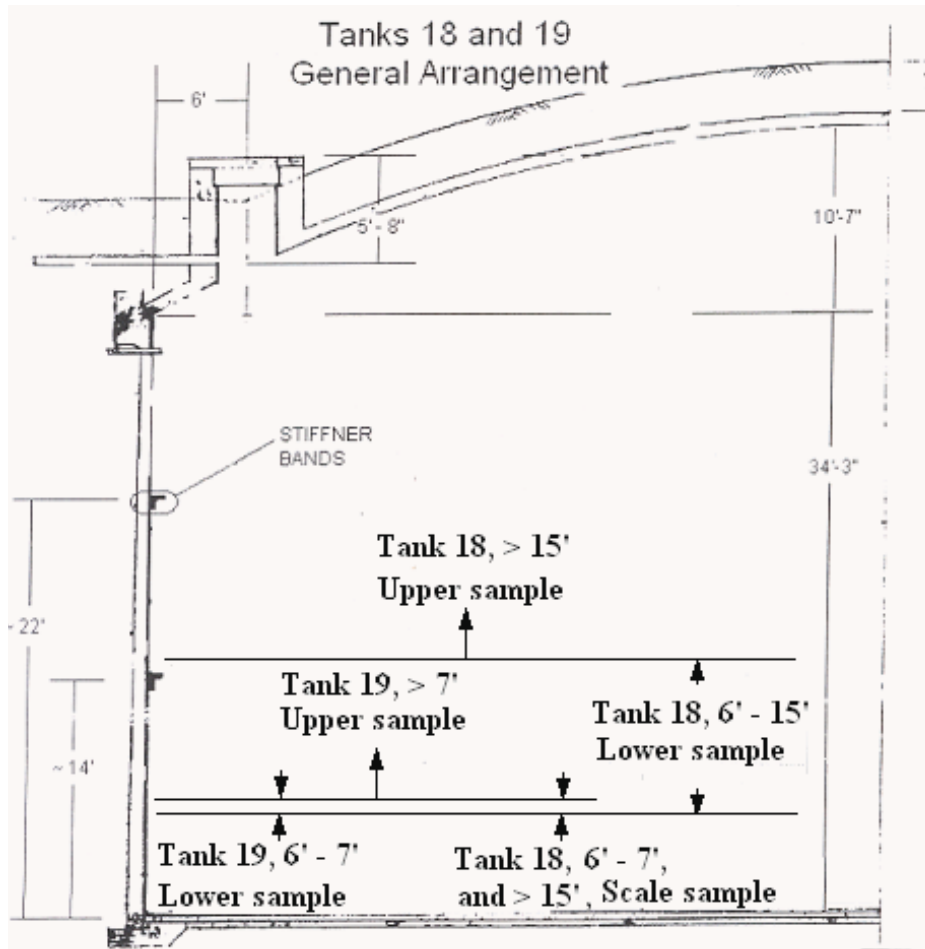


Figure 1: Construction and Elevation View of Mast Installation in Tanks 18 and 19

2.2 SAMPLER DESCRIPTION

Fabrication of two identically designed wall samplers and a performance evaluation were required from SRNL (Savannah River National Laboratory) for FTF Engineering (Thaxton, D. [1]), SRR (Savannah River Remediation, LLC). In addition, technical support for full scale testing in T-Area and sampling activities in Tank 18 and Tank 19. A sampler is shown in Figure 2; the sampler mast assembly is shown in Figure 3; and the FTF Tanks 18 and 19 are shown in Figure 4.

Although the fabrication and installation of the mast were the responsibility of FTF Engineering and SRR Construction, the mast installation is discussed in this report to summarize SRR project results, as well as SRNL research. In short, the sampler machined small samples from the tank walls, and the mast positioned the sampler into the waste tanks to machine these wall samples to establish the activity of waste tank wall surfaces.

Much of the testing was performed using the same sampler that was installed in the waste tanks to collect samples. The other sampler was used to complete EDL testing in parallel with SRR installation and testing.

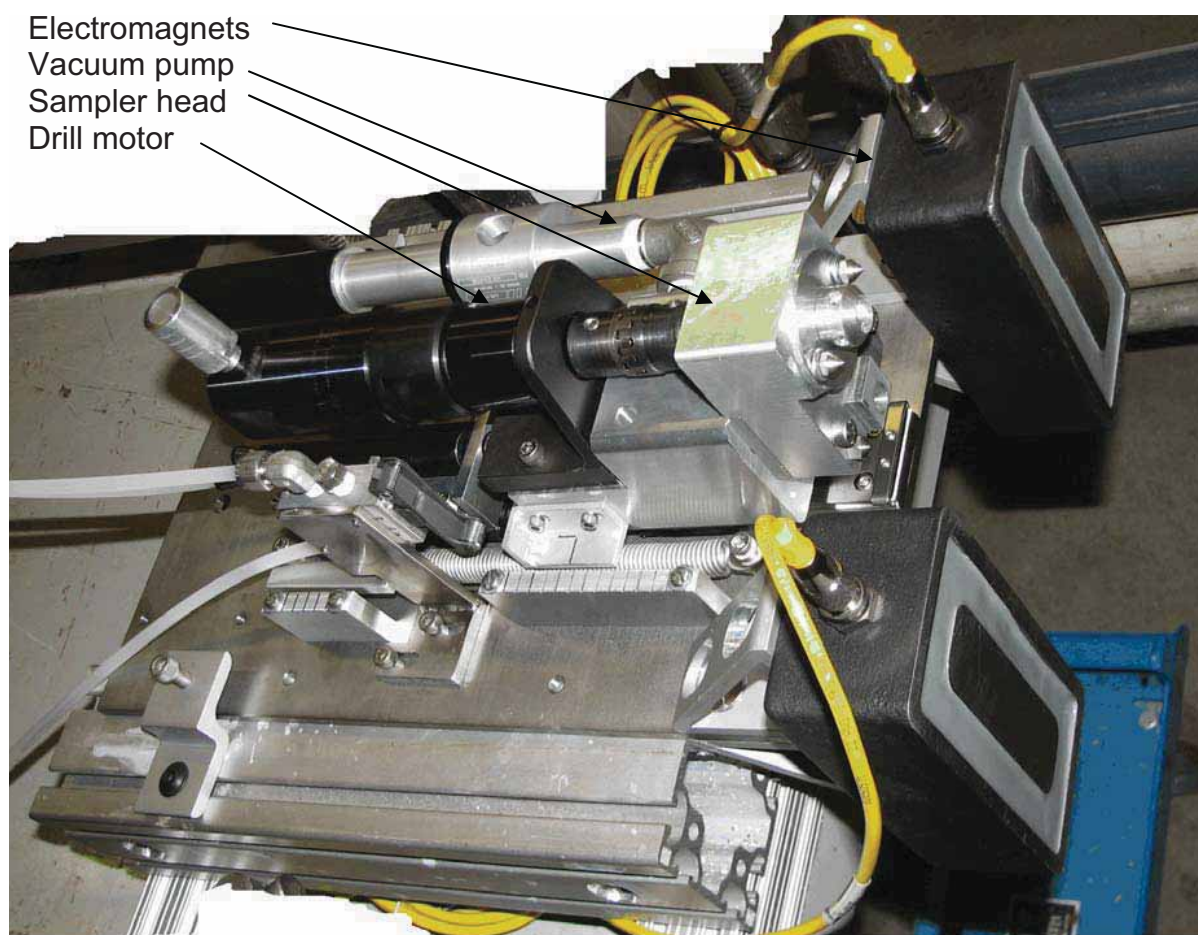


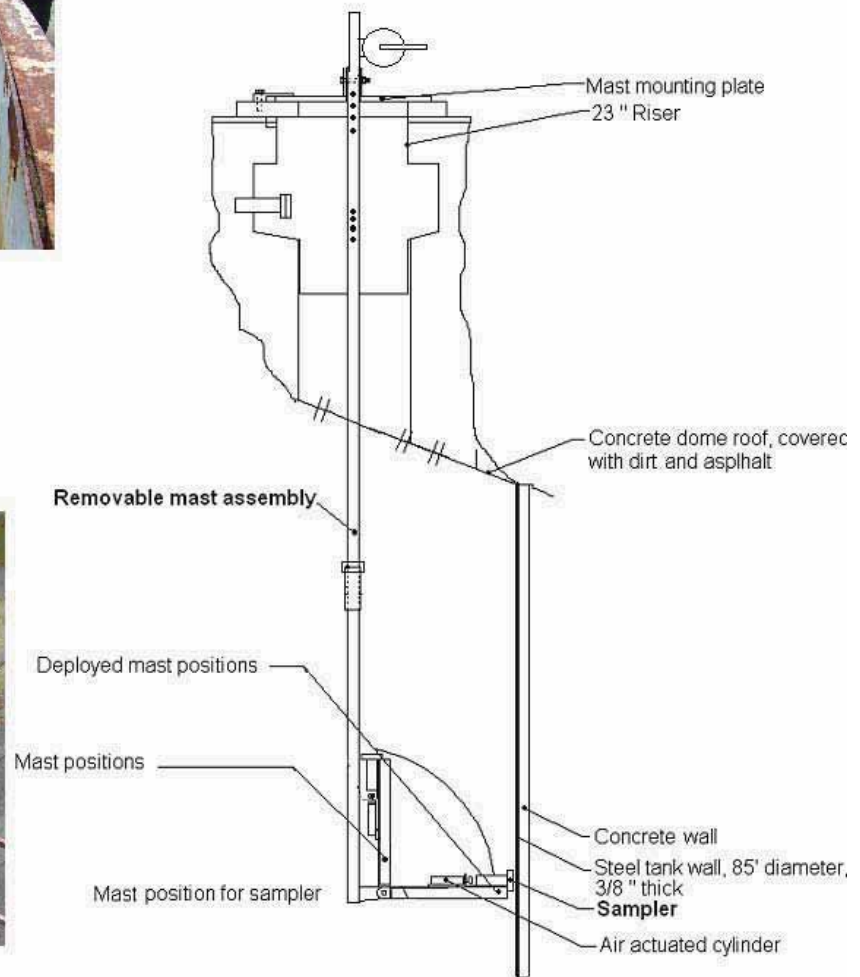
Figure 2: SRNL Sampler Assembly (unmodified)



Full scale testing



Sampler and mast assembly



Sampler and mast assembly layout

Figure 3: Elevation View of Mast Installation in Tanks 18 and 19



Figure 4: Tanks 18 and 19

2.3 SAMPLE REQUIREMENTS

The sampler and the mast were used to collect samples from the tank walls at two different elevations in each tank. Numerous references document the requirements and work performance (Leishear, R., Fowley, M. France, T., and Jackson, M. [2 - 10]). At each elevation, the sampler was designed to drill shallow holes (0.500" diameter by 0.060" maximum depth) in the walls of the 1.3 million gallon, nuclear waste storage tanks to obtain samples of the waste on the wall, the corrosion layer on the wall, and the base metal below the corrosion. Samples areas were selected to ensure that the samples provide representative corrosion for tank surfaces above and below typical waste levels in the tank during waste storage. One set of samples was collected above typical waste levels in the tanks where more corrosion was expected (Wiersma, B. [11 - 12]), and the other set of samples was collected below typical waste levels in the tanks where less corrosion was expected. Success was achieved when: 1) the sampler machined down to exposed shiny steel surfaces, 2) materials were collected from the surfaces; 3) and sample surface areas were determined.

2.4 WASTE TANK SURFACES

Sampling was performed which collected both corrosion and waste from the tank walls. Corrosion and waste accumulation on the walls of Tank 18 and 19 are shown in Figure 5,

Figure 6, and Figure 7. Note that salt accumulation in Tank 19 appears to be negligible, while waste may be as thick as 3/8 inch, or more, in some areas of Tank 18. The exact thickness of waste was difficult to distinguish, but the shadows from the nuts on the 5/8 " diameter bolts on the wall stiffener were compared to the shadows of the waste to provide a crude approximation of the waste thickness. Thick waste on the walls prevented the sampler electromagnets from holding the sampler to the wall for collecting a corrosion sample of the wall surface. To collect steel corrosion samples, the sampler was positioned to ensure that samples were collected in locations where waste deposits were thin on the wall surfaces, since a primary goal of sampling was to discern the activity contained in the tank wall corrosion layer. To collect a scale sample, the sampler was located on the thicker waste deposits on the wall, and samples were collected from the wall without drilling into the steel surface.

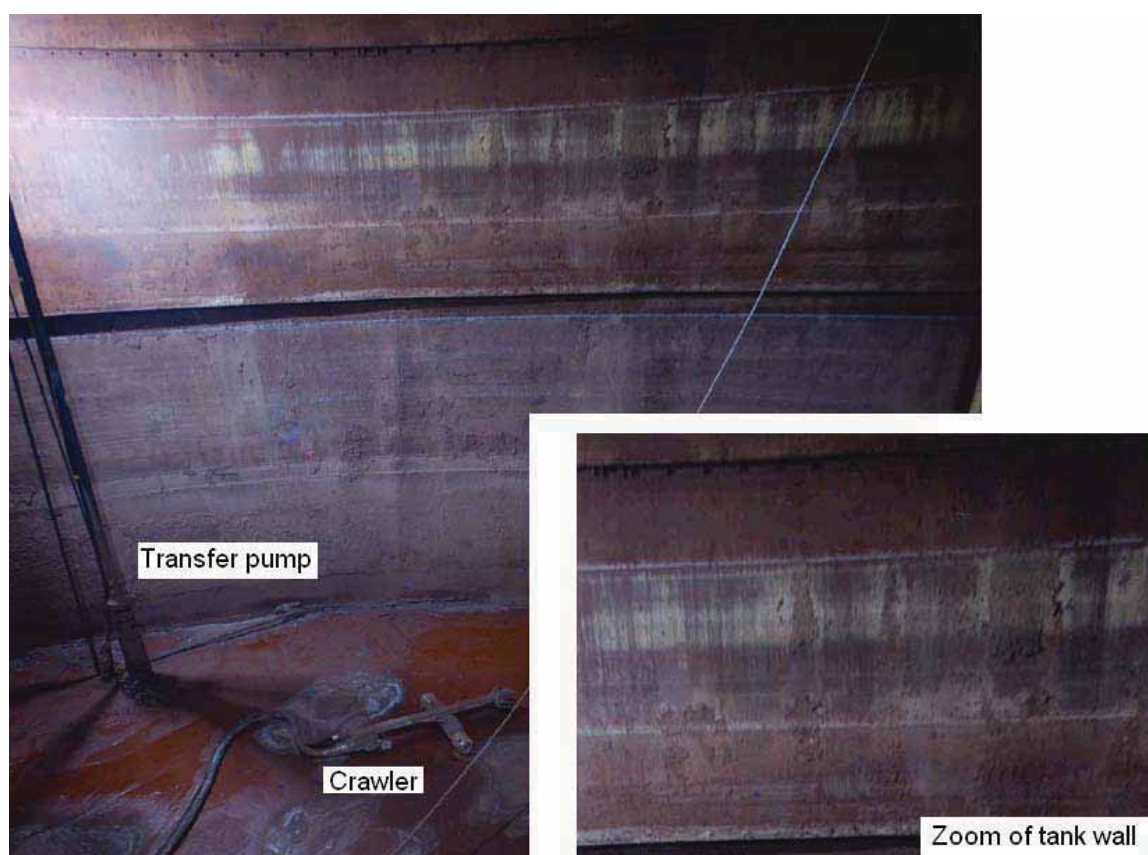


Figure 5: Tank 18 Wall and Tank Bottom



Figure 6: Tank 18 Wall Details



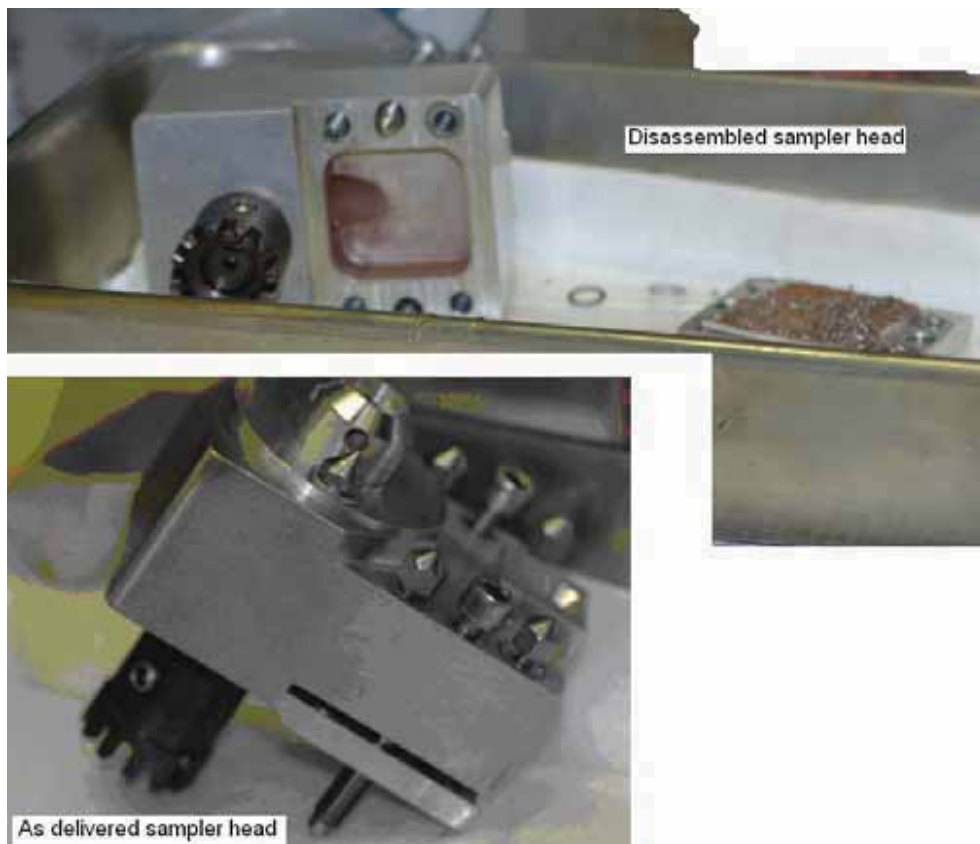
Figure 7: Tank 19 Wall and Tank Bottom

2.5 ANALYSIS

Activity analysis was the reason for obtaining the tank wall samples discussed in this report, where the micro-Curie content will be measured for the samples, and radionuclides will be

identified in a separate report. To better handle the wall samples, a removable sampler head was part of the sampler (Figure 8). Once the wall samples were collected in this head, the radioactive samples were transported to SRNL for analysis. Along with the surface areas associated with the samples, those test results will be provided to SRR engineering to further evaluate residual nuclear waste activity on the tank walls in Tank 18 and Tank 19. Consequently, this report is confined to a discussion of the fabrication and testing of the sampler at SRNL as well as the collection of samples from the waste tanks.

In particular, the sampler collection efficiency and the estimated surface area for each sample were required. What percentage of material drilled from samples was collected by the sampler in laboratory conditions? What was the surface area for waste tank samples transported to SRNL for analysis?



Tank 18

Figure 8: Sampler Head Delivered from FTF to SRNL

3.0 SRNL SAMPLER DESIGN AND OPERATION

3.1 SRNL EQUIPMENT DESCRIPTION

The SRNL equipment required for testing consisted of samplers, removable sampler heads for the samplers, a wall plate installed in EDL to mimic the tank walls, and sample coupons used to validate sampler operation. The equipment setup is shown in Figure 9. Two samplers

were fabricated: one to complete testing at EDL, and one for use by FTF after extensive testing of the sampler to validate operation. Attached to each sampler was a removable sampler head, which contained a drill bit to obtain the samples and a filter to collect machined particles as they are vacuumed from the wall surface. These heads were self contained units, designed to be removed and transported to SRNL for processing after tank samples were obtained. The wall plate was a 4 feet by 3 feet curved plate installed at EDL, and the sample coupons were 1 inch by 1 inch by 3/8 inch thick steel plates, which were bolted to the wall plate for machining by the sampler. The sampler was attached to the wall plate by electromagnets while samples were drilled from the plate. The mast assembly was not installed at EDL.

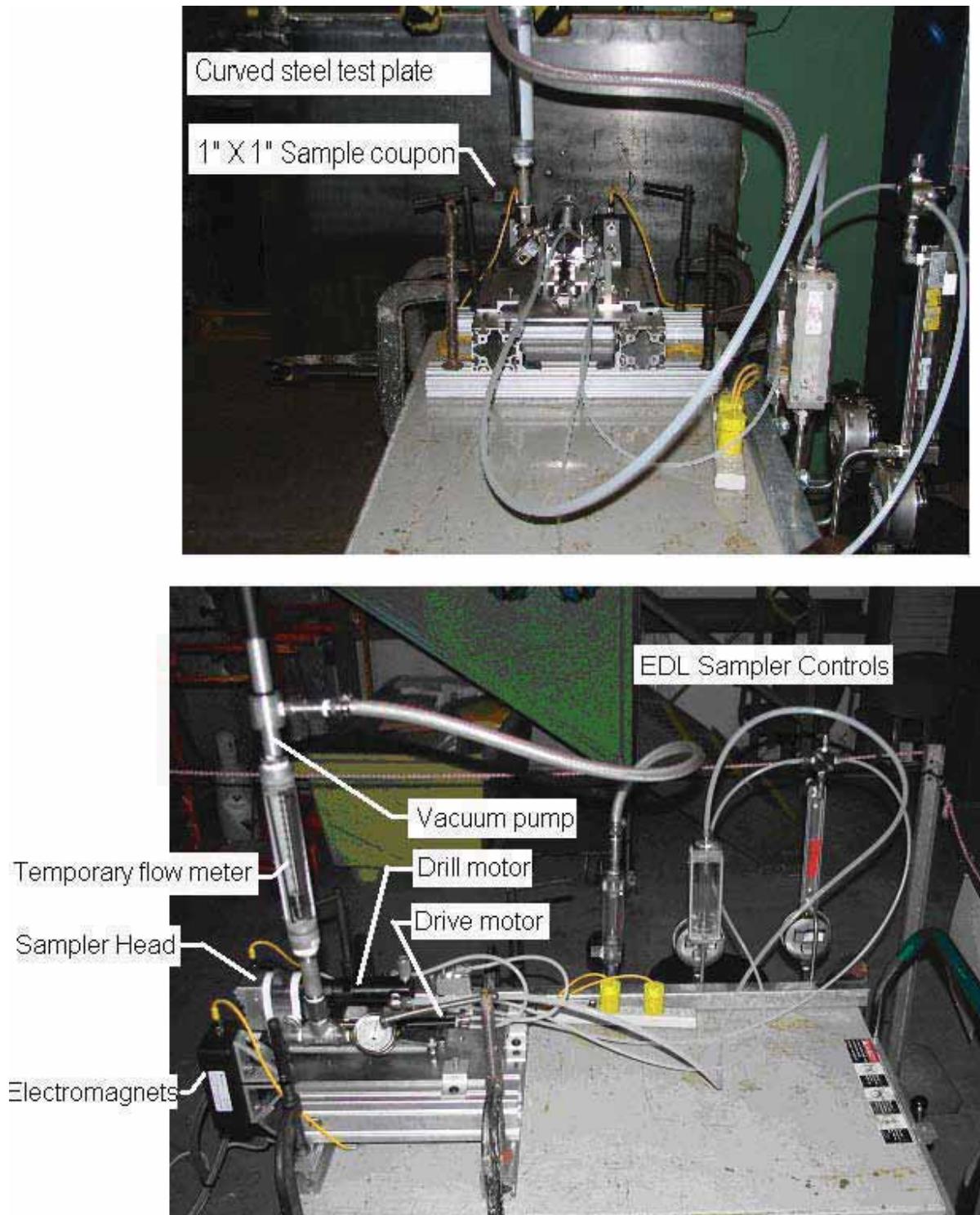


Figure 9: EDL Test Setup and Sampler Components

3.1.1 SRNL Sampler Assembly

The sampler was originally designed by Oak Ridge National Laboratory (ORNL), subsequently modified by West Valley (Thomas, T., and Drake, J. [13 - 14]), and modified again by SRNL. The ORNL design is also discussed in detail in Appendix A (Killough, S.). Although referred to here as a sampler, the equipment is also referred to as a burnishing tool or an end effector, which is the action component deployed by a robotic arm. The sampler was successfully used at Hanford to obtain samples from a concrete walled tank and then modified at West Valley to obtain samples from a steel walled tank. The SRNL modifications included changes in the controls, the mounting plate, springs, filter selection, and added electromagnets.

The main components of the sampler are the drill motor, the linear motor (drive motor), the vacuum pump, sampler head, and controls, as shown in Figure 10 and Figure 11. Material is machined from the wall, and passes through the sampler head where it is collected on the sampler filter. The work instruction for operating the sampler at EDL is provided in Appendix G. A discussion of the sampler components and controls provided later in this report clarifies sampler operation.

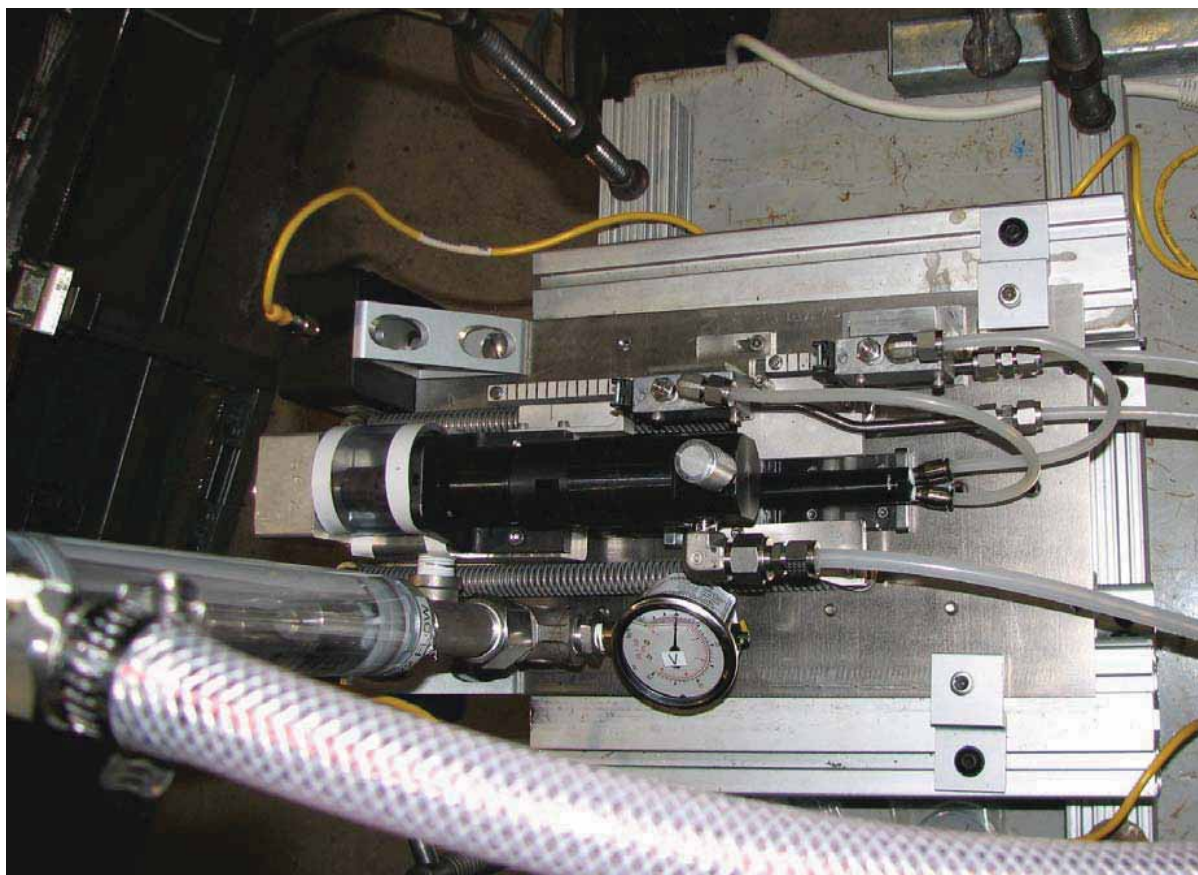


Figure 10: Sampler Assembly Installed for Testing (modified)

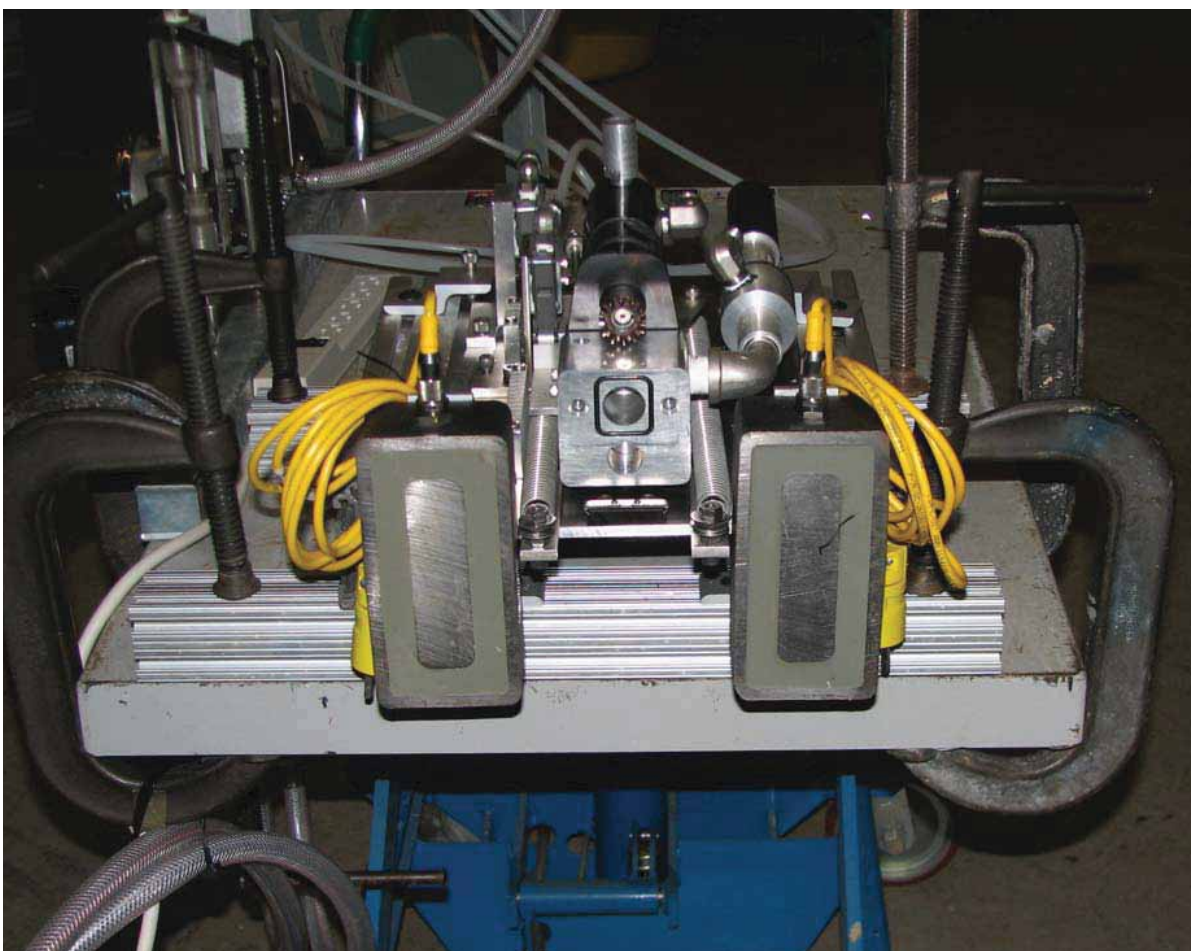


Figure 11: Sampler Assembly with Sampler Head Removed, Front View

3.1.1.1 Final Sampler Design

The final sampler design is shown in Figure 12 through Figure 15. Not only were the controls redesigned, but springs were changed to compensate a resonance problem, which is discussed in Section 5.2 of this report. The equipment was air operated, and supply pressures were altered after testing began.

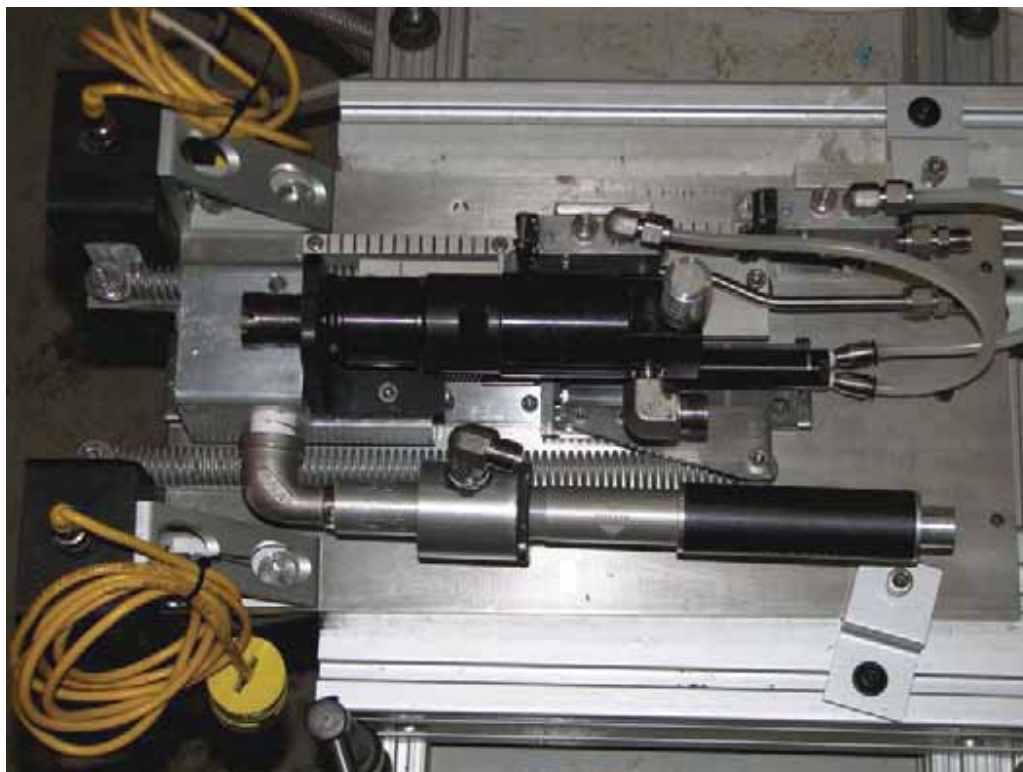


Figure 12: Sampler Assembly with Sampler Head Removed, Side View

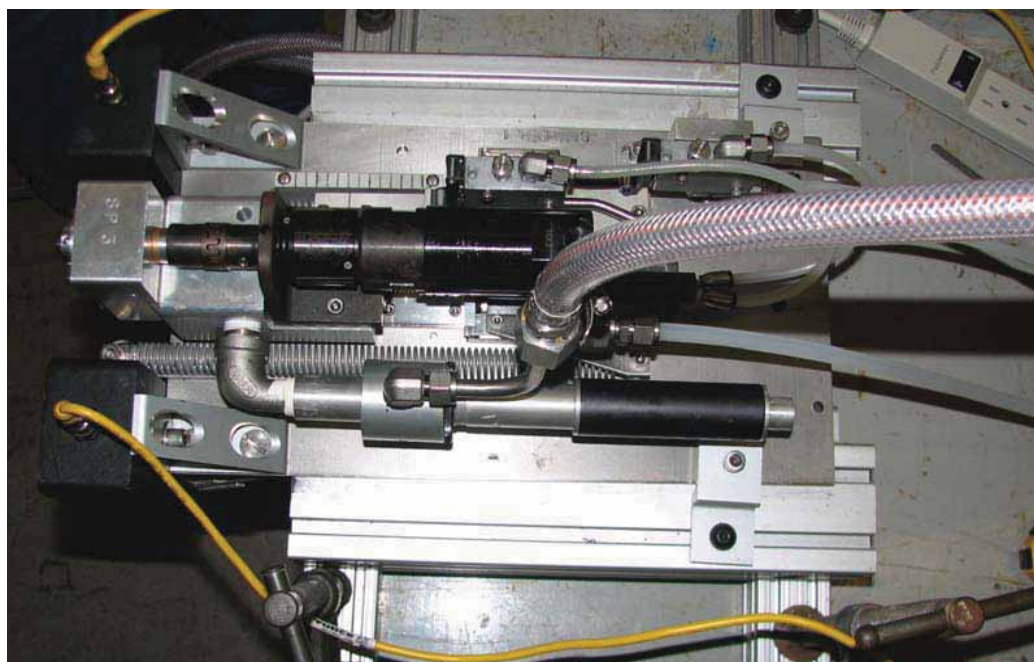


Figure 13: Sampler Assembly with Sampler Head Installed

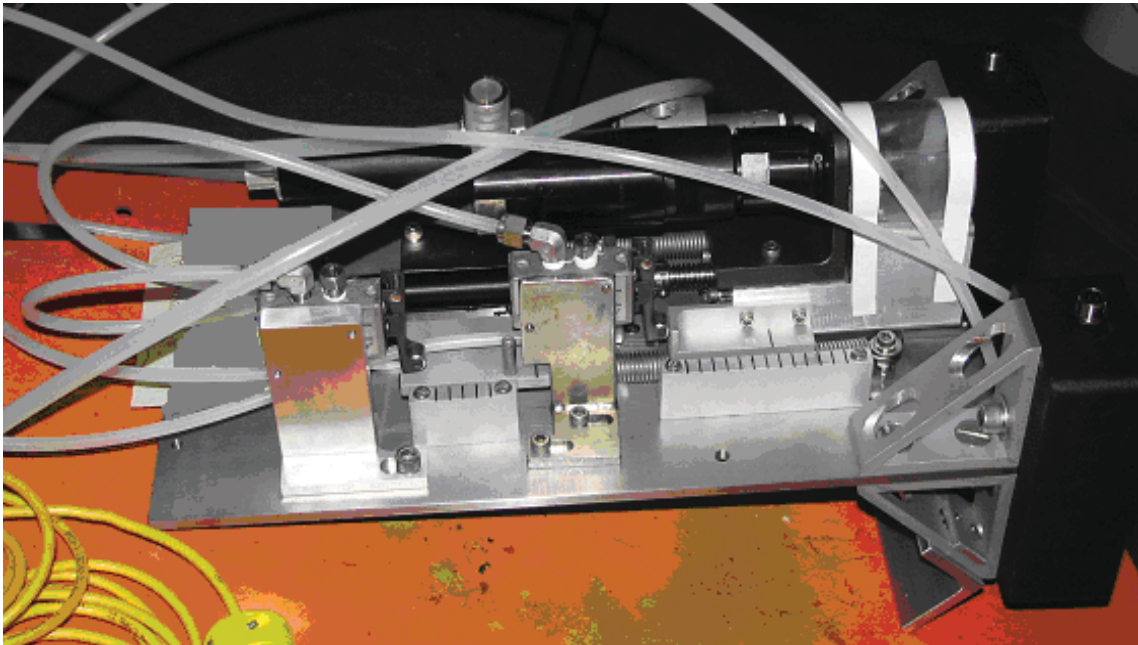


Figure 14: Delivered Sampler Assembly

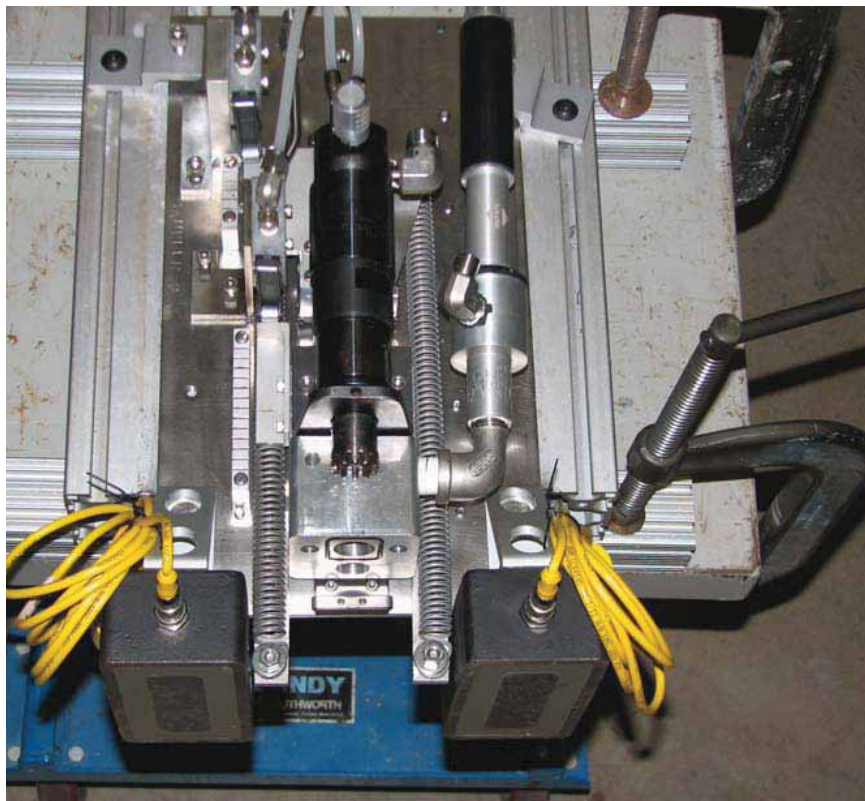


Figure 15: Delivered Sampler Assembly Without Sampler Head

3.1.1.2 Electromagnets and Springs

Two, 1500 pound force, electromagnets held the sampler to the wall when energized. For design, the magnets were first derated to 750 pounds each, since they were rated for a one inch thick plate. The actual tank wall was only 3/8 inch thick, which lowered the magnetic force. They were again derated for a potential 0.030 inch gap. Per the manufacturer, a 0.030 inch air gap causes a 90 % reduction in force, which yielded a 75 pound force for each magnet for a 0.030" air gap. Although electromagnetic properties of waste are unknown, this distance provides an approximation of the working distance from the wall at which the electromagnets are expected to operate. The springs on the sampler each provided a counteractive maximum force of 37 pounds when fully extended during sampler operation. Consequently, for waste thicknesses over approximately 1/32", the electromagnets were not expected to effectively hold the sampler to the waste tank wall.

The electromagnets caused other effects that were observed during testing. The electromagnets caused some residual magnetism in the wall plate which deteriorated slowly, but the magnets could be tilted slightly to break the small residual magnetic field. Also, the collected metal chips in the sampler head were all magnetized, which caused collected steel samples to cling together as a single mat of fibers attached to the sampler filter (Figure 22).

3.1.1.3 Operating Parameters

The EDL sampler operating parameters (Figure 16) for the air driven components (vacuum, drill motor, and linear motor) were initially chosen to simulate operating conditions expected at the tanks, which were based on the available air supply and the requirements of the components. However, testing at T-Area yielded different parameters, since the final SRR design of the mast assembly had higher tubing pressure drops than anticipated, and the SRNL design was already complete. To minimize costs, the SRNL operating pressures were changed to equal the operating pressures and drill speeds of the final SRR design. In short, EDL operating pressures were selected to provide comparable flow rates and drill speeds to those measured in T-Area on a fully assembled mast and sampler assembly with installed controls, hoses, and tubing.

Linear motor control Drill motor control Vacuum Eductor control

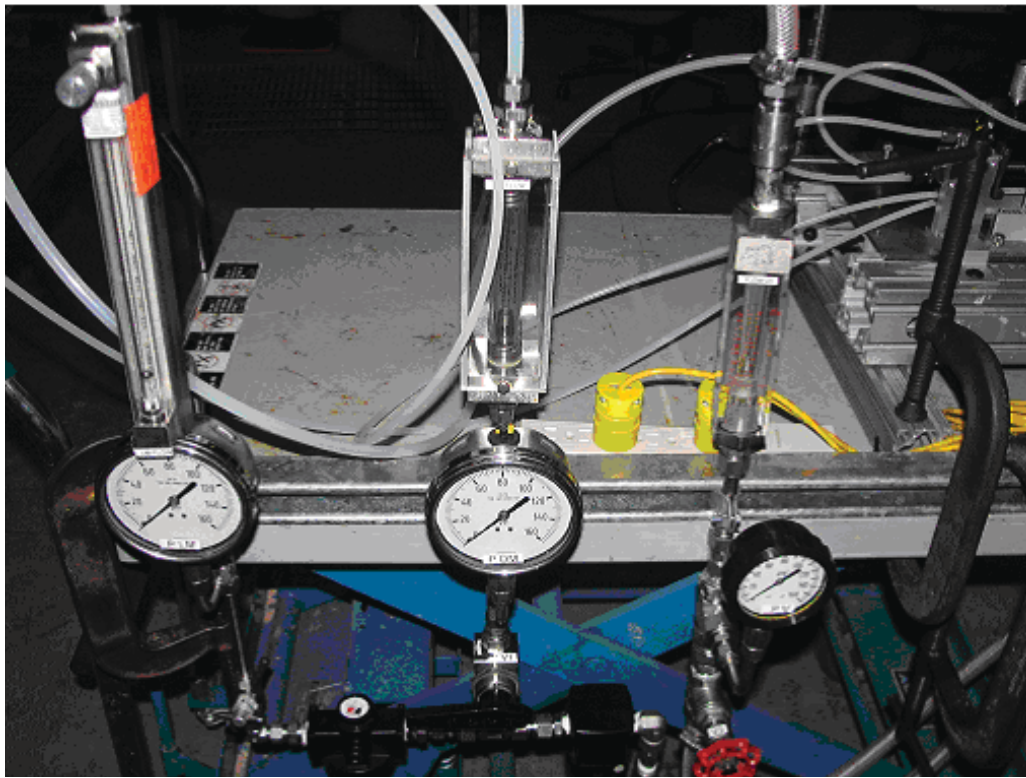


Figure 16: EDL Sampler Controls

The initial settings at EDL were 80 psig (15.2 scfm) for the vacuum supply, 90 psig (22.0 scfm) for the drill motor supply, and 40 psig (1.3 scfm) for the linear motor supply, which was controlled by a pressure regulator. These flow rates initially optimized sampler drilling and collection performance.

When the sampler system pressures and flow rates were changed, some parallel testing was already completed at EDL. Consequently, tests performed at earlier flow rates were performed again. Some of the data for sampling steel coupons is recorded in this report for both before and after flow rates were changed. In other words, some tests were re-performed as required to ensure that test results were consistent with FTF sampler operations. The details ensuring that test pressure and flows were conservative with respect to expected waste tank flows and pressures follow in the next paragraph.

Comparable supply pressures were 100 psig at T-Area, EDL, and FTF. Final flow rates were measured during full scale testing where supply pressures were 100 psig, and EDL operating conditions were set accordingly.

- The drill speed was 450 rpm and air flow was set to obtain this speed at EDL.
- The T-Area vacuum flow rate varied between 9.7 to 11.2 scfm, and the EDL vacuum flow rate was set slightly below this range to provide conservative test results. The

reference vacuum flow rate was measured on a rotameter operating at 100 psig on the full scale equipment, with rotameter readings of 3.5 – 4.0 cfm. Consequently, the minimum vacuum scfm was found to equal $3.5 \text{ scfm} / 0.358 = 9.7 \text{ scfm}$, where 0.358 is a conversion factor to change pressurized flow rates to flow rates in terms of standard atmospheric conditions (see Appendix F).

- The linear motor operating pressure was set to 70 psig, which was the operating pressure of the full scale sampler assembly. Comparable conversions were applied to find scfm requirements for required flows used for rotameters in EDL, and the lab notebooks record operating pressures and flows for all tests.
- To ensure conservative test results, the final EDL settings were 100 psig (24.4 scfm) for the drill motor supply, 50 psig (9.4 scfm) for the vacuum supply, and 70 psig (2.1 scfm) for the linear motor supply. These final test pressures were used to obtain the test results reported in the conclusions of this report.

3.1.1.4 Drill Motor

The drill motor was a non-lubricated, air operated motor. The drill was operated at approximately 450 rpm, which was in the typical speed range required to drill steel. Lubricating the motor temporarily increased the speed by about 100 rpm when occasional lubrication was required. Since multiple holes were drilled with some of the sampler heads at EDL, lubrication was required. An original design assumption was that lubrication would not be required, since few holes were planned. Although the introduction of oil into waste tanks is prohibited, FTF determined that minimal oil lubrication was not a concern for these tanks undergoing closure. Only a few drops of oil were added, and most of this oil discharged through the vacuum eductor before the sampler was operated in the tanks.

3.1.1.5 Drill Bit Design

The drill bit design was the same as the original ORNL design, and the drill depth at the tip was 0.060 inches to provide at least 0.030 inches of sample depth at the drill perimeter for most testing and sampling. Deeper 0.125 inch holes were used for only one sampler head. Primary requirements for drilling were:

- A minimum depth is drilled into the tank wall to ensure that damage does not affect structural integrity of the wall.
- Drilling is performed without lubrication to prevent mixing of oil with nuclear waste, which could potentially generate mixed waste.

The drill bits were modified, 1/2 inch diameter, HSS (high speed steel) end mills, which were tapered 0.025 inches from the center to the outer radius of the bits, resulting in a slightly conical tip with a drill point angle of 169° (Figure 17). The recommended drill point angle for drilling steel is 118°. Using a sharper drill point angle results in a deeper hole, and minimizing the depth of the hole was a requirement for sampling the tank wall. Initially, ORNL used a flat tip end mill to minimize the depth of cut into the tank wall, but chattering of the end mill prohibited drilling the concrete wall. Modifying the end mill permitted

effective drilling. West Valley also experienced chattering on the steel walled waste tanks and difficulty with drilling. To improve drill performance they increased the drill speed, changed the spring, and increased the drill point angle, but those drill point and speed changes were not included in the SRS (Savannah River Site) design. West Valley also found that the tank walls had to be cleaned additionally to remove waste before samples could be collected. Other improvements to the drill bit design were also possible and were related to the relief and rake angles of the bit, and the angle of the bit with respect to the wall.

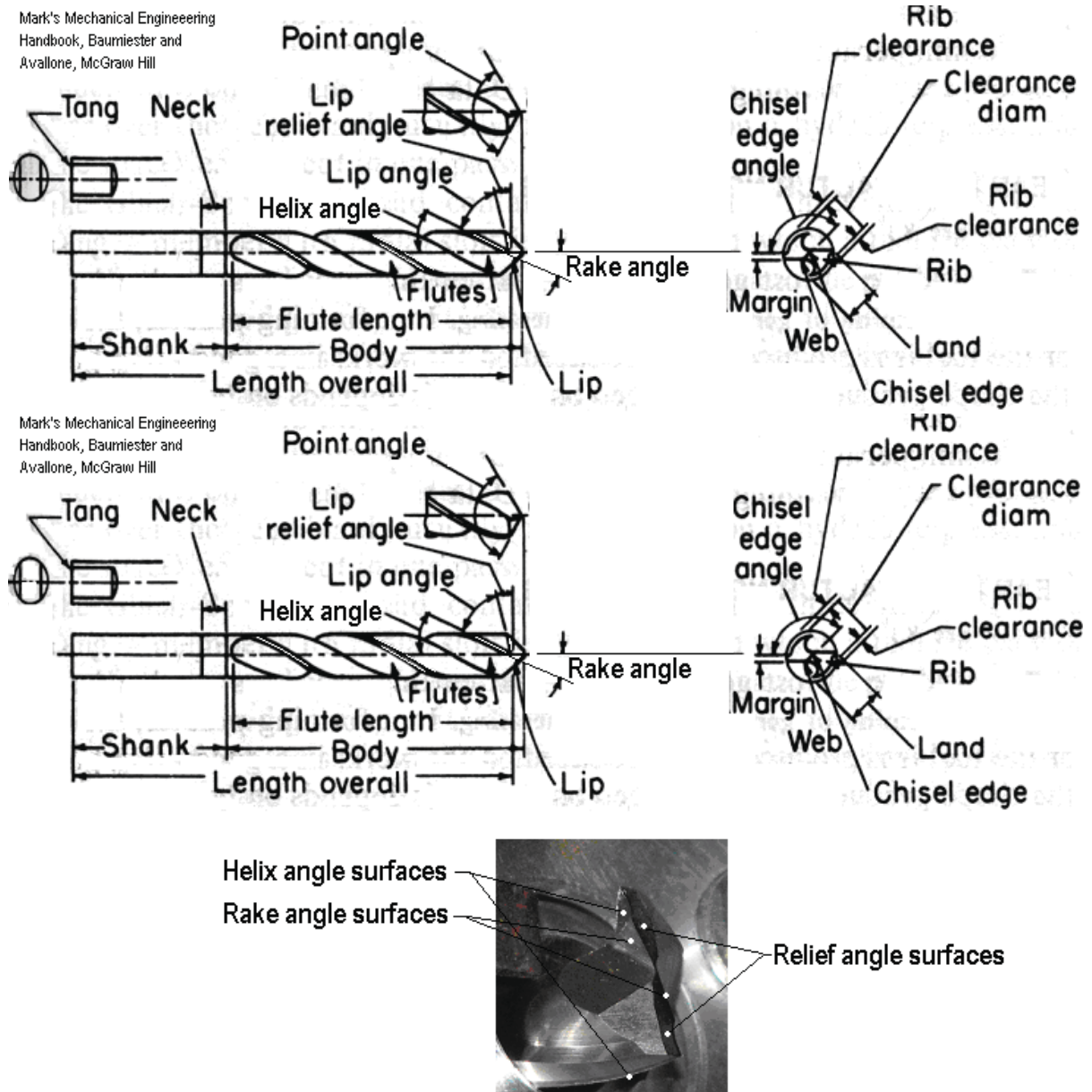


Figure 17: Drill Bit Terminology

The relief angle is the angle of cutting edge with respect to the surface, and this angle directly affected drill bit chattering. EDL testing showed that as the relief angle between the surface

and the bit decreased, drilling performance improved as the size and length of the chips increased. This observation agrees with machine tool literature, and can be explained in terms of vibration and drill bit surface area.

Refer to Figure 17 to see the relief angle surface. As more relief surface area is pressed against the wall material, more force is applied to the drill bit. When either a rusted or painted surface is drilled, the relief surface presses into the softer material. Accordingly, more force is impressed on the drill bit. When the relief angle is increased, less surface area is exposed to the rust, and forces are decreased, which may seem counter intuitive since increasing the relief angle actually sharpens the cutting edge. However, the contact area between the drill and surface is the dominating effect for chattering. Also, chatter decreases as the material hardness increases, and the contact area between the drill and wall surface decreases.

For this design, chattering occurred when rusted surfaces were drilled. Since the magnitude of vibration due to chattering is related to the forces on the relief surface, vibration increased as the relief angle decreased. Then the vibration increased, the drill bit spent less time in contact with the surface, and drill bit life decreased.

The rake angle is the angle machined in the two drill flutes, which is typically 90° to the surface. The rake angle is different than the helix angle, and is machined into the helix surface near the drill point. Again, see Figure 17. Material is cut by the chisel edge between the relief and rake surfaces. Theoretically, a decrease in the rake angle to the surface increases material removal as the sharper rake angle cuts a deeper groove in the base material. This effect was not investigated.

The angle of the drill bit centerline to the surface also affected drilling. When the drill was perpendicular to the surface, an angle of 5.5° existed between the conical bit surface and the wall. When the drill bit was slightly tilted, the angle between the bit and the surface decreased on one side of the drill, and drilling performance decreased as indicated by smaller chip sizes. Sampler assembly was controlled to ensure that the bit was perpendicular, and each sampler head was tested at EDL where the depth of a single drilled hole was measured around its circumference to ensure that the drill was normal to the surface and performed properly before shipping to FTF. In full scale testing in T-Area, the mast position was intentionally changed to cause one magnet to touch the wall, while the other magnet was 1/8 inch from the wall. When this action was taken, drill chips were compared to chips obtained with a properly aligned drill bit, and the chips were noticeably smaller indicating decreased performance. Therefore, camera inspections at the waste tanks ensured that the sampler was properly aligned to the wall before electromagnets were energized. Once the electromagnets were turned on, the force on the drill bit was controlled by the linear motor and the springs.

3.1.1.6 Linear Drive Motor and Spring Control

The linear drive motor is also a non-lubricated, air operated motor. It actuated an ACME screw to slowly advance the sampler head toward the wall in about 30 seconds. The total time to drill a hole in the EDL test plate typically varied from 2 – 3 minutes. Four minutes

was the total operating time recommended to SRR for waste tank sampling, since sampler drilling progress cannot be directly monitored or observed.

The spring force applied to the drill directly affected the size of the chips. The control system forced the drill bit against the wall, and then fully extended the springs, so that the springs exerted the only forces on the drill bit tip. Increasing the force increased the size of the drilled chips. Depending on the spring force, a range of chip sizes was obtained that varied between small particles to long curls, similar to the effect of changing the relief angle on the drill bit.

3.1.1.7 Vacuum Eductor

The vacuum eductor had an adjustable air flow and vacuum pressure to pull air through the sampler head from the drill bit. The vacuum eductor acted as an air pump, as shown in Figure 18. A vacuum is produced in the entrainment section of the eductor, which draws air from the suction. Then the air exits the eductor discharge. The flow rate at EDL was adjusted to obtain a maximum suction, and the adjustment nut was then glued in place to prevent accidental maladjustments of the vacuum.

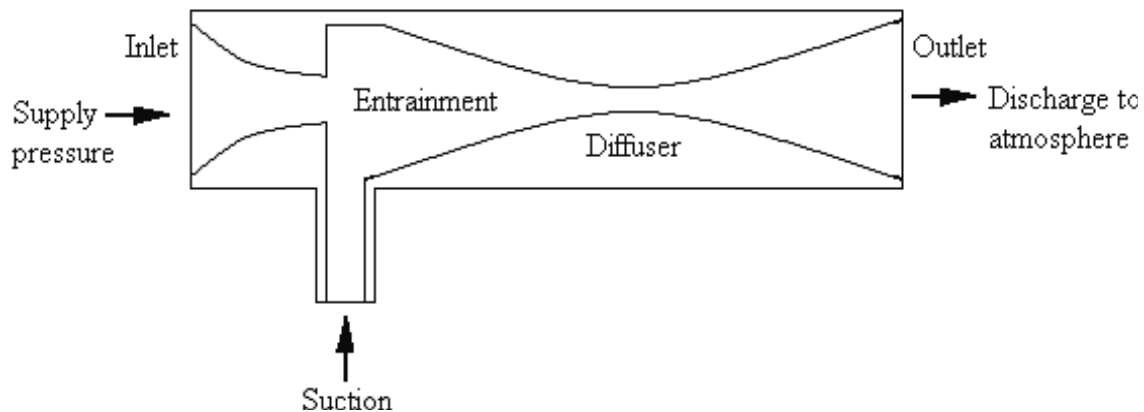


Figure 18: Typical Eductor Design

Testing at EDL showed that the vacuum collected all material that was drilled. To verify vacuum performance, the sampler was attached to the wall test plate, and a white tape was stretched between the bottom of the electromagnets to capture any falling particles. The tape was replaced between several tests, and typically no particles were captured. In one set of tests a few minute particles were captured as shown in Figure 19 and Figure 20, but these particles were considered to have negligible effects on testing. Also, during salt testing, material surrounding the drill site was observed to break loose from the wall and be pulled into the sampler head. In other words, not only did the sampler collect all of the material within the sample area, but there was potential to collect material outside of the sample area. Consequently, SRNL recommended to SRR that the vacuum be turned off immediately after drilling was complete, and before the sampler was retracted from the wall.



Figure 19: White Tape Used to Collect Chips Falling From the Drill Bit

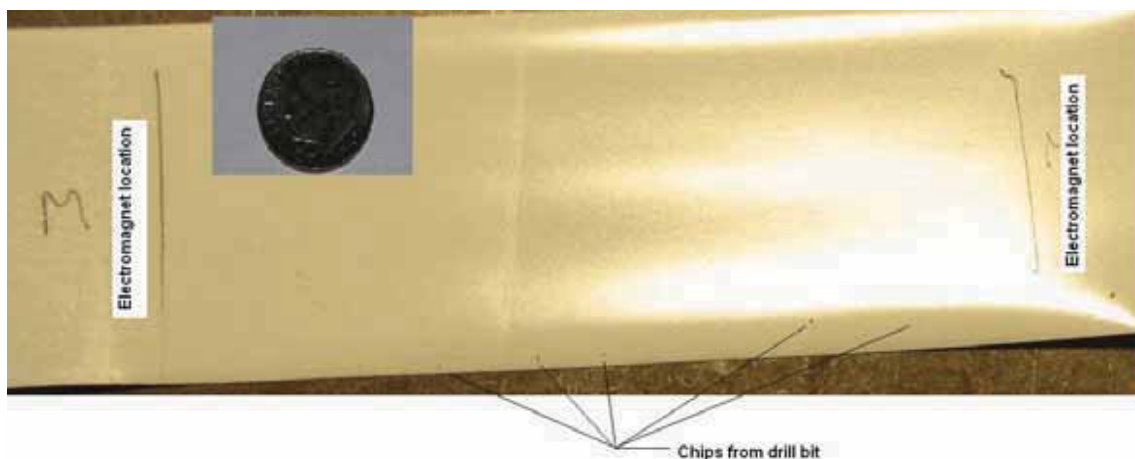


Figure 20: Chips from Drill Bit Following Drilling of Three Holes

3.1.1.8 Sampler Heads

Nine sampler heads were manufactured at SRNL for testing and sampling. They were identified and stamped as TK 18-1, TK 18-2, TK 19-1, TK 19-2, and SP1 through SP5. Each

sampler head consisted of a small aluminum block containing a drill bit in the upper portion and a filter in the lower portion (Figure 21). Figure 22 through Figure 25 show the basic construction of a sampler head.

Prior to shipping to SRR, all fabricated sampler heads and drill bits were tested, including verification of drilled hole depths which were typically $0.060'' \pm 0.005''$. The minimum hole depth was then $0.055''$, which ensured that at the minimum depth requirements were met. That $0.050''$ requirement equaled $0.025''$ for the drill angle plus $0.030''$ inches to ensure an adequate depth for the drill sample through the waste and corrosion layers.

Although most testing and sampling was performed for $0.060''$ holes, the depth was increased. For the last sample at Tank 18, a $0.125''$ drill bit depth setting was used. Since the electromagnets were releasing from the tank wall during testing in T-Area, an increased drilling depth was added to the design to aid in drilling. The primary problem with drilling during test was found to be associated with resonance, and changing the drill bit length added little improvement to the design.

The drill bit was driven by a multi-jaw coupling connected to the drill motor, which rotated in a bronze, oil impregnated thrust bushing. The tip of the drill bit protrudes from the front of the head but was surrounded by an aluminum, spring-actuated collar, or shroud, which permits air flow through the sampler and prevents loss of material at the drill bit. The air flow through the sampler head passed through the openings (four equally spaced holes) in the drill bit collar. The flutes of the drill bit directed the shavings and debris removed from the wall surface into the drill cavity and then into the filter cavity, where the material was captured by the filter.

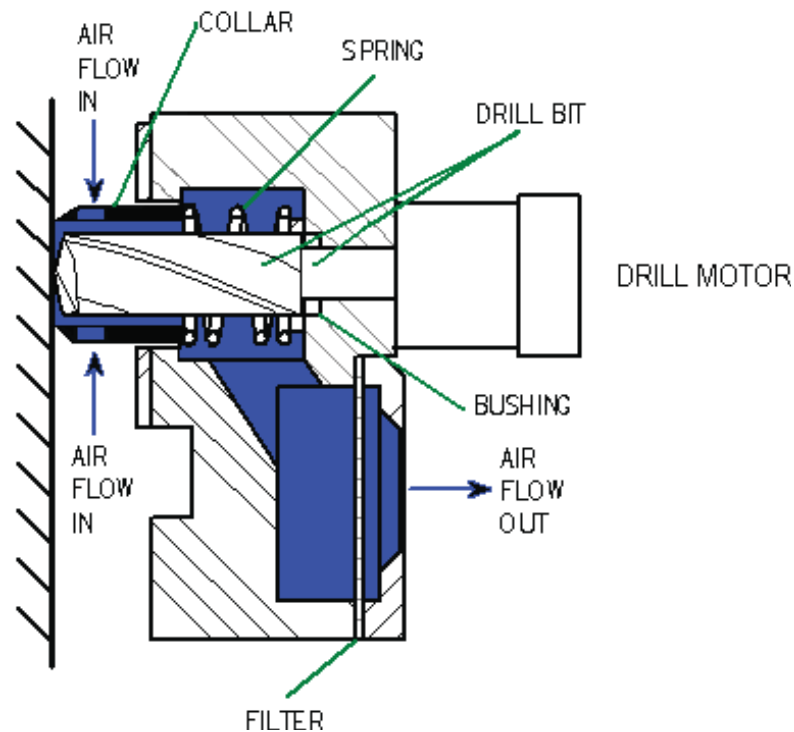


Figure 21: Flow Path Through the Sampler Head



Figure 22: Test Sample Prior to Initial SRR Delivery, One 0.060" Deep Hole

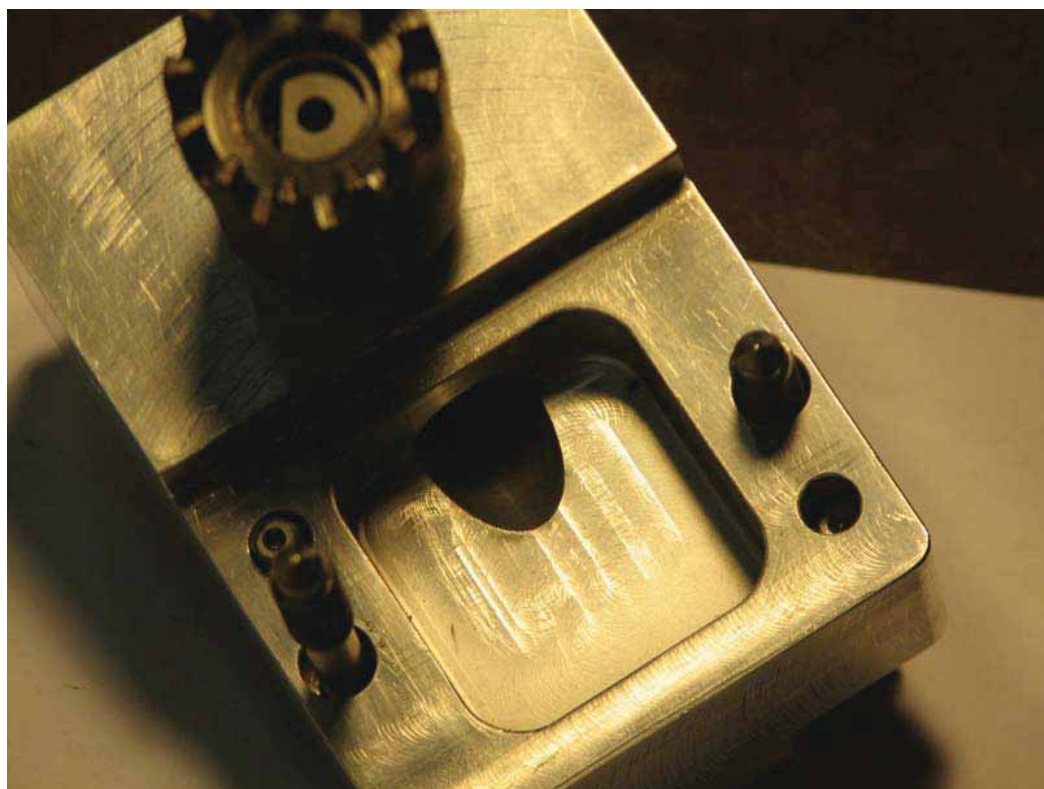


Figure 23: Sampler Head and Filter Housing



Figure 24: Sampler Head Drill Bit Shroud



Figure 25: Sampler Head Drill Bit

3.1.1.9 Filters

HEPA filters were used by ORNL and West Valley, but fiber material filters were used at SRNL. Thin High Efficiency Particulate Air filters (HEPA filters) were fabricated from a particulate fiber glass material (Pall Filters, 0.3 micron, 0.014 inch thickness), which was rather fragile. Initial testing at EDL demonstrated that when the filters were compressed between the sampler housing and the filter retaining plate, the filters were cut along the compression line (Figure 26). Since there was a risk of lost material passing through the cut and around the filter, a different filter was selected (Cole Parmer, polypropylene felt, 5 micron, 0.060 inch thickness). The filters were cut 1 - 3/4" X 1 - 3/4". The surface area exposed to the vacuumed material was 1 - 1/4" x 1 - 1/4" with 1/4" radii on all 4 corners. The opening in the sampler head, downstream of the filter, was 3/4" diameter. Although the sampler design could have been altered to use the HEPA filter, a thicker fibrous filter was expedient and was shown to provide equivalent results during steel sampling at EDL. Three fibrous filters would have provided filtration similar to the HEPA filter, but one filter was initially considered adequate. In retrospect, the sampler may have been readily adapted for multiple filter use, since the sampler housing was later modified.

That modification included spacers that were added to ensure uniform compression of the fibrous filter between the sampler housing and the filter retention plate. To minimize personnel radiation exposure at the FTF tank tops, the spacers were installed by EDL. Spacers were also required to prevent tilting of the drill bit. Tilting of the drill caused the drill bit to lie flatter to the wall, and drill smaller chips, or not drill at all. To prevent tilting, the filter required uniform compression. At EDL compression was controlled by careful assembly of the sampler to ensure that the drill bit did not tilt with respect to the wall surface and drill improperly.

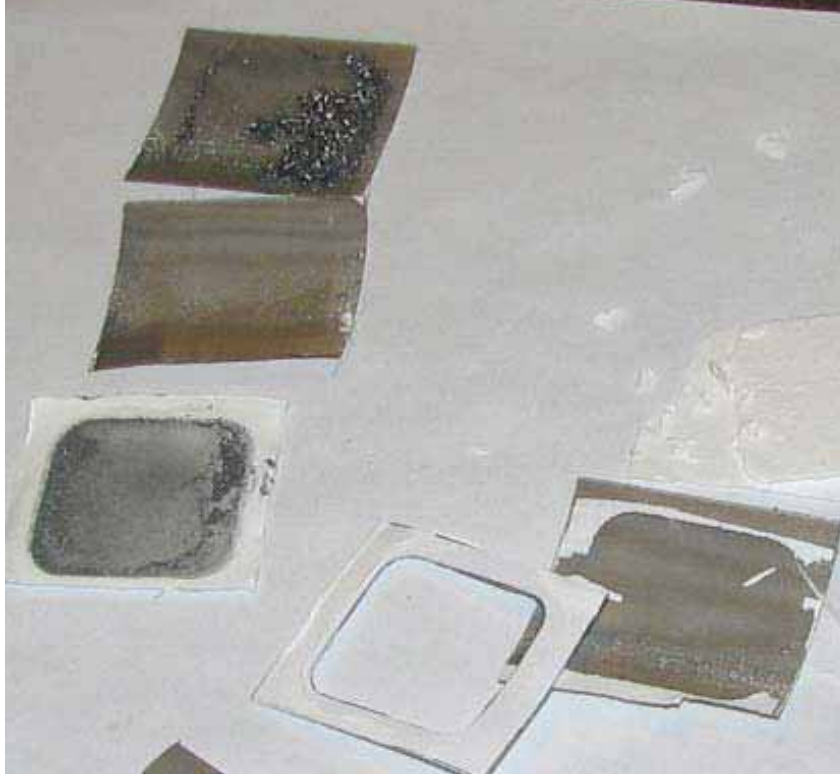


Figure 26: Unacceptable HEPA Filter Design

3.1.1.10 Sampler Controls

The control system Process and Instrumentation Diagram (P&ID) for the EDL sampler is shown in Figure 27. Testing showed that the sampler controls needed modification. An additional limit switch was installed to prevent the sampler from jamming at the end of retraction. Without control system changes, the sampler would have failed in the waste tank.

The P&ID shows pertinent components. As mentioned, the vacuum eductor, drill motor and linear motor were all powered by the EDL air supply at 100 psig. The supply pressure to the eductor was set by manual valve V3. The supply pressure to the drill motor was set by manual valve V1. The supply pressure to the linear motor was set by regulator R1 and isolated by manual valve V2. Advance and retract operations were controlled by the 4-way valve V4 and by the two limit switches in the linear motor flow control loop. Advance moved the sampler toward the wall, and retract withdrew the sampler. The limit switches prevented the linear motor from driving to either full travel position. The limit switches were two Mead Fluid Dynamic, Inc., model LTV-15 4-way control valves. They were engaged by depressing a roller leaf and disengaged by releasing the roller leaf. The limit switches are shown in Figure 28.

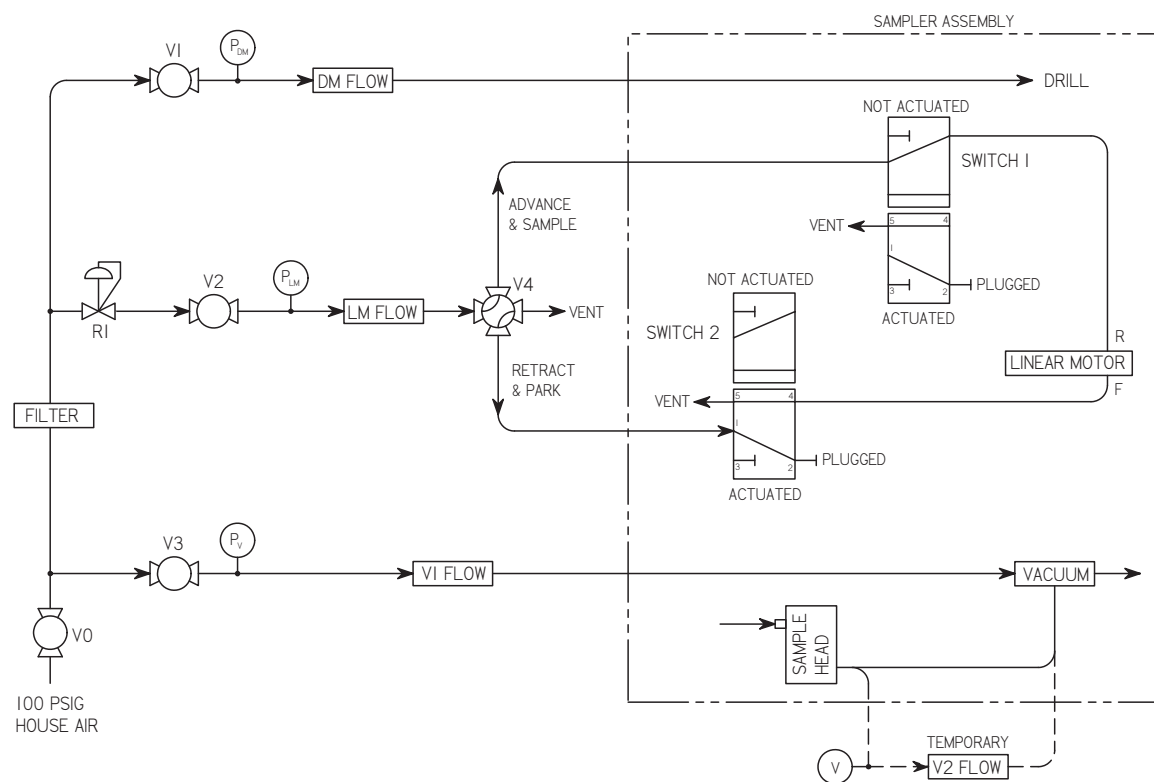


Figure 27: EDL Sampler Controls, P&ID

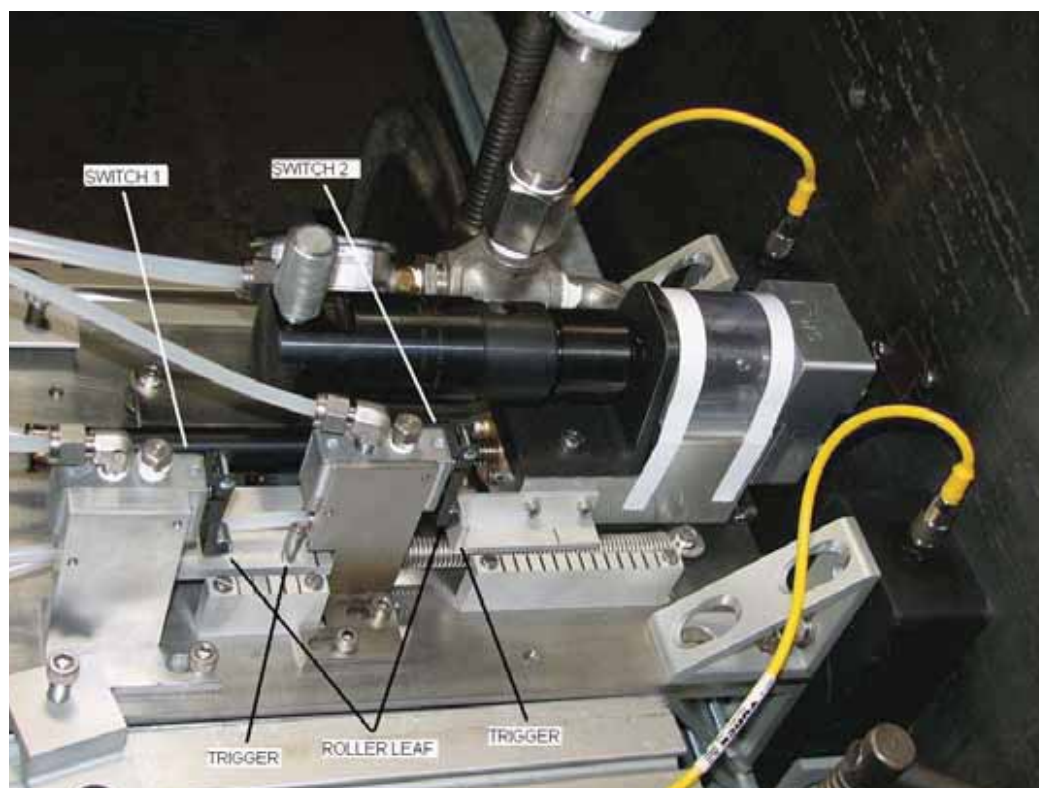


Figure 28: Sampler in the Fully Retracted Position

The sampling sequence started with the linear motor fully retracted. The 4-way valve V4 was off (positioned between ports), switch 1 was not actuated and switch 2 was actuated (roller leaf compressed by trigger), as shown in Figure 29. The terms actuated and not actuated are terms provided in the vendor literature for the controls.

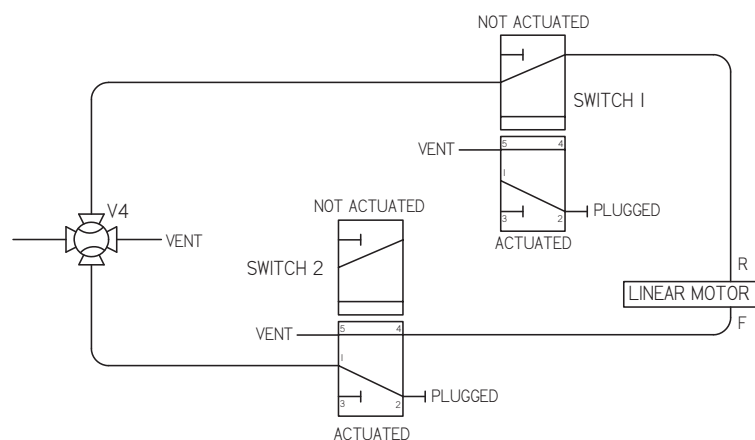


Figure 29: SRNL Linear Motor, Fully Retracted

Sampling was initiated by manually setting V4 to the ADVANCE & SAMPLE position. Switch 1 remained not actuated and switch 2 was actuated initially (with air venting out of

the switch) then became de-energized (with the air venting out of V4) as the linear motor advanced towards the plate and released the trigger (Figure 30).

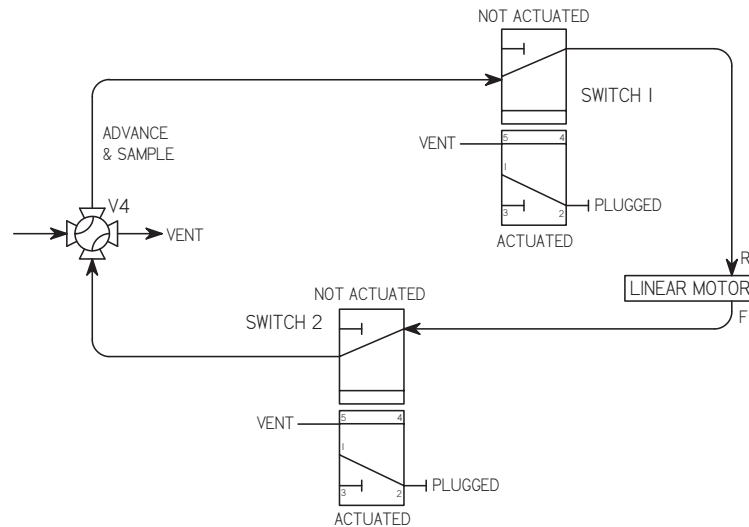


Figure 30: SRNL Linear Motor, Advancing

The sample was taken and switch 1 was actuated as the linear motor reached the fully advanced position (the roller leaf was depressed by the trigger). Switch 2 remained de-energized and V4 was manually set to the off position (Figure 31).

3.1.1.11 Drill Advancement

During drilling, the final 2 minutes of the initially recommended 4 minute drill time were required to advance the drill only 1/16". The widely spaced black lines on the sampler were inadequate to gauge this slight motion of the sampler head. Even so, the bulk motion of the sampler prior to, and after, drilling could be judged by the relative motion between markings on the sampler. Some insight into advancement of the drill was discerned from the rotation of the ACME screw on the linear drive motor. In general, the drill obtained material as the screw rotated. However, there were times when rotation occurred periodically, and minimal material was collected. At EDL, screw motion was easily observed, but in the waste tank, the motion could only be observed by camera. Camera positions were recommended by EDL Engineering to FTF Engineering to view the ACME drive screw advancement in the waste tanks. Even so, drill advancement could not always be discerned.

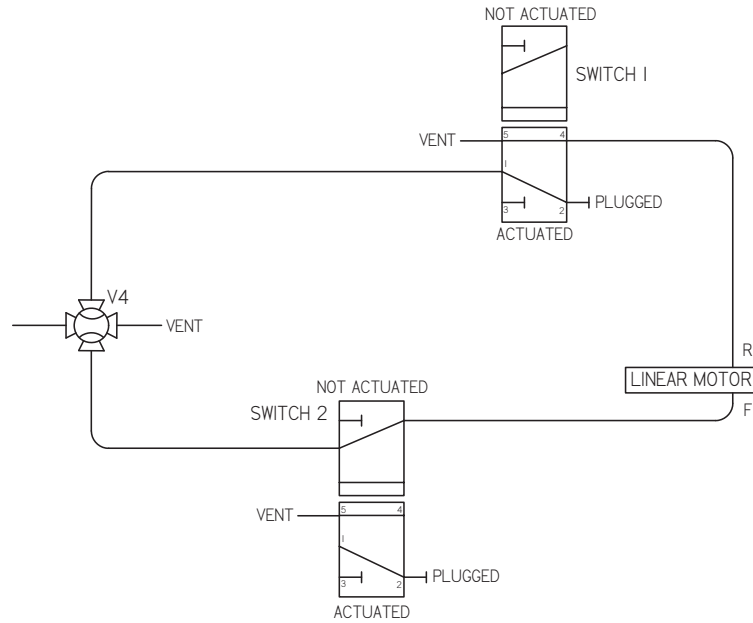


Figure 31: SRNL Linear Motor, Fully Advanced

Retraction was started by manually setting V4 to the RETRACT & PARK position. Switch 1 was initially actuated (with air venting out of the switch), then became not actuated (with air venting out of V4), as the linear motor retracted away from the plate and released the trigger (Figure 32).

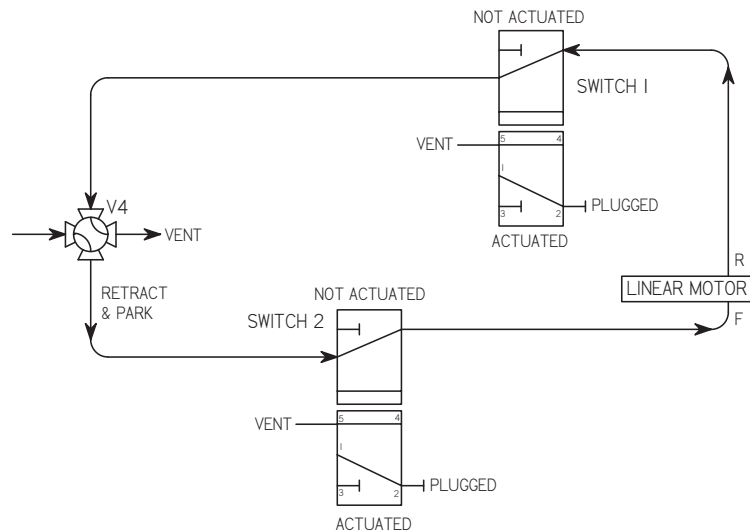


Figure 32: SRNL Linear Motor, Retracting

Switch 2 was actuated when the linear motor reached the fully retracted position (the roller leaf was depressed by the trigger). Switch 1 remained not actuated and V4 was manually set in the off position to complete the sequence and prepare for the next sample.

3.1.2 EDL Sampler Evaluation

Nearly 100 holes were drilled at EDL and T-Area to evaluate the performance of the samplers, 41 holes were drilled in the EDL test plate alone. Holes were drilled in the EDL test plate and at T-Area to validate sampler operation before waste tank installation, and test coupons were drilled at EDL to assess sampler performance.

The test setup is shown in Figure 33. The test plate was built of A36 steel (Figure 34), which has a comparable hardness to the A285 steel sample coupons, and the steel plate used to fabricate the waste tanks. The test plate was rolled to an 85 foot diameter, which was equal to the waste tank diameters. A recess was machined into the test plate, so that the flat test coupons could be flush mounted to the plate, using bolts at two corners of the coupons. Four milling machine mounting holes were drilled into the test plate to ensure precision machining of the recess and proper mounting of the test coupons. A metal frame with brackets was installed on the plate to assist alignment of the sampler to the coupons.



Figure 33: EDL Sample Setup

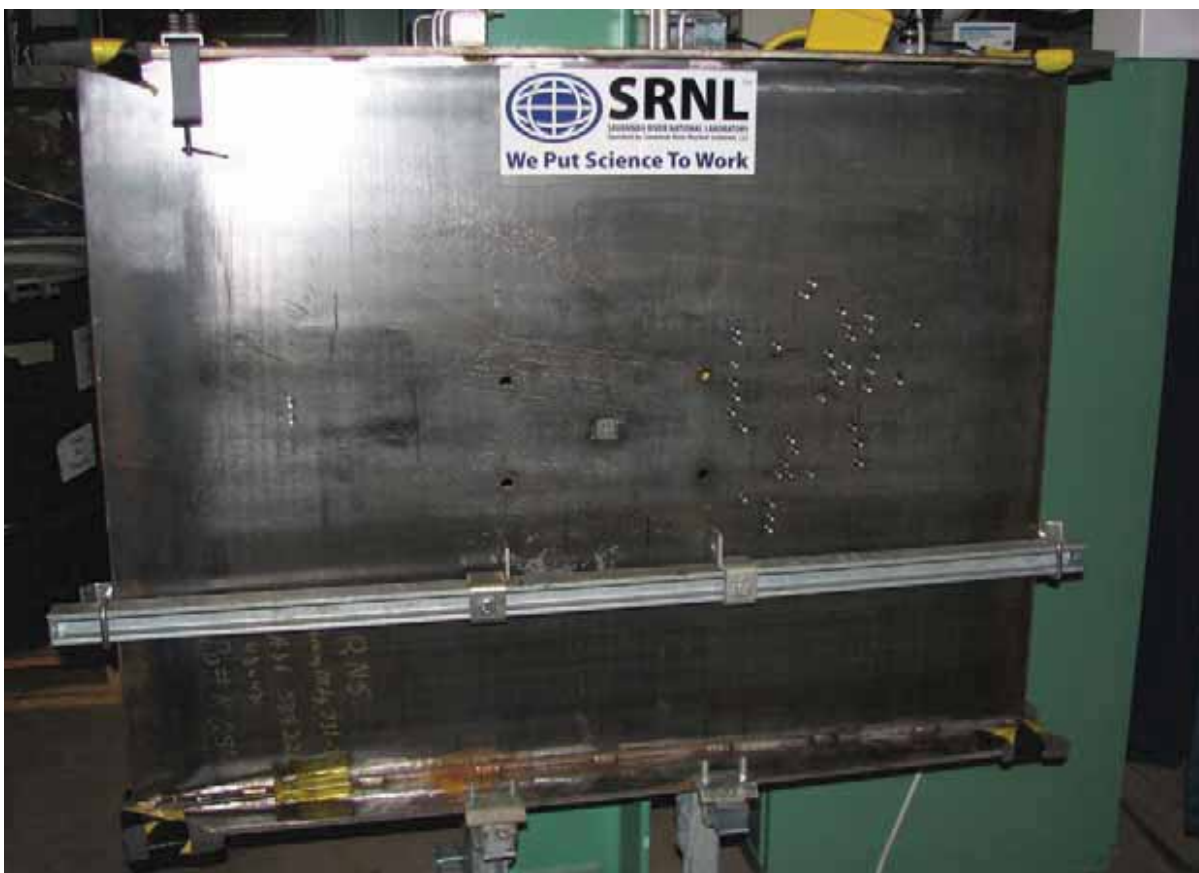


Figure 34: EDL Test Plate

3.1.3 Sample Coupons

To simulate tank conditions, several different sample types were evaluated, using sample coupons. Each set of sample coupons was made from A285 steel, which is similar to the steel used for tank construction per T. Hooper, SRR. The tanks were constructed to the 1952 ASME Boiler Construction Code, where the 1960 DuPont specification for tank construction specified that tank walls met the Boiler Code material requirement for P-1, UCS-23. One set of samples were rusted steel plates with a layer of salt; one set of samples were electronic discharge machined (EDM) steel plates with a salt layer on each coupon; and one set of samples were polished plates without salt coatings. Sample preparations are described in Appendix C.

After the sample coupons were machined, masses of the coupons and filters were weighed before and after drilling for comparison. For the metal samples, only steel chips were collected and weighed. For the salt samples, only salt was machined and weighed with the filter. For the rusted samples, combined corrosion, steel and salt were weighed with the filter. Sample coupons are machined for testing as shown in Figure 35, and a typical coupon coated

with salt is shown in Figure 36. The coupons are later drilled during testing, as discussed in Sections 4.2.4 and 4.2.5.



Figure 35: Prepared Test Coupons



Figure 36: Typical Sample with Salt Deposition

3.1.4 Waste Characteristics and Test Samples.

Residual salts were expected in the tanks, since salts often collected on the tank surfaces in addition to a corrosion layer. The salt layer in waste tanks is hygroscopic, and absorbs sufficient moisture in summer months to become transparent on wall surfaces. For test purposes, salts were built up on sample coupons where salt deposition thickness was poorly controlled within the 0.030 inch thickness, as described in Appendix C. Although additional chemicals are present in waste tank salts, the salts used for sampling provided a comparable salt simulant. Salts may have been present on the walls of Tank 19, but the waste observed in Tank 18 was significantly different than salt. The salt tests performed at EDL are not representative of actual tank conditions, but tests were performed for the best simulant available. Tests were also performed in parallel with sampling of the tanks, and material differences between test and tank conditions were identified while salt testing was in progress, just prior to sampling of the waste tanks.

As noted, the actual waste characteristics for Tank 19 may have included salt, and Tank 18 contained waste on the walls that was not initially considered for sampler design. The sampler was initially designed to collect samples from a surface with 0.004" – 0.006" of corrosion and a maximum salt thickness of 0.025". EDL sample coupons were prepared accordingly for evaluation of collection efficiencies. Even though salt accumulation on the walls was not observed during waste tank sampling, EDL testing with salts provided considerable insight into sampler performance and collection efficiencies.

4.0 EDL TESTING

4.1 SAMPLER COLLECTION EFFICIENCIES

How much of each type of material is collected? The efficiency of the sampler to collect material can be determined for individual materials. The efficiency is calculated from the masses measured before and after drilling, where the collection efficiency of the sampler is expressed by the percent of material collected by the sampler head compared to the amount of material removed from the coupons. Collection efficiencies were determined by the following equations.

$$CE = 100 \cdot M_S / M_C \quad (1)$$

$$M_S = M_{S2} - M_{S1} \quad (2)$$

$$M_C = M_{C1} - M_{C2} \quad (3)$$

CE is the collection efficiency of the sampler expressed as a percentage; M_S is the total mass of material collected by the sampler head; M_{S1} and M_{S2} are the sampler head masses before and after sampling; M_C is the total mass of material removed from the coupons; M_{C1} and M_{C2} are the coupon masses before and after sampling.

From these equations an uncertainty analysis was conducted prior to testing to determine the optimum coupon size that would provide the greatest accuracy of the results. Consequently, the size of the sample coupons was chosen to reduce the uncertainty but also to ensure machinability during sampling.

Collection efficiencies were markedly affected by salt properties. The collection efficiency was 99.6 +0.4 / - 2.2 % at expected operating conditions. Calculated efficiency values over 100 % are due to the theoretical uncertainties of the instrumentation. For the salt samples, the measured collection efficiency was 82.1 +17.1 / - 24.9 %. The salt simulant used for testing was expected to be similar to salt coatings on the tank walls, where the salts are very hygroscopic. That is, the salts liquefy somewhat during short term testing. Overnight, the samples liquefy completely at standard shop conditions. In the waste tanks, the salts have been observed to liquefy during the summer into a transparent film, and solidify to a white film on the walls in cooler months. Tank 18 was spray washed in 2002 using low pressure and low volume. Tank 19 was spray washed in 2001 and was pressure washed using high pressure in 2009. A thin film of salt may, or may not, be present after pressure washing.

Waste tank sampling was performed during summer, and the thin transparent film (0.004”) was initially expected in the waste tanks.

In EDL testing, a test anomaly was noted due to salt liquefaction. The liquid passed through the filter, and salt accumulation was observed in the tubing downstream of the sampler head, following tubing disassembly. The effects of this phenomenon were not investigated for other than test conditions. Tests for the rusted, salt coated coupons are also affected by salt properties. Neither salt liquefaction effects on efficiency or efficiency of corrosion alone were investigated. Given this limitation of the rusted, salt coupon results, the collection efficiency is $99.3 \pm 0.7 / - 3.7 \%$. The following discussion supports these statements.

4.2 TEST PREPARATION

4.2.1 Test Specifications

Required testing consisted of three series of tests; one series using polished steel coupons, one series using coupons with a layer of salt, and one series using coupons with a layer of corrosion and a layer of salt (Table 1). A series consisted of three separate sample pairs, where two coupons were sampled using one filter. Two samples per filter duplicated the sampling technique initially planned for Tanks 18 and 19.

Table 1: Test Specifications

Series Number	Test Number	Test Name	Coupon Coating	Number of Coupons Sampled per Test
1	1	Polished Steel	None	2
	2	Polished Steel	None	2
	3	Polished Steel	None	2
2	4	Salt	Salt	2
	5	Salt	Salt	2
	6	Salt	Salt	2
3	7	Salt + Rust	Corrosion + Salt	2
	8	Salt + Rust	Corrosion + Salt	2
	9	Salt + Rust	Corrosion + Salt	2

4.2.2 Test Procedure

Testing consisted of installing a sample coupon into the test plate, and drilling a sample to the required depth. To document test results, sampler heads, filters, and coupons were weighed before and after sampling, and the depths of sample holes were measured.

After weighing, the filter was installed in the sampler head. The head was attached to the sampler. The coupon was attached to the test plate. The sampler, which was mounted to a mobile lift table, was moved to place the electromagnets against the plate. The sampler was

then operated. A metal frame, attached to the EDL test plate, aided the alignment of the sampler to the coupon. Sampler position was verified and then the electromagnets were energized. The flow to the eductor was first initiated and set to test conditions. Then the flow to the drill motor was started and set to test conditions. The flow to the linear motor was started to advance the drill to the coupon. The supply air to the linear motor was set and maintained by a pressure regulator. A stopwatch was started when the linear motor was started to measure the advance time. The advance time was complete when the cone-head screws contacted the plate. A feeler gauge was used to determine when contact was made, and in addition, the vibration of the drill bit could be felt through the plate, which was a good indicator of completion of the sample. At the end of the sample, the vacuum and drill motor were stopped. The linear motor was started in retract and the stopwatch was started to time the retract event. At the end of the retraction, the air supply to the linear motor was stopped, and the equipment was put in a safe condition.

Final weights were obtained after sampling was complete. The head was carefully disassembled to remove the filter and loose debris, and the loose debris was added to the filter and weighed. The coupons were weighed and the sampler head was then weighed. The pre-test and post-test masses were used to determine the collection efficiencies of the tests.

4.2.3 Mass of Material Collected by the Sampler Head

As testing progressed, it became apparent that all of the material removed from the coupons was not collecting on the filter. During initial testing of steel, a small portion of material passed through the filter as indicated by staining of the downstream side of filters. A somewhat larger portion was retained in the internal passageways of the head. Some material was deposited on the surfaces of the passageways (Figure 37), and some continuous chips from the drill bit were entangled with the collar spring and the drill bit (Figure 38). From this EDL finding, two efficiencies were presented in this report: collection efficiencies of the filters only and collection efficiencies of the entire sampler heads. These efficiencies are reported in the conclusion of this report. Also, as a result of this finding, sampler heads were completely disassembled and thoroughly emptied at EDL during testing and in the SRNL lab after delivery of samples from Tank 18 and Tank 19. The filter cavity, the drill cavity, and the passage between them were all carefully cleaned to obtain all sampled material from the tanks.

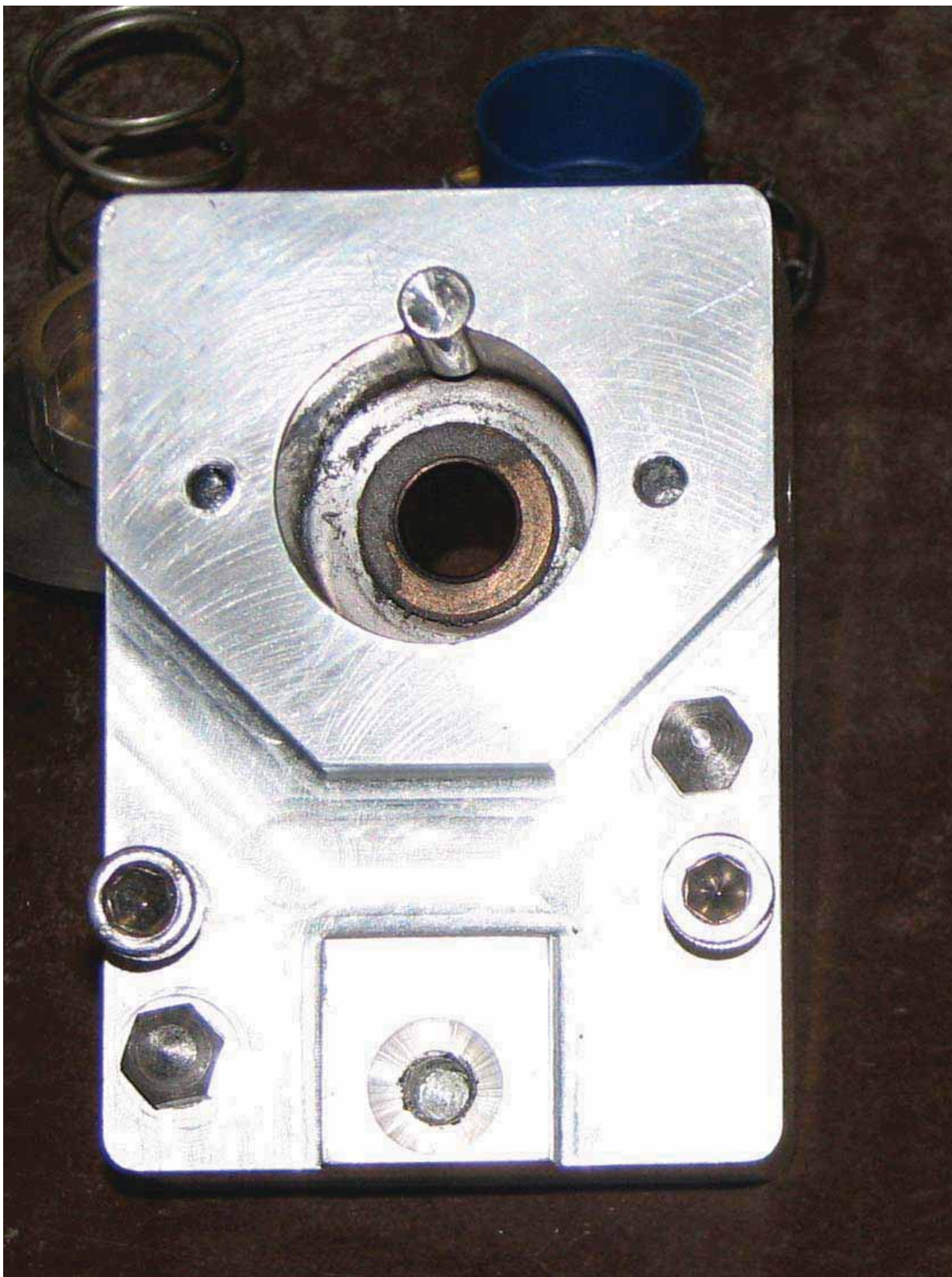


Figure 37: Material Coating the Sampler Surfaces Following Steel Sampling

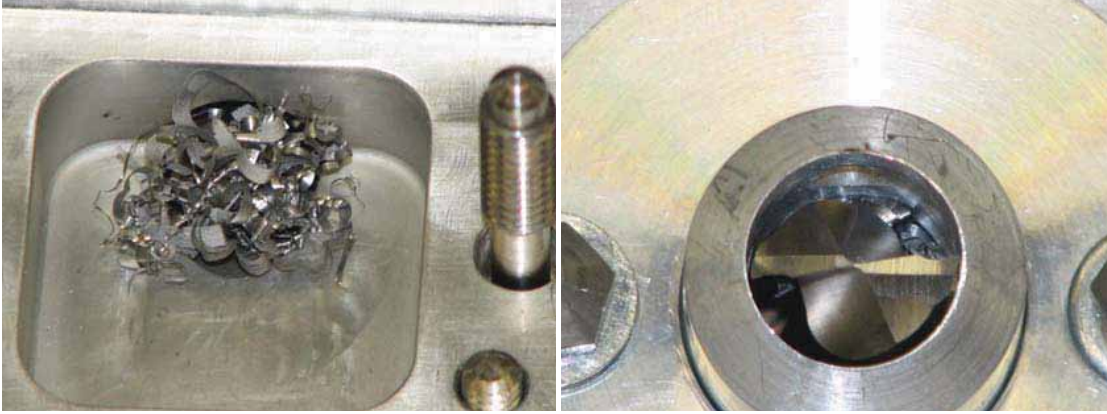


Figure 38: Large Chips Clogged in Drill Cavity

For the filter only collection efficiency, the mass of material collected by the filter only (M_{SF}) was determined by subtracting the pre-test mass of the filter (M_{SF1}) from the post-test mass (M_{SF2}).

$$M_{SF} = M_{SF2} - M_{SF1} \quad (\text{filter only}) \quad (4)$$

For the entire head collection efficiency, the mass of material collected by the entire head (M_{SH}) was determined by subtracting the pre-test mass of the head (M_{SH1}) from the post-test mass of the head (M_{SH2}) and included the mass collected by the filter (M_{SF}).

$$M_{SH} = M_{SH2} - M_{SH1} + M_{SF} \quad (\text{entire head}) \quad (5)$$

4.2.4 Mass of Material Removed from Steel Sample Coupons

The mass of material removed from the polished steel coupons (Figure 39 and Figure 40) was determined by subtracting the post-test coupon mass from the pre-test coupon mass. To duplicate planned sampling operations of sampling in the tanks, two coupons were sampled for each test. Therefore, the mass removed from the coupons (M_C) was the post-test mass of each coupon (M_{Ca2} and M_{Cb2}) subtracted from its corresponding pre-test mass (M_{Ca1} and M_{Cb1}).

$$\begin{aligned} M_{CP} &= M_{Ca1} - M_{Ca2} + (M_{Cb1} - M_{Cb2}) \\ \text{or} \quad M_{CP} &= M_{Ca1} + M_{Cb1} - (M_{Ca2} + M_{Cb2}) \end{aligned} \quad (\text{polished steel coupons}) \quad (6)$$

M_{CP} is the mass removed from the polished steel coupons.



Figure 39: Typical Drilled Steel Sample Coupon

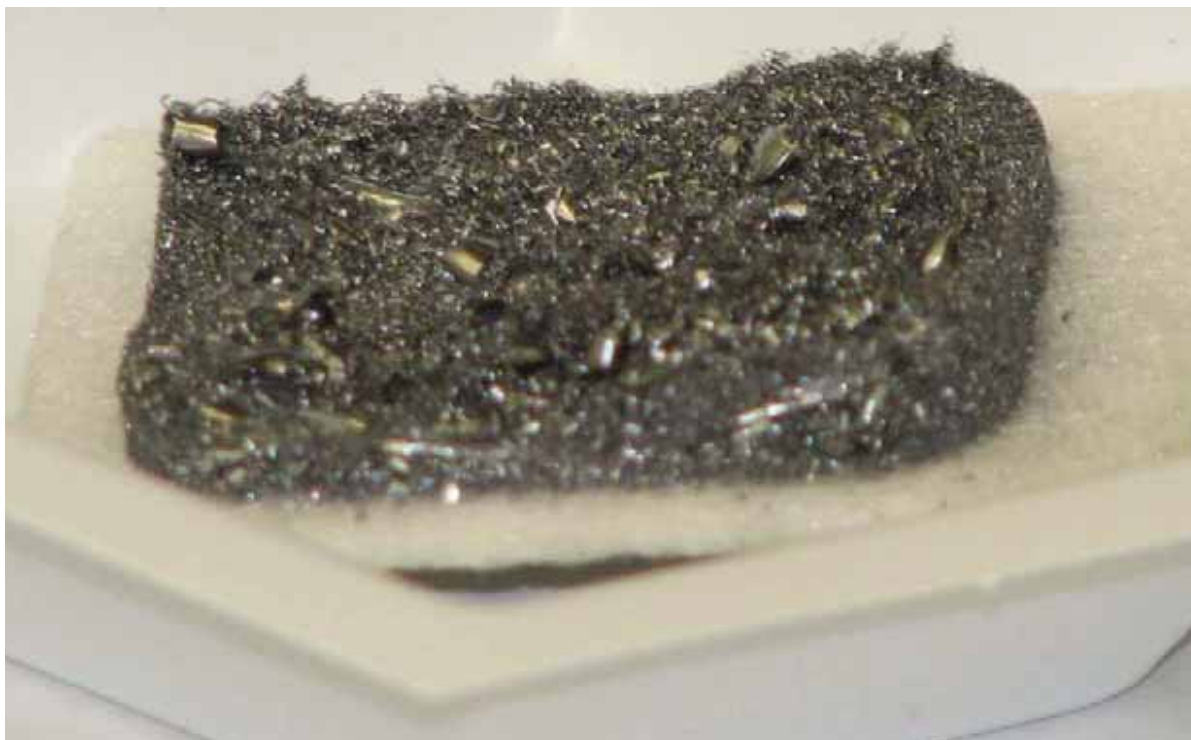


Figure 40: Collected Steel Sample Removed From Sampler

4.2.5 Mass of Material Removed from Salt Sample Coupons

Determining the mass of material removed from the coupons was complicated for those with salt residue. The salt cake was hygroscopic, which made acquiring a stable pre-test and post-test mass difficult. Techniques were developed to minimize liquefaction of salts, and ensure that pre-test weights did not change during measurements. A salt sample liquefying at atmospheric conditions is shown in Figure 41. Another complication with the salt and corrosion/salt coupons arose during initial testing. The salt layer was structurally unstable, and the salt had a tendency to crumble or break apart upon contact. Crumbling and breakage was noticed when the collar contacted the salt layer and while drilling into the steel of the coupon, due to vibrations caused by the bit. Figure 42 shows a Salt + Rust coupon after sampling; a portion of the left side of the salt layer, outside of the collar, broke off during the sample operation. An undamaged Salt sample is shown in Figure 43, and a typical sample collected on a filter is shown in Figure 44, where some of the salt was shown to liquefy and pass through the filter.

Collection efficiencies were shown to be directly related to the mass of the sample collected as compared to the mass of the salt collected: the larger the sample, the greater the efficiency. One implication is that, an excellent efficiency may be obtained by simply increasing the size of the sample collected (i.e. increase drill depth).



Figure 41: Liquefying Salt Sample



Figure 42: Salt + Rust Sample Coupon with Portion of Salt Cake Detached



Figure 43: Undamaged Salt Sample



Figure 44: Collected Salt Sample

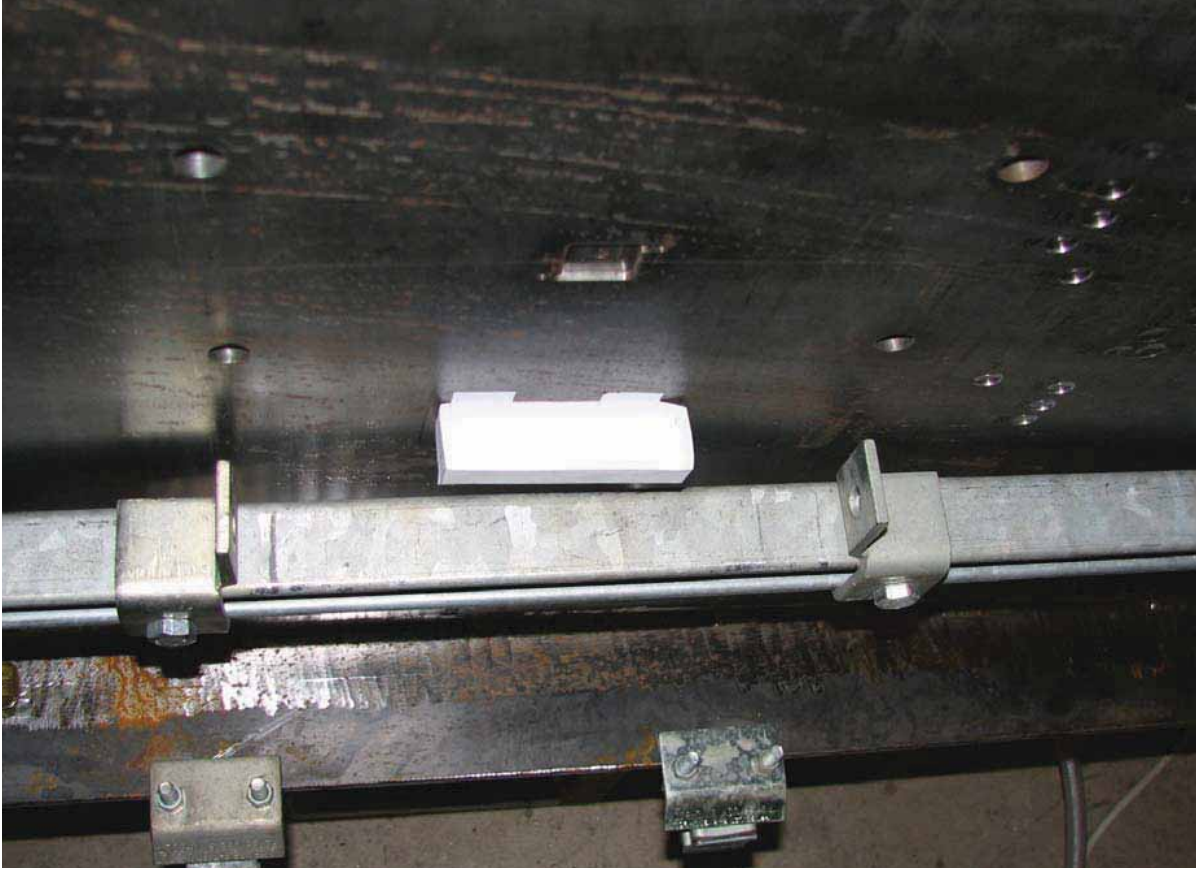


Figure 45: Collection Tray Mounted on EDL Test Plate

The problems associated with structural instability of the salt layer were addressed by different methods. First, a collection tray was attached to the plate directly below the coupons. Any salt material falling from the coupon was caught by the tray (Figure 45). The amount of material that fell into the collection tray was determined by subtracting the pre-test mass of the collection tray (M_{CT1}) from the post-test mass (M_{CT2}). The mass of the material that fell into the collection tray was added back to the post-test masses of the coupons. Therefore, for coupons with salt, Equation 6 yields:

$$\begin{aligned}
 M_{CR} &= M_{Ca1} + M_{Cb1} - [M_{Ca2} + M_{Cb2} + M_{CT2} - M_{CT1}] \\
 &\text{or} \quad \text{(coupons with salt residue)} \\
 M_{CR} &= M_{Ca1} + M_{Cb1} + M_{CT1} - M_{Ca2} - M_{Cb2} - M_{CT2} \quad (7)
 \end{aligned}$$

Second, the operating sequence of a sampling process was changed. During initial testing with salt, some loose material outside of the collar was vacuumed into the head as it retracted from the coupon. This produced a biased result due to the additional material collected. The sequence of operation was changed so that the vacuum and the drill motor were stopped prior to retraction. This allowed loose material outside of the collar to fall into the collection tray during retraction.

Several actions were taken to limit the hygroscopic effects on sampling, and resolve the mass instability issue of the salt coupons. Samples were transported to and from testing in sealed containers. The items with salt (coupons, filters, sampler head, and collection tray) were kept in a desiccator when not used for testing. Trays of desiccant were placed in the enclosure of the analytical balance when the items with salt were being weighed (Figure 46 and Figure 47). Samples were allowed to dry after coupon drilling and before weighing. These practices established and maintained a relatively consistent moisture level of the salt for the weighing process. Also, an uncertainty due to hygroscopic effects was derived from multiple, repeated masses of items with salt and applied to the uncertainty of the collection efficiency (Appendix B).



Figure 46: Sampler Weighing Station



Figure 47: Sampler Weighing with Installed Dessicant

4.3 EDL TEST RESULTS

Collection efficiencies constitute the required EDL test results. Before considering the collection efficiencies, closing comments about EDL sampler operation are provided.

4.3.1 Sampler Operation and Testing at EDL

Much of the sampler operation was discussed above to describe the basic sampler operation. Sampler adjustments were made during testing, which affected material drilling and sampler operating times.

4.3.1.1 Sampler Material Removal

The amount of material removed was affected by the depth of the drilled hole, which was set by adjusting the two cone head screws on the sampler head adjacent to the drill bit. By adding or subtracting shims to the base of two cone head screws, the drill depth was controlled since the sampler is designed to advance the drill bit until the two points touch the wall. The Salt coupons had a drill depth of 0.00 inches, i.e. only the salt cake was removed; and the other coupons had a drill depth of 0.060 inches or 0.125 inches. The 0.0 inch drill depth removed a relatively small amount of material compared to the other coupons, where the mass of sample the sample material was approximately 0.3 grams for salt coupons versus as much as 2.5 grams for the Salt + Rust coupons. Salt collected on the filter had a tendency to liquefy, wick through the filter, as evidenced by observation of the passageway downstream of the filter which revealed very fine particulates of a salt residue.

4.3.1.2 Operating Times for the Sampler

During testing, the sampling time was measured for different materials and operating conditions to establish the completion time for a sample. In addition to monitoring the sampling time, measuring the gap between the cone-head screws, or points, and the plate or coupon was another method to determine when sampling was complete. Sampling was complete when the points touched the plate, and sampling times were initially on the order of 3 minutes or less, and a sampling time of 4 minutes was established to ensure a complete sample. Later, after changing operating parameters and changing the drill-force springs with stiffer springs, the sampling was typically complete in about 1 minute. Even so, a 4 minute operating time was still conservatively recommended to SRR. Occasionally, sampling took longer than 4 minutes due to dulling of the drill bit, and a shallower hole was drilled. Before bits dulled, up to a dozen holes could typically be drilled in the A285 steel coupons or the A36 wall plate, which had comparable hardness. When drilling in steel twice as hard as the A285 steel, only a few holes were drilled per bit, and the bits were significantly dulled after the second hole. The effect of harder steel can be seen in coupons Spare 6 through Spare 11 (Figure 48). A significant amount of drilling data was obtained.

4.3.1.3 Drilling

Drill data was obtained for test coupons and the steel test plate, as shown in Figure 48. The figure shows the drill depth setting and the corresponding actual depth of drilled holes. Since the settings varied from the actual drilled depths, all samplers were tested for drill depths at EDL to ensure that samples were drilled to the correct depths in FTF and T-Area.

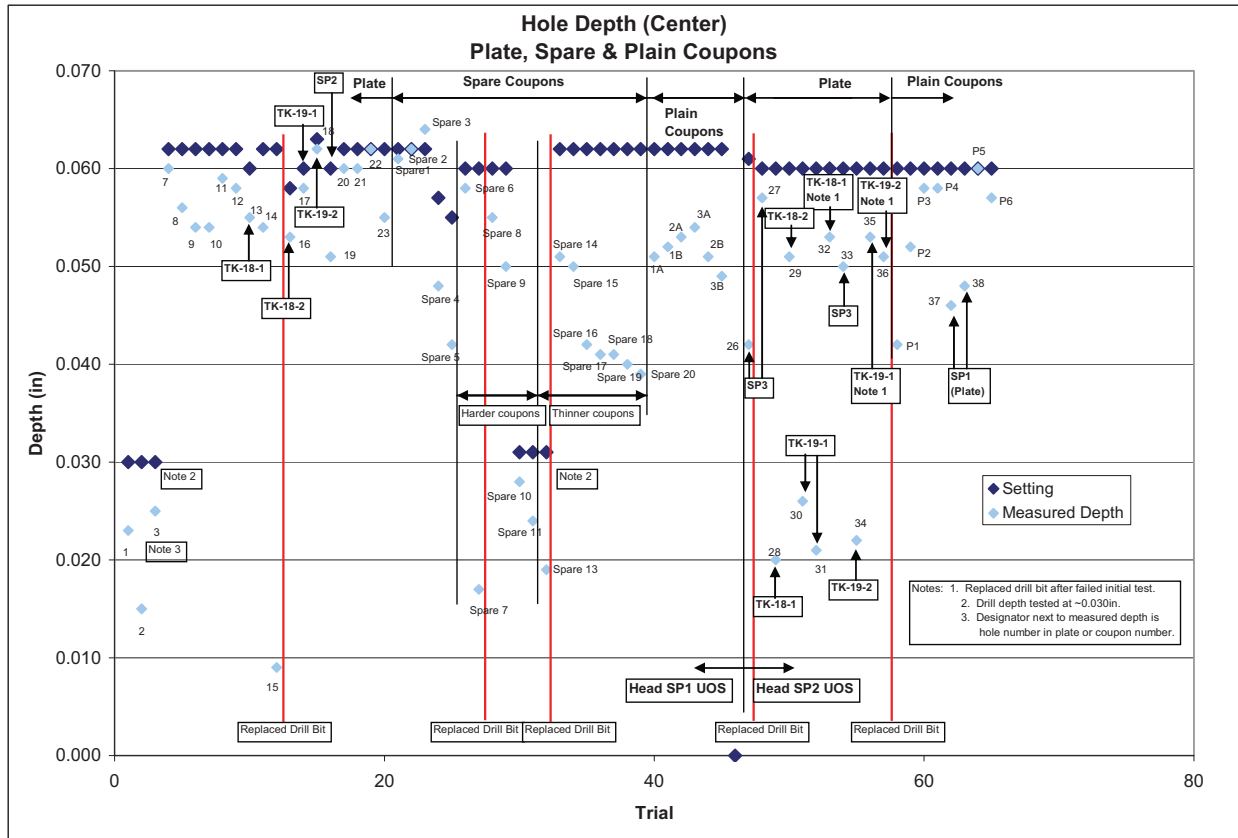


Figure 48: Hole Depths of Samples

4.3.2 Calculated Collection Efficiencies

Collection efficiencies are listed in Table 2 and are graphically depicted in Figure 49. The figure also includes results from initial testing with sample coupons prior to changing the operating parameters. Results are listed in the table from two different calculation procedures. The first calculation procedure determined the efficiency using only the masses of the filter and the collected sample material. The second calculation procedure used the masses of the sampler head, the filter, and the material. From the table, consistently higher efficiencies were calculated from the second calculation procedure. Consequently, EDL endorsed this procedure, and recommendations were followed during SRNL disassembly of all FTF samples to clean out the entire sampler assemblies instead of only the filter cavities of the samplers. Both efficiencies and uncertainties are listed in the table.

The calculated efficiency results strongly reflect material properties. The calculated efficiencies listed in the table reflect instrument uncertainties, and the efficiencies theoretically exceed 100 percent. However, actual efficiencies are limited to a maximum of 100 percent. Consequently, the efficiencies are noted in the body of the report to be limited to 100 %. Then, efficiencies for polished steel ($99.6 \pm 0.4 / - 1.5$ and %, and 99.6 ± 0.4 % / - 2.2 %) were comparable both before and after operating parameters were changed at EDL. The possibility of efficiencies greater than 100 % is due to instrument errors. The salt efficiencies

varied widely ($82.1 \pm 17.1\%$ / -24.9%). High efficiencies were obtained ($99.3 \pm 0.7\%$ / -3.7%) for the Salt + Rust samples, but efforts to specifically evaluate rust capture by the filters or the effects of salt thickness on efficiency were not pursued.

Calculated uncertainties are listed along with collection efficiencies in Table 2. The uncertainty of each individual test was calculated using the tolerances of the respective instruments and, in the case of coupons with salt, included a large uncertainty due to hygroscopic effects. The uncertainty of the average was based on the standard deviation of the three respective tests and also included the instrument uncertainty and hygroscopic uncertainties (Appendix B). Note that the average uncertainties are considerably larger than the individual uncertainties. The increase in uncertainty is due to the small sample population of three tests. The accuracy of the uncertainty could have been increased with a greater number of tests, but the required accuracy requested from SRR was met with three samples. For example, the recommended 95 % confidence level for the three initial steel coupons listed in Table 2 is $\pm 2.2\%$. If only two coupons were tested at EDL, the total uncertainty would have been on the order of $\pm 6.4\%$, assuming a similar distribution of test results. If ten or thirty coupons were used, the uncertainty would have been on the order of 1.2% or 1.1% , respectively. Accordingly, three tests are commonly performed in laboratory testing to achieve reasonable accuracy, while limiting costs.

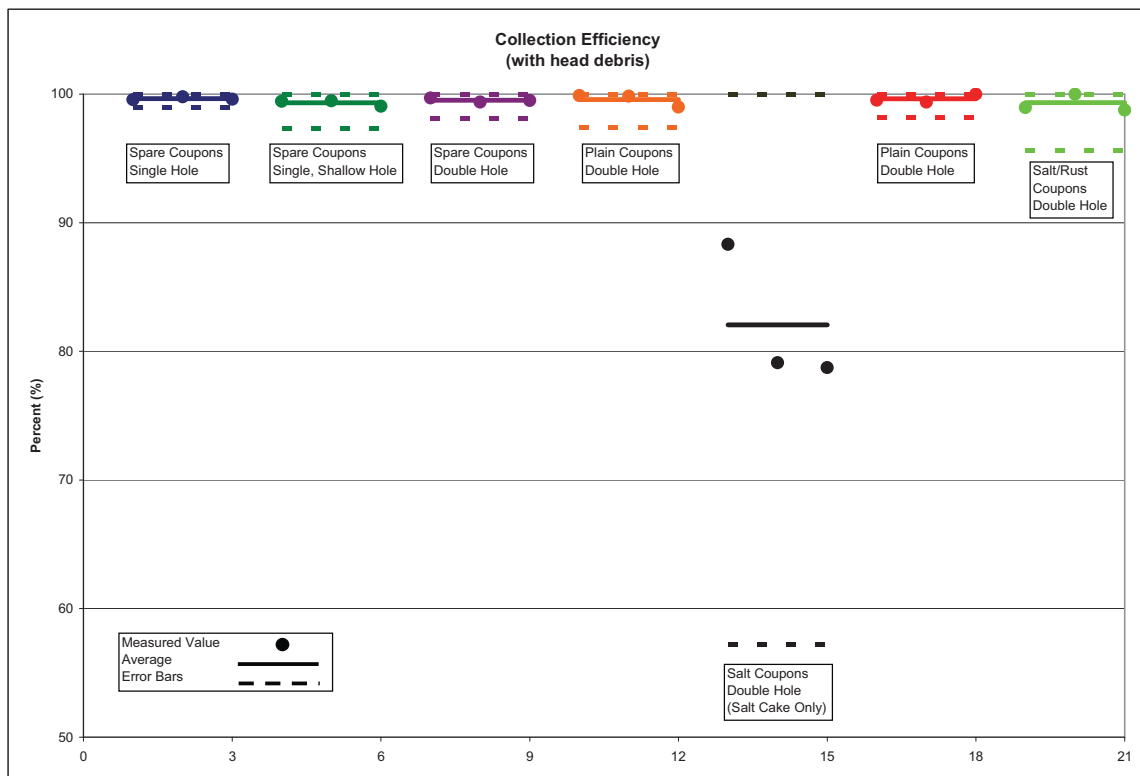


Figure 49: Collection Efficiencies

Table 2: Collection Efficiency Test Results from EDL

Test	Filter and material		Head, filter, and material	
	Collection Efficiency (%)	+/- Uncertainty ¹ (%)	Collection Efficiency (%)	+/- Uncertainty ¹ (%)
Polished ⁶ steel, before changes	98.3	0.2	99.9	0.2
Polished ⁶ steel, before changes	99.0	0.2	99.8	0.2
Polished ⁶ steel, before changes	97.5	0.2	99.0	0.2
Average	98.3	3.2	99.6	2.2
Salt	85.8	8.3	88.3	8.5
Salt	42.4	6.6	79.1	7.8
Salt	74.3	6.5	78.7	6.7
Average	67.5	97.2 ²	82.1	24.9²
Polished steel, after changes	101.0 ³	0.2	99.5	0.2
Polished steel, after changes	71.0	0.1	99.4	0.2
Polished steel, after changes	75.5	0.1	100.0	0.2
Average	82.5	69.7 ⁴	99.6	1.5
Salt + Rust	88.7	0.9	99.0	0.9
Salt + Rust	96.5	0.8	100.3 ⁵	0.8
Salt + Rust	94.6	0.8	98.8	0.9
Average	93.3	17.5 ⁴	99.3	3.7

1. The uncertainty of each individual test included the instrument uncertainty and hygroscopic uncertainty, which was applied only to coupons with salt. The average uncertainty was based on the standard deviation of the three respective tests and included the instrument and hygroscopic uncertainties (as applicable).
2. A large variation in collection efficiencies was evident. The salt coupon tests collected salt only (no metal), which meant a much smaller mass of material collected compared to the other tests. Significant variations in the efficiency were caused by small salt masses compared to relatively large instrument errors, hygroscopic material changes, and lost material through the filter.
3. This efficiency greater than 100% was caused by added material shaved from the ID of the collar surrounding the drill bit. The drill bit cut into the drill collar on only one occasion.
4. The unexpectedly large uncertainty for the second set of polished steel coupons and the Salt + Rust coupons was due to a significant amount of material becoming entangled in the components of the sampler head for a few of the tests.
5. This efficiency greater than 100% was most likely due to cumulative instrument uncertainty.
6. Two polished steel tests were conducted, one prior to EDL operational changes resulting from T-area tests and one after.

5.0 SRR MAST DESIGN AND INSTALLATION

5.1 MAST AND SAMPLER COMPONENTS

The SRR mast design used the EDL supplied sampler and sampler heads. The completed assembly consisted of several major components, shown in figures (Figure 50 and Figure 51).

The installation procedures for Tanks 18 and 19 consisted of numerous steps, related to the equipment. The mast assembly was encased in a flexible plastic sleeve to maintain radioactive contamination control. Although not used in T-Area, the sleeve connected to a yellow plastic hut built for working with the sampler. As the mast was lowered, the sampler was accessed in the hut. The base of the sampler was a 3 inch thick plate designed to cover 23 inch openings at the tank tops, referred to as risers. The vertical mast was raised, or lowered through this plate and fixed in position to obtain required heights for wall samples. A cantilevered arm was hinged at the bottom of the mast, and the controls were connected at the top of the mast. The sampler was positioned near the end of the arm, and was lowered into position using a cable connected to a manually operated winch, which was located above the tank. On the arm the bubble in a leveling device was observed. This device was fabricated from a carpenter's level. When the arm was lowered, the bubble in the level was observed with a remote camera to level the arm to ensure perpendicularity to the wall at either T-Area or FTF. Once the arm was leveled, an air actuated cylinder then guided the sampler along the arm until the electromagnets touched the wall. The mast mounted camera was then used to ensure that the electromagnets were properly aligned before energizing the electromagnets. The level was re-checked, and sampling was performed. To obtain samples, the sampler control system, though different from the EDL control system, performed the same functions as the EDL controls. The SRR control system is shown in Appendix H. A mast mounted camera and a fixed focal length camera mounted to the bottom of the sampler were used to determine that the sample was complete. The recommended time to machine a sample was used to direct the sampling effort, but success was established by simply looking at the wall surface after drilling, i.e., shiny steel was the objective. After collecting a sample, the mast was raised until the sampler head was accessible in the hut. Extended tools were used to disassemble the captive hardware on the sampler head and minimized personnel radiation exposure. The head was then placed in a paint can for transport. The sampler head was then changed to repeat the process for other samples, or the mast was removed from the tank.

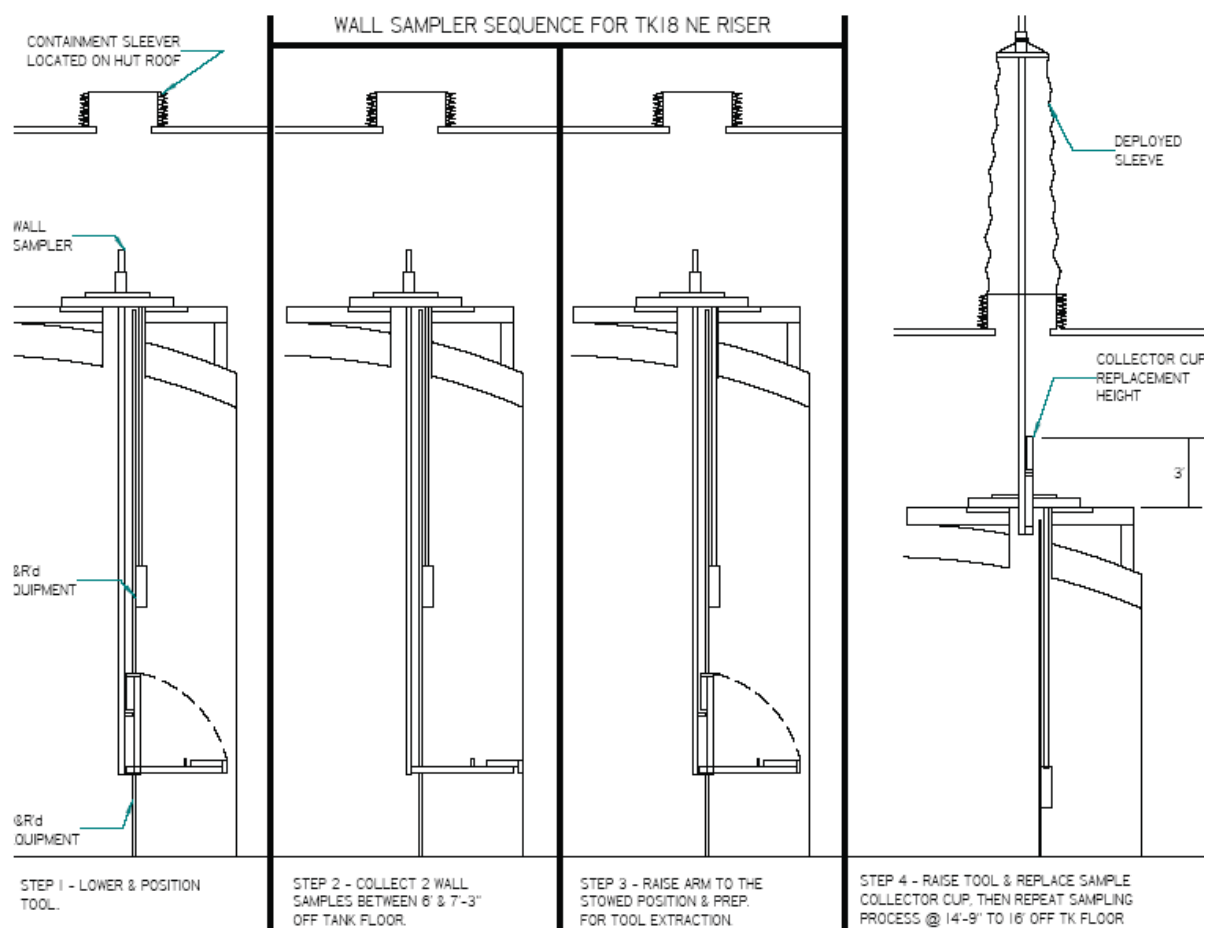


Figure 50: Installation Procedure for Tank 18

(T. France)

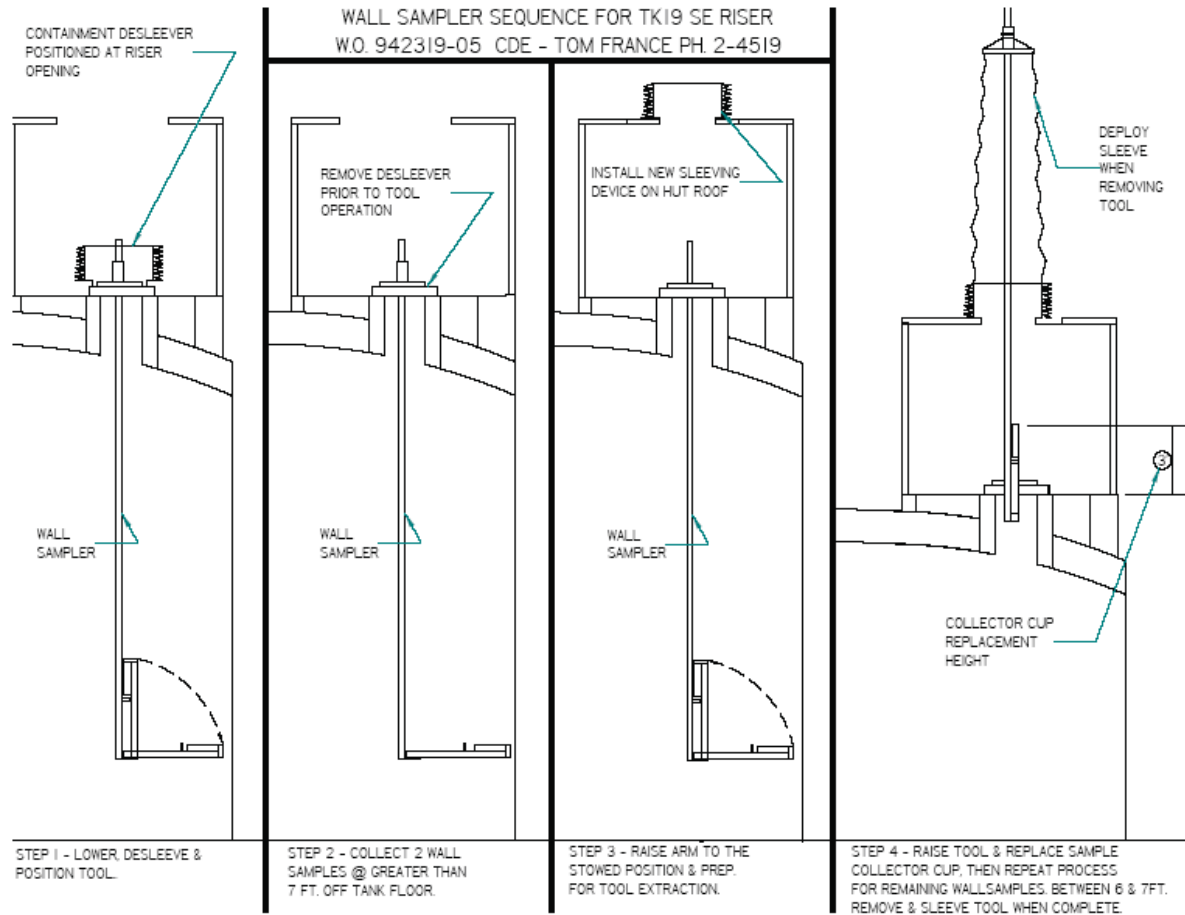


Figure 51: Installation Procedure for Tank 19

(T. France)

5.2 MAST AND SAMPLER EVALUATION IN T-AREA

To ensure sampling success in the waste tanks, the completed mast, sampler, and controls were evaluated at full scale in T-Area. Evaluation consisted of installing the mast by crane through a full scale riser opening, lowering the mast into position, operating the sampler, removing the mast assembly by crane, and removing and packaging a sample. These steps were performed using the same mast mounted camera equipment available to FTF. Other than the huts at the tank tops and contamination concerns, T-Area testing conditions were comparable to FTF. Installation of the assembly in T-Area is shown in Figure 54 through Figure 60. A few minor changes were made to the mast, but it functioned as designed, and workers learned to operate the equipment efficiently before working in FTF. The first holes were successfully drilled in a clean ground surface on the Full Tank wall, (Figure 61). Initial attempts to drill rusted surfaces were ineffective.

5.2.1 Rust Concern in T-Area

The sampler was shown to be unreliable on rusted surfaces, which meant that similar results could be expected in FTF. Typically, only one or two holes could be drilled before the bit became dull and drilling could not proceed. Occasionally, the mast was pushed by hand toward the wall to obtain a sample. In one case, a tested sampler would not drill a hole, and the sampler head was returned to EDL where it successfully drilled a hole in the EDL test plate, using the spare sampler. Also, a standard portable drill successfully drilled holes in the wall in T-Area. EDL investigated and resolved the problem as discussed below.

5.2.2 Resolution of for Sampler Resonance Failure Mechanism

Materials testing and vibration analysis were used to resolve the fact that the sampler would only drill one hole in a rusted surface, and even one hole was not certain. First, hardness testing showed that the hardness of the Full Tank wall was comparable to materials tested at EDL. Portable Vickers hardness testing equipment was used to measure the force on a small striker. This data was converted to Brinell hardnesses, and materials were eliminated as a major contributor to drill bit failure. Following hardness testing, vibration analysis was performed to resolve the problem. The root cause of inadequate drilling was identified as drill bit chattering, induced by the coupling of the resonant frequency of the spring with a critical speed of the motor.

The vibration of the drill motor was measured, the natural frequency of the spring was measured, and the two frequencies were compared to show that the system was resonant. For resonance to occur, one of the natural frequencies of a structural component must be excited by a cyclic force of the same frequency. In this case, the frequency of drill bit chattering due to motor rotation equaled the spring frequency (cycles per second), and the system was unstable. The soft rust material permitted chattering to start at the drill bit tip, and the bit oscillated on and off of the surface, which increased the wear rate of the drill bit. This resonant condition is typically referred to as a motor critical speed.

Although operating at a critical speed was not previously identified, the chattering problems at West Valley, Oak Ridge, and now SRS were clearly related to system resonance of the drill / spring system. The springs were replaced with stiffer springs, which permitted drilling of six holes in the rusted tank wall surfaces in T-Area. Since only two holes were planned to be drilled with each sampler head, this improvement was adequate to move the sampler assembly to FTF. Further improvements to drill bit life could have been made by modifying the drill bits, using a different spring design, or other alternatives, but the design was complete. Holes were successfully drilled in rusted surfaces.

With respect to the critical speed problem for this design, vibration analysis clearly showed that drill bit chatter occurs in some cases for the initial design of the Tanks 18 and 19 wall sampler. Changing the spring increased end mill bit life during testing by reducing resonance. Figure 52 shows vibrations for drilling a hole, where expected vibrations occurred at multiples of running speed at approximately 485 rpm (cpm, cycles per minute). The lower frequency rubbing vibrations due to drilling are seen at the left of the figure. Some minor

vibrations at multiples of one times running speed are observed, which were due to normally expected vibrations due to motor rotation. Of interest to chattering, vibrations at multiples of two times running speed ($f = 485 \text{ rpm} \cdot 2 = 970 \text{ cpm}$, cycles per minute) occurred, which are the result of chattering, or tapping, of the two drill bit flutes during each revolution. In T-Area drilling of rusted surfaces, the springs were also observed to vibrate excessively at higher mode frequencies during chattering.

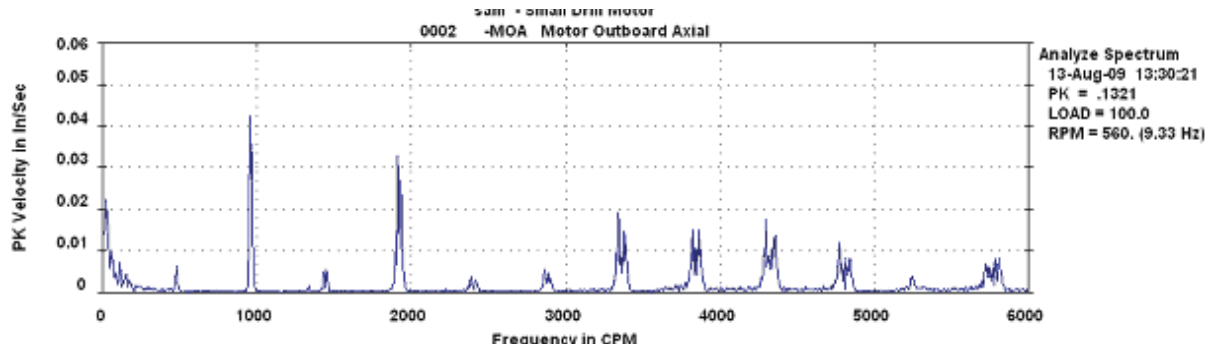


Figure 52: Motor Vibration Before Spring Change

To determine modal frequencies, the first mode was measured by hanging a weight on each spring, letting the weight drop, and counting the vibration cycles. First mode frequencies, f_i , were identified as approximately 120 cpm and 180 cpm for the two springs; McMaster - Carr, 94135K44 and 94135K46 respectively. Higher mode frequencies were calculated from $f = (i) \cdot (\text{first mode})$, where i equals the mode and f equals the frequency.

The resonant condition is described by Figure 53. In the figure transmissibility is shown, which is described in detail in Appendix E. Appendix E develops new vibration theory to explain the sampler resonance problem, where Figure 15 of the attached paper is the basis for Fig. 53. In this case, the transmissibility shows the amplification of vibration due to chattering. The effects of replacing the spring are also shown in the figure. To use the figure, f/f_i is required, where $f/f_i = \text{critical speed} / \text{natural frequency}$. For the original spring, the frequency equals $f/f_i = 970 / 120 = 8.08$. Assume damping of $\zeta = 0.005$, which is a typical minimum for springs. Then, the transmissibility is read directly from the figure as 56.8. This value means that any vibration at the drill bit tip is multiplied by a factor of 56.8, or more.

For the replacement spring, the relationship between the two springs is required, and this relationship is defined by the spring equation, and the transmissibility, TR , equation

$$F = -k \cdot x \quad (8)$$

$$TR = x_{max} \cdot k / F \quad (9)$$

where k is a spring constant, x is the deflection, x_{max} is the maximum deflection, and F is an applied force. Per manufacturer's data, the original spring deflects 5.75" for a 21.39 pound force, and the spring operated with a 5" deflection on the sampler. The replacement spring deflects 5.50" for a 37.13 pound force, and operated with a 7" deflection. To use the figure, a ratio of spring constants is required. Using the above data,

$$\frac{k_1}{k_2} = \frac{x_1 \cdot F_2}{F_1 \cdot x_1} = \frac{\frac{5}{5.75} \cdot 21.39}{\frac{6}{7} \cdot 37.13} = 0.5844 \quad (10)$$

A second transmissibility curve is generated by multiplying 0.5844 (Equation 10) times the original spring response curve to obtain the replacement spring response curve in the figure. Using $f/f_i = 970 / 180 = 5.39$, the transmissibility is read directly from the figure as 8.3. Accordingly, the transmissibility was decreased from 56.8 to 8.3; a factor of 684 %. The forces induced during chattering were reduced by a factor of more than six.

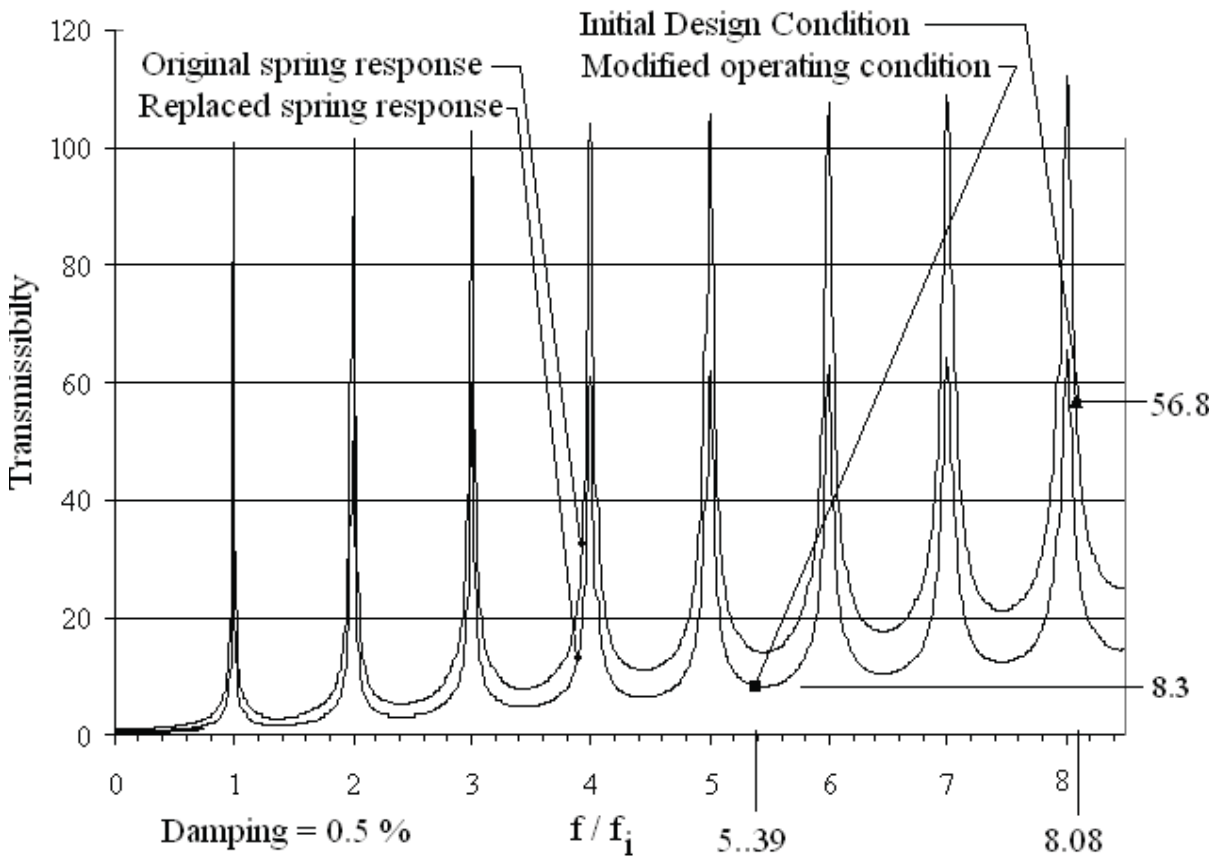


Figure 53: Sampler Resonance

In other words, the soft layer of rust permitted the start of chattering and the interaction of the chattering with the resonant spring caused the spring to resonate as observed by excessive vibrations during sampler operation. The increased surface area in contact with the drilled material increased the force on the bit to initiate chattering. The spring vibration in turn exaggerated chattering and rapidly dulled the tip of the bit to reduce the number of drilled holes. On unrusted plates, 10 - 12 holes were drilled with a single bit before getting dull. Bits that would not drill a rusted plate were later found to easily drill an unrusted plate. The unique test results were explained through resonance.

The replacement spring decreased resonance affects and increased the number of drilled holes. Changing the relief angle on the drill bit also improved drilling, but was not fully investigated. West Valley noted that changing the drill bit point angle also improved performance. Replacing the spring resulted in successful drilling of six holes in steel, which concluded testing. Testing at T-Area also concluded that the sampler does not operate properly near 100° F, which were well above the expected tank temperatures during testing. Heating of components may have loosened parts, and decreased damping, thereby increasing resonant effects. Vibration data was not collected after the springs were replaced. Again, further investigation was not pursued, since the sampler drilled half a dozen holes at expected design conditions.

Recommended improvements to minimize drill bit chattering are to further investigate drill bit relief angle and drill point angle effects, increase the spring force, and install damping to lower the resonant response of the sampler. Drill changes seem to be the most promising recommendation. The springs could be eliminated, but low frequency resonant vibrations from the mast would then couple to the sampler and affect chattering. A stronger electromagnet can be used to improve drilling of thick materials on the tank walls, but significant increases in force are limited by the size of the electromagnets with respect to the riser opening in the tank top.



Figure 54: Sampler Lowering into a Simulated Riser Opening



Figure 55: Sampler Passing Through a Simulated Riser Opening

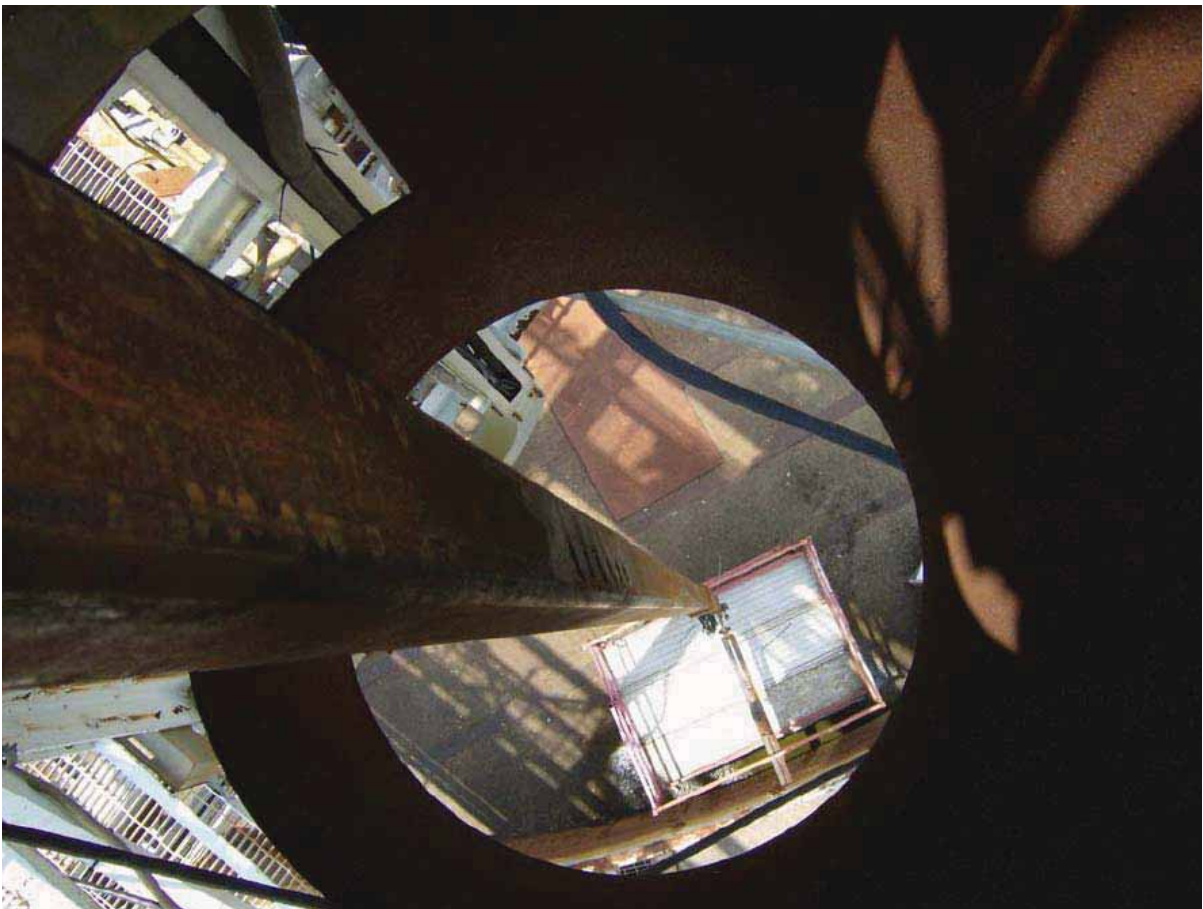


Figure 56: Plan View of Installed Sampler in T-Area



Figure 57: Mounting Plate and Mast in T-Area



Figure 58: Mast Arm in Vertical Position



Figure 59: Mast Arm in Leveled Position



Figure 60: Sampler Attached to Wall in T-Area



Figure 61: Samples at T-Area on an Unrusted Surface

5.3 MAST AND SAMPLER INSTALLATION IN FTF

The mast assembly was lowered by crane into the two tanks until the desired sampling elevations were reached in each tank. FTF engineering established the recommended elevations to acquire representative samples for characterization of the activity in the tanks (Table 3). Sampler operations were similar to those performed in T-Area, but an additional video camera was installed in other tank risers to provide an overall view of the mast and sampler. Photos of sampler installation above and inside the tank are shown in Figure 62 through Figure 65.

Table 3: Elevation Requirements for Tank Samples

Sample requirement	Tank 18, Upper	Tank 18, Lower	Tank 19, Upper	Tank 19, Lower
Elevation from tank bottom, ft	>15	6 - 15	>7	6 - 7



Figure 62: Mast and Sampler Installation in Tank 19



Figure 63: Mast and Sampler Installation in Tank 19

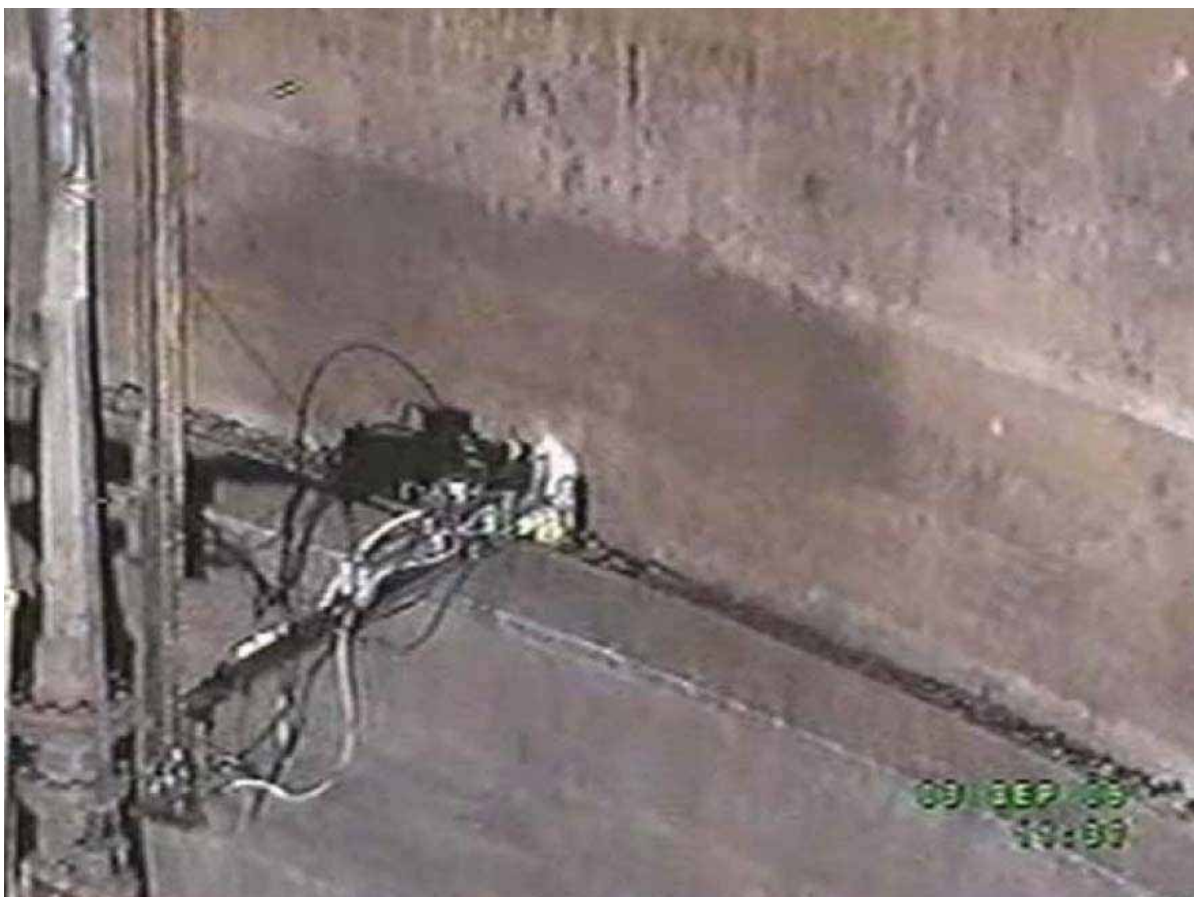


Figure 64: Sampler Installed in Tank 18, Upper Sample



Figure 65: Close-up of Sampler Installed in Tank 18

6.0 FTF SAMPLING RESULTS

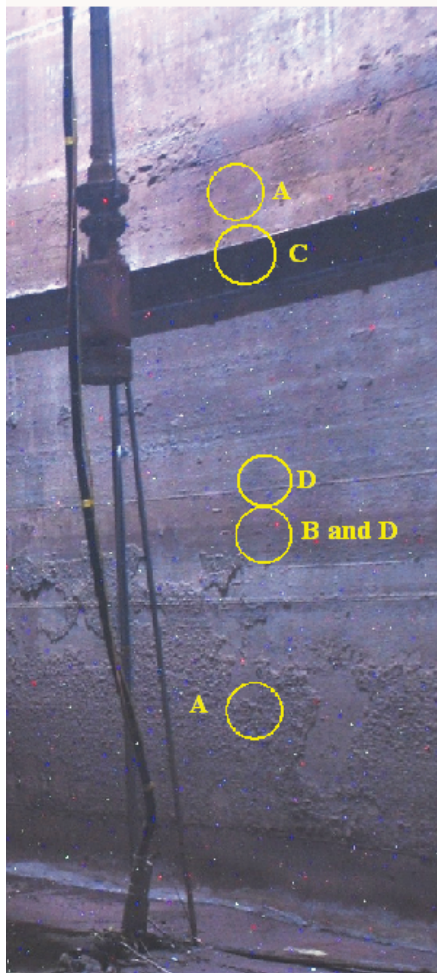
6.1 FTF SAMPLING

Samples were obtained below the Northeast riser in Tank 18 and Southeast riser in Tank 19. The performance of the sampler varied between Tank 18 and Tank 19. Even so, samples were collected from each tank at the required elevations. Results that completely fulfill sampling requirements are referred to as the Tank 18 upper sample, Tank 18 lower sample, Tank 19 upper sample, and Tank 19 lower sample. One of the sample attempts provided negligible sample material, and is listed in the table as the second sample attempt. Performed testing is summarized in Table 4, Figure 66 and Figure 67. These test results are discussed below.

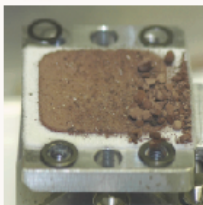
Table 4: Tank 18 and Tank 19 Test Summary

Sampler Head Number	Tank	Elevation from tank floor ft	Drill time, min	Rad rates, @ 2" mrem, extremity	Figure number	Date	Results
TK 18-2	18	19' 8-7/16"	0.17	2000	Figure 80	9/2	Scale sample: Brown material, 1/16" – 1/8" diameter stone shaped material, similar to dried clay. Two shallow holes and some chips from the waste on the wall. One shallow hole appeared black at the bottom of the hole.
		6' 3"	2				
		6' 6"	5				
		6' 9"	4.5				
		7' 0"	6				
SP3	18	10' 3-7/16"	4	---	Figure 82	9/3	Second sample attempt: Two small waste chips removed. Negligible material.
		9' 9-7/16"	13				
TK 18-1	18	17' 0"	8	1500	Figure 68 Figure 84	9/3	Tank 18 Upper sample: Bare metal on one hole. Exposed corrosion in the bottom of the second hole. Reddish brown dust like material and some metal chips.
		17' 1"	0.82				
SP4	18	10' 7/16"	10.5	4000	Figure 70 Figure 72 Figure 89	9/24	Tank 18 Lower sample: Bare metal on one hole, black crystalline material and some metal chips, small chip on second hole. Drill depth was changed to 0.125".
		11' 6-7/16"	24				
TK19-1	19	7' 3"	4.32	13	Figure 74	10/7	Tank 19 Upper sample: Two complete holes drilled, numerous metal chips.
		8' 0"	4.45				
TK 19-2	19	6' 9"	4.43	37	Figure 90	10/7	Tank 19 Lower sample: Two complete holes drilled, numerous metal chips.
		7' 0"	4				

Tank 18 Northeast Wall
Approximate sample locations



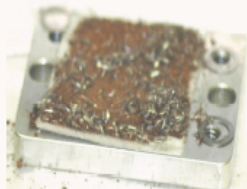
Sampled solids
on collection filter



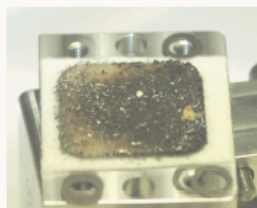
A. First sampler attempts



B. Second sampler attempts



C. Tank 18 upper samples

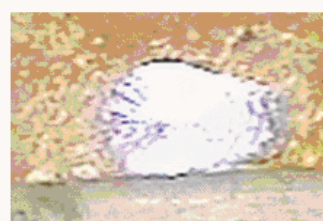


D. Tank 18 lower samples

Material removed
from wall



B. Failed attempt with second sampler



C. Completed upper samples

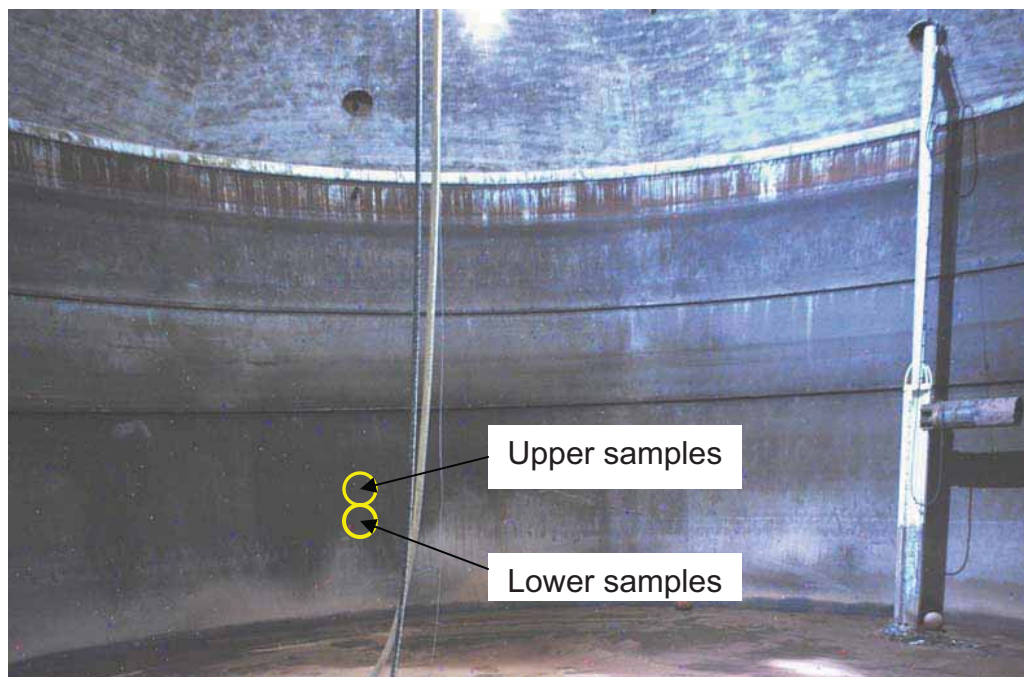


D. Completed lower samples

Figure 66: Tank 18 Wall Sampling Results

Note: Location C is above the stiffener.

Tank 19 Southeast riser, Approximate sample locations



Upper samples

Lower samples

Sampled metal on collection filter



Material removed from the wall



Figure 67: Tank 19 Wall Sampling Results

6.1.1 Tank 18 Samples

In Tank 18, at least one sample was obtained at each of the required elevations, and sufficient material was collected for SRNL analysis. The walls were not pressure washed, and accumulated waste on the walls prevented the electromagnets from operating properly. Several samples were collected.

For the scale sample, material was collected at several locations, and most of the material was collected between 6 feet and 7 feet, where the scale thickness appeared to be about 3/8 inch thick. The scale sample was the first sample to be collected using the sampler.

The second attempt failed to collect an adequate sample.

When the upper sample was collected, the sampler and arm were wedged between the tank wall and an abandoned transfer pump, as shown in Figure 64. When the sampler was operated to collect the upper sample, a large vibration response due to drill bit chattering shook the sampler between the wall and the transfer pump. The effects of resonance had been reduced, but not eliminated. The sampler would have vibrated with forces many times higher if the spring design had not been changed, and a sample would not have been collected. Even so, a sample was ground from the wall steel surface as the drill bit scraped horizontally along the tank wall.

For the lower steel sample, the sampler did not initially collect material. The mast was shaken at the tank top, and the drill bit scraped down along the wall and ground off a sample, which included surface steel from the tank wall.

6.1.2 Tank 19 Samples

In Tank 19, the walls were cleaned by pressure washing and the sampler drilled holes as expected. Two holes were drilled with each of two samplers and the samplers were transported to SRNL.

The only concern with respect to sampling occurred when the arm of the mast was inadvertently lowered to a vertical position during the Tank 19 lower sample, and chips could have fallen from the sampler drill opening. One sample hole was drilled for the sampler head, and the arm was lowered while raising the mast before the second hole was drilled. To determine if metal chips could have fallen from the drill opening, one of the actual sampler heads full of radioactively contaminated metal chips was demonstrated to retain chips after delivery to SRNL. The sampler head was vigorously struck with a screw driver with the drill opening facing downward, and no chips fell from the sampler. The magnetic properties of the chips prevented any material loss from that sampler head.

To complete the FTF experimental results, discussions follow to consider surface area calculations which provide a description of the sampler performance in the tanks, a discussion to describe sampler materials delivered to SRNL for activity analysis, and finally a concise summary of the FTF sampling.

6.2 SURFACE AREA ESTIMATES FOR TANK 18 AND TANK 19 WALL SAMPLES

The sampler design used for obtaining wall samples for these two tanks was successful in both Tank 18 and Tank 19 for collection of material down through coatings and corrosion to steel surfaces. In Tank 19, two ½ inch diameter by 1/16 inch deep holes were drilled into the wall for each of two sampler heads: a total of four holes. The surface area for each sampler equals the area of two 0.500 + 0.020”-0.000” diameter holes, based on the fact that laboratory testing showed that all holes drilled with the sampler were within these tolerances. Pairs of samples were taken above and below 7 feet in Tank 19. In Tank 18, holes were not drilled at all, but instead the sampler drill bit scraped, or ground, material down to bare steel on the tank wall. Although more than one sampling was attempted at the upper and lower levels, only one sample attempt at each level collected wall material down to bare steel. Additional material was removed from the wall and collected in the sampler heads, but its volume cannot be calculated, and was conservatively neglected here. That is, only the area of exposed steel was used here to conservatively estimate surface areas. Surface areas were estimated to determine the activity (μ Curies) per unit area for the sample areas only.

The Tank 18 surface area estimate is conservative since the use of a smaller surface area increases the prediction of total activity per unit area. That is, the radioactive material collected in the Tank 18 sampler heads was collected from a larger surface area than the surface areas provided in this report, and consequently any activity calculated using the material collected in the sampler and this surface area will yield a higher activity per unit area, which may be conservative by as much as 75%, or more, in Tank 18. Inspection of the lower Tank 18 sample in Figure 71 shows that the exposed steel area is nearly ¼ of the total area machined by the sampler. Considering the fact that a second hole was also attempted with the sampler head, the 75% estimate is reasonable. Inspection of the upper Tank 18 sample shows that the calculation error is probably much less than 75%, but the error cannot be determined since the amount of material scraped from the wall outside of the bare metal area is undetermined as is the material collected at the second drill site. In short, surface area calculations were based on minimum calculated areas. For the Tank 18 upper samples, the calculated surface area exceeded 0.196 in² (0.00136 ft²), and for the Tank 18 lower samples, the surface area exceeded 0.063 in² (0.000437 ft²).

In Tank 19, the calculated areas were in the range of 4% less than actual surface areas. This error is based on the errors observed in testing at EDL, where test holes varied in size due to wobbling of the drill bit in the sampler head. The surface area for the upper samples was 0.393 in² (0.00273 ft²), and the surface area for the lower samples was the same, 0.393 in² (0.00273 ft²). Billy West (Certified Visual Testing Level II, ASNT SNT-TC-1A, ANSI/ASNT Cp-189-2001, and NAS 410), who performs SRR camera and video inspections and evaluations for waste tanks, reviewed the draft calculation area estimates, and agrees with the surface area estimates for the wall samples collected from Tank 18 and Tank 19.

6.2.1 Tank 18 Wall Samples

Surface areas were required for Tank 18 samples at both the upper and lower sample elevations. Those calculated areas follow.

6.2.1.1 Tank 18 Upper Wall Samples

This conservative surface area estimate considered only one of the sample attempts, which is shown in Figure 68. Figure 69 shows a small chip collected for the second sample. The only discernable dimensions in the photo are the widths of the stamped characters in the sampler head and the vertical diameter of the ground area. The character widths (No. 8, letter punch) vary from 0.200 – 0.250 “depending on the stamping depth. The vertical diameter equals the ½ inch diameter drill bit hole, which was measured during numerous EDL (Engineering Development Lab) shop tests to vary between 0.504 and 0.520 inches, where the minimum hole diameter could be 0.500”, depending on wobbling of the drill bit in the sampler head. The character size can be used to scale the size of the cleared area. The slight ridges of material at the edges of the ground area are caused by the squared edge of the drill bit. These deductions demonstrate that the vertical dimension of the ground area equaled, or exceeded ½ inch diameter. The cleared area was nearly 11/16 inch long, but the shadowed areas on the steel surface were chatter marks from the drill, which may contain corrosion products or waste on the surface. Since the shadowed areas were indiscernible, only the shiny steel surfaces were considered. Consequently, the surface area was estimated as the area of a ½ inch diameter circle, such that

$$\text{Surface_Area}(\text{Tank_18_upper}) = \frac{\pi \cdot 0.500^2}{4} = 0.196 \text{ in}^2$$

Also note that a scarred area about ¾ of an inch to the left of the bare steel may be the beginning of sampling, when the sampler started to vibrate between the wall and transfer pump. Additional material may have been collected by the sampler as it moved along the tank wall.



Figure 68: Tank 18 Upper Sample, Steel Removed from the Wall

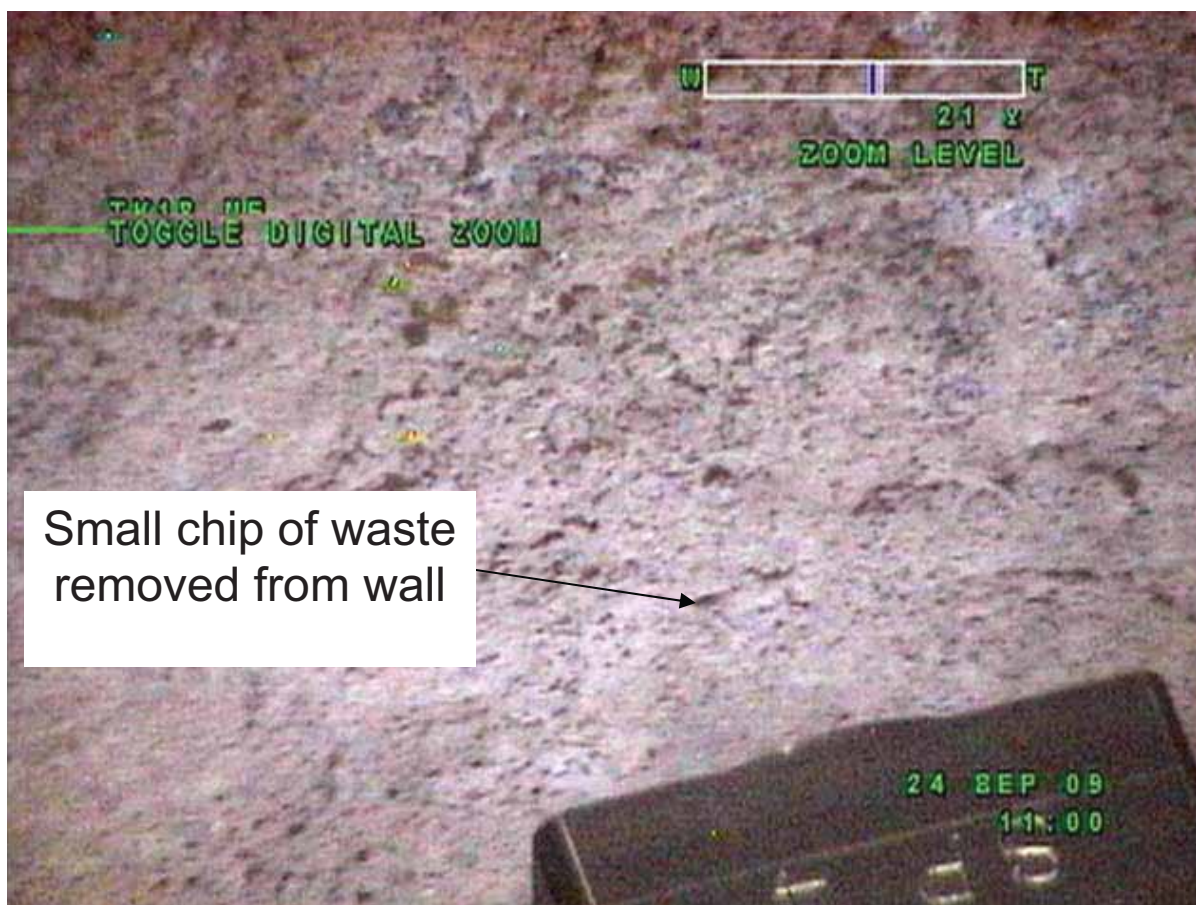


Figure 69: Tank 18 Lower Sample, Small Chip of Waste Removed from the Wall

6.2.1.2 Tank 18 Lower Wall Samples

Again, only one sample attempt was conservatively calculated here, since only one sample exposed a shiny steel surface on the tank wall, as shown in Figure 70 and Figure 71. Figure 72 shows the second hole, which was drilled down to the corrosion layer, as indicated by the dark spot at the bottom of the hole where the color change from light to dark indicates the interface of two different materials. Figure 73 shows the approximate surface area of the hole. For this figure, the exposed steel diameter was smaller than the drill bit diameter, and the only reference dimension was the stamped character height on the sampler head (No. 4 letter punch). Again, measured dimensions for these punches vary between 0.200 and 0.250 inches, depending on the depth of the punch. Conservatively assuming that the character is 0.200 inches, the exposed steel area slightly fills more than half of a 0.400 inch diameter circle. Material removed from the surface above the exposed steel was also conservatively neglected, since the amount of material cannot be quantified. Then,

$$\text{Surface_Area}(\text{Tank_18_lower}) = \frac{\pi \cdot 0.400^2}{4 \cdot 2} = 0.063 \text{ in}^2$$

During this lower sampling, the mast was moved horizontally at the tank top, the drill bit moved down the wall, and then collected the sample to bare metal.



Figure 70: Sampler Head and Tank 18 Lower Sample Area



Figure 71: Tank 18 Lower Sample Area

(Same as Figure 70, but without sampler head)



Figure 72: Partially Drilled Hole at Upper Level in Tank 18



Figure 73: Dimensioned Tank 18 Lower Sample Area

6.2.2 Tank 19 Wall Samples

Since holes were completely drilled in Tank 19 as shown in Figure 74 and Figure 75, the surface areas were calculated directly from the diameters of the drilled holes, which were noted to equal 0.500 – 0.520 inches. Both the upper and lower samples each contained material from two drilled holes and the total surface area for collected material therefore equaled

$$\text{Surface_Area}(\text{Tank_19_upper}) = \text{Surface_Area}(\text{Tank_19_lower}) = 2 \cdot \frac{\pi \cdot 0.500^2}{4} = 0.393 \text{ in}^2$$



Figure 74: Typical Drilled Hole in Tank 19



Figure 75: All Four Drilled Holes in Tank 19

6.3 SAMPLER MATERIAL COLLECTION FOR TANKS 18 AND 19

After delivery to SRNL, all sampler heads were disassembled and carefully cleaned to ensure that all material was collected for analysis. A delivered sampler head, and initial disassembly is shown in Figure 76, Figure 77 and Figure 78. In Tank 18, sample material thicknesses varied from 1/16" to approximately 3/8" during testing, where the exact thickness was not determined. In Tank 19, material was not observed on the tank walls. Sample results varied for each sampler head.

Five discrete locations were sampled for the Tank 18 scale sample, and two locations were selected for each of the other samples. The Tank 18 scale sample collected a material which looked like small, reddish brown, dried clay like, pebbles about 1/8 of an inch in size. The dust from this sample was easily cleaned from the sampler head surfaces (2000 mRem extremity) (Figure 79 - Figure 81). Although this sampler head was used at multiple locations at both higher and lower sample elevations, and the collected sample is referred to as the scale sample. The second sample attempt collected negligible material even though chips appeared to be removed from the waste during sampling (Figure 82 and Figure 83). The Tank

18 upper sample collected steel chips from machining the surface and also collected a fine, brown, dust like material (1500 mRem extremity), which could not be brushed from the sampler head surfaces and (Figure 84 - Figure 86). More material than usual passed through the filter for this sample. Figure 80 shows material being cleaned downstream of the filter. For steel testing, filters were noticed to be stained on the downstream side of the filters due to incomplete filtering, but particles did not accumulate downstream. This sample indicated that particle size may affect filter efficiency. Further investigation was not pursued. The Tank 18 lower sample collected a small amount of black, dust like, perhaps crystalline, material in addition to some steel chips machined from the surface (4000 mRem extremity) (Figure 87 - Figure 89). In other words, the material was visually distinct in each sample. Also, negligible extremity radiation rates were expected from the corrosion layer, and dried waste on the tank wall surfaces varied up to perhaps 3/8 inch or more at different wall locations. While holes were not properly drilled like those drilled at EDL and T-Area, Tank 18 sampler heads clearly collected corrosion products from the tank wall. Sampling occurred on several days over several weeks in FTF.

In Tank 19, two holes were drilled with each sampler head (13 and 37 mRem extremity), and samples were machined similar to EDL test results (Figure 90 and Figure 91). All Tank 19 sampling was completed in less than a day.

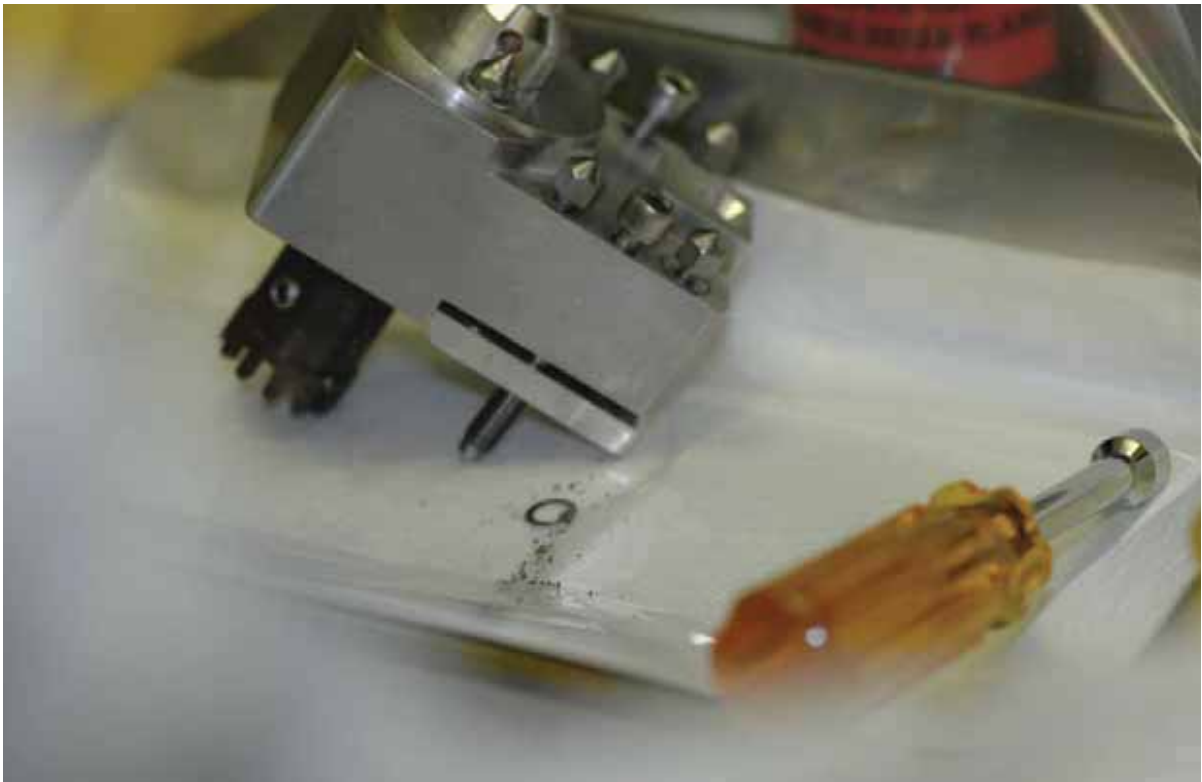


Figure 76: Delivered Sampler Head

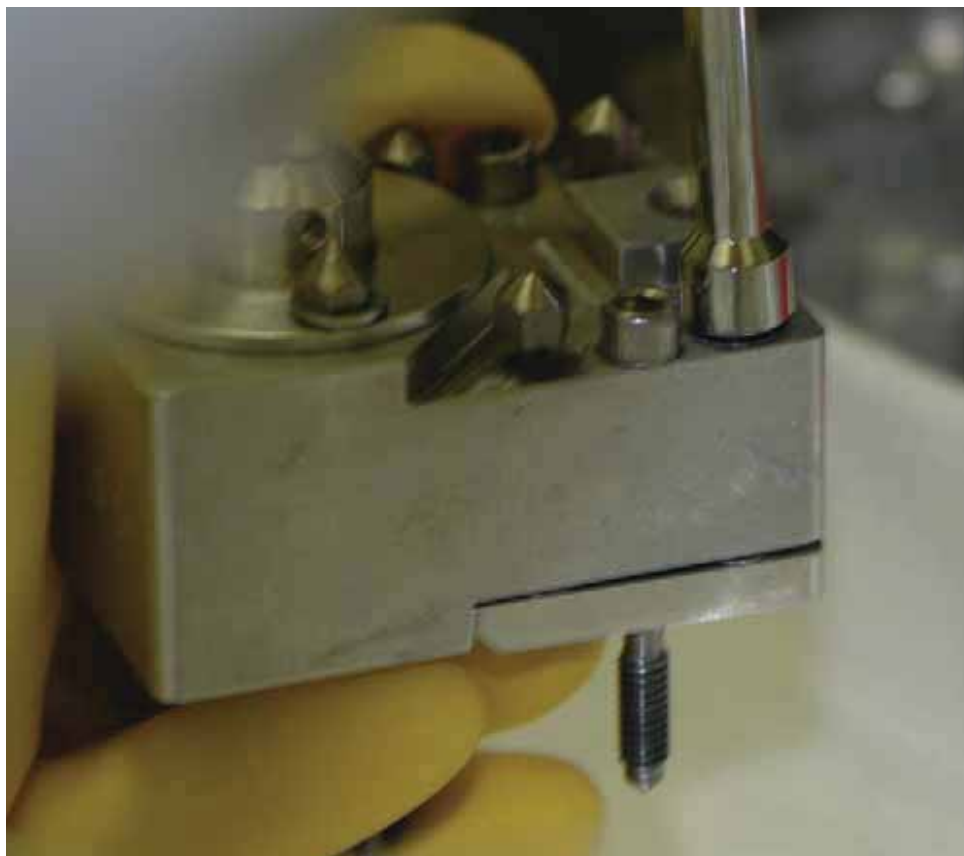


Figure 77: Sampler Head Disassembly



Figure 78: Disassembled Drill Collar

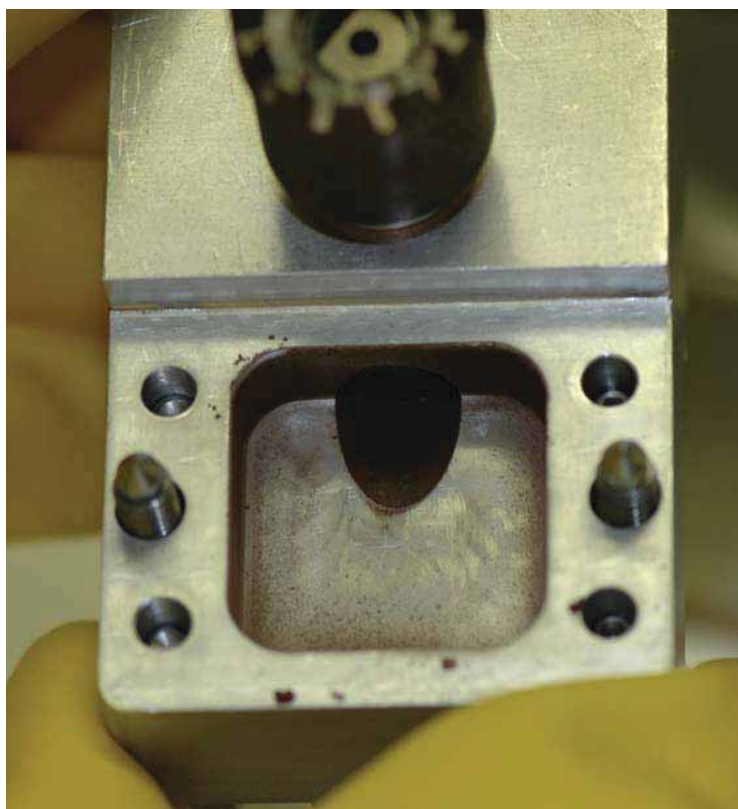


Figure 79: Filter Cavity, Tank 18 Scale Sample, TK 18-2



Figure 80: Collected Material, Tank 18 Scale Sample, TK 18-2



Figure 81: Drill Cavity, Tank 18 Scale Sample, TK 18-2



Figure 82: Collected Sample, Second Tank 18 Sample Attempt, SP3



Figure 83: Drill Cavity, Second Tank 18 Sample Attempt, SP3

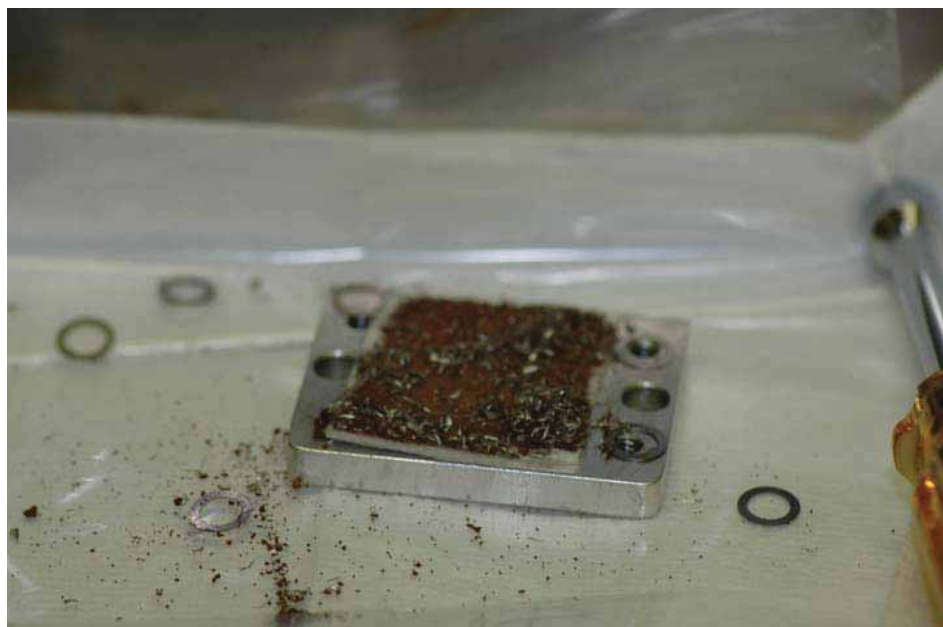


Figure 84: Collected Sample, Final Tank 18 Upper Sample, TK 18-1



Figure 85: Filter Cavity, Final Tank 18 Upper Sample, TK 18-1



Figure 86: Filter Plate, Final Tank 18 Upper Sample, TK 18-1

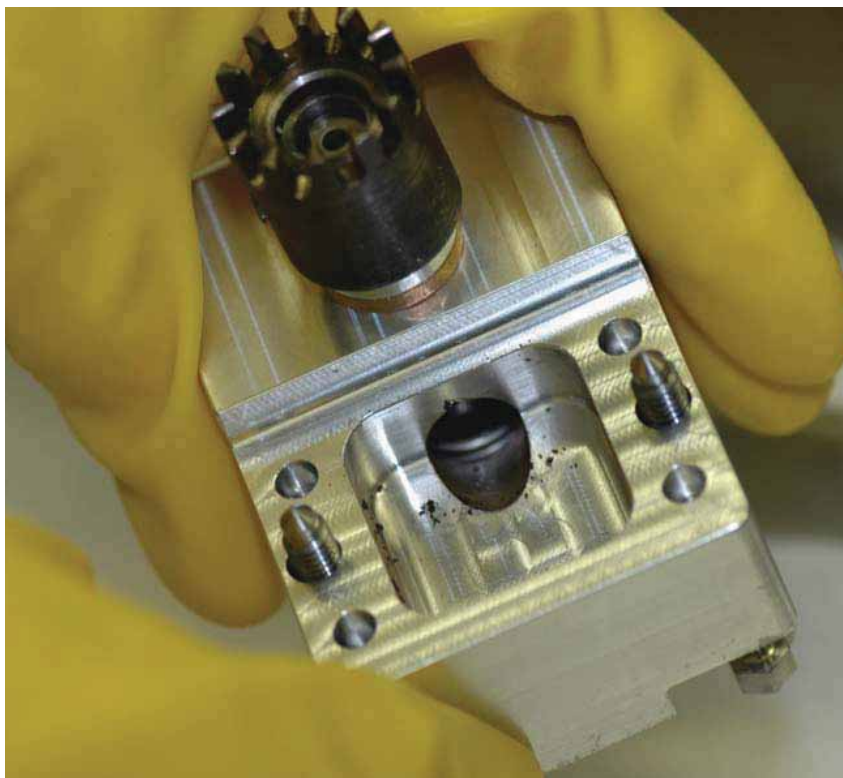


Figure 87: Filter Cavity, Final Tank 18 Lower Sample, SP 4

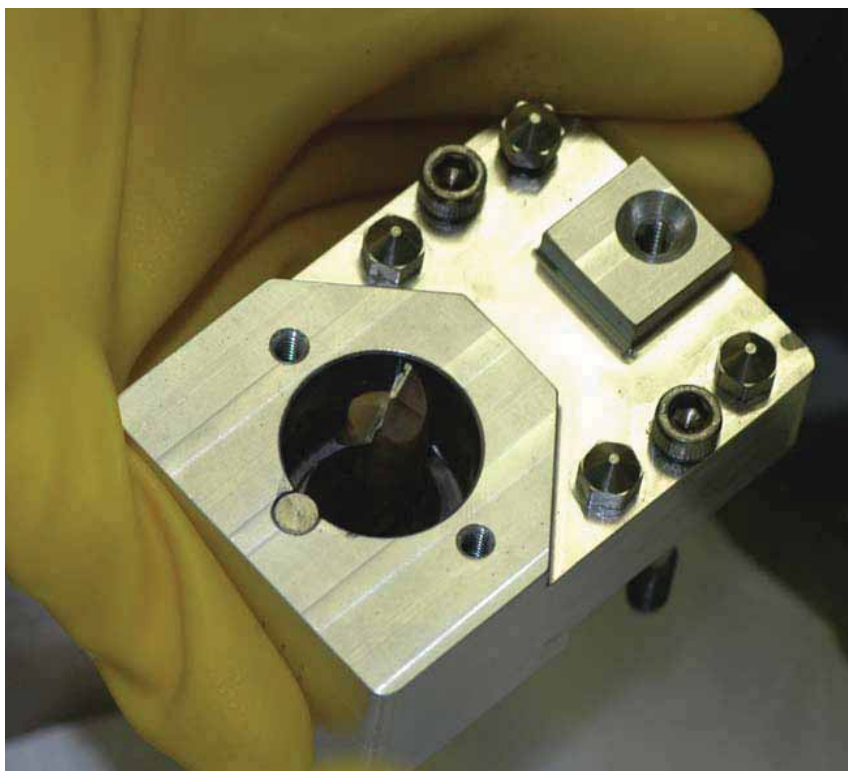


Figure 88: Drill, Cavity, Final Tank 18 Lower Sample, SP 4

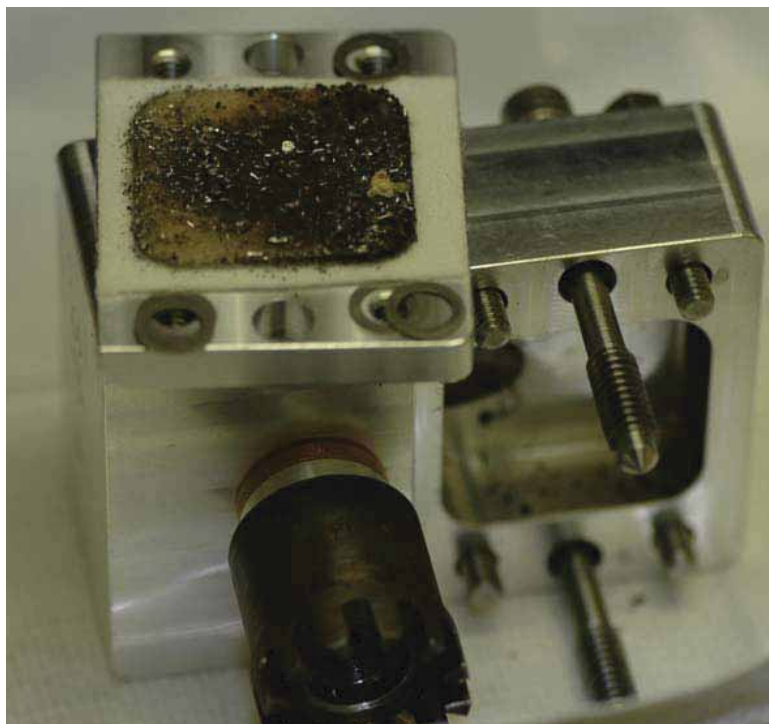


Figure 89: Collected Sample, Final Tank 18 Lower Sample, SP 4



Figure 90: Collected Sample, Final Lower Sample, Tank 19, TK 19-2 (Upper Sample showed similar results)



Figure 91: Filter Cavity, Final Lower Sample, Tank 19, TK 19-2

6.4 SUMMARY OF DESIGN IMPROVEMENTS

SRS corrected the resonant frequency chattering problem in order to make the sampler operate as designed. The design was also simplified to minimize cost.

SRS success showed that the steel was bright and shiny as expected once the corrosion layer was machined through. In the West Valley report, a key assumption of their analysis was “that the dark center of the burnish indicated penetration into the base metal since very little of the burnish locations appeared to reflect light as a shiny surface would with the optimal lighting and cameras angle.” Testing at SRS showed that vibrations prevented adequate drilling, and that the black hole at the center of the burnish, or hole, was in fact the corrosion layer. An essential element of success was the use of an electromagnet by SRS. The magnet eliminated additional resonant vibrations from the long mast, hanging from the tank top. The West Valley design successfully collected material from tank walls, but one may conclude that their report indicates that corrosion material was not effectively collected. A description of typical equipment used at West Valley and other facilities is shown in Figure 92.

In contrast to the complex robotic system, the SRS design was simplified. The design used manual controls, a sampler and mast with attached cameras, and a single truck equipped with video equipment. From the video truck, directions were remotely reported by radio to the technicians operating the equipment in the hut on top of the tanks.

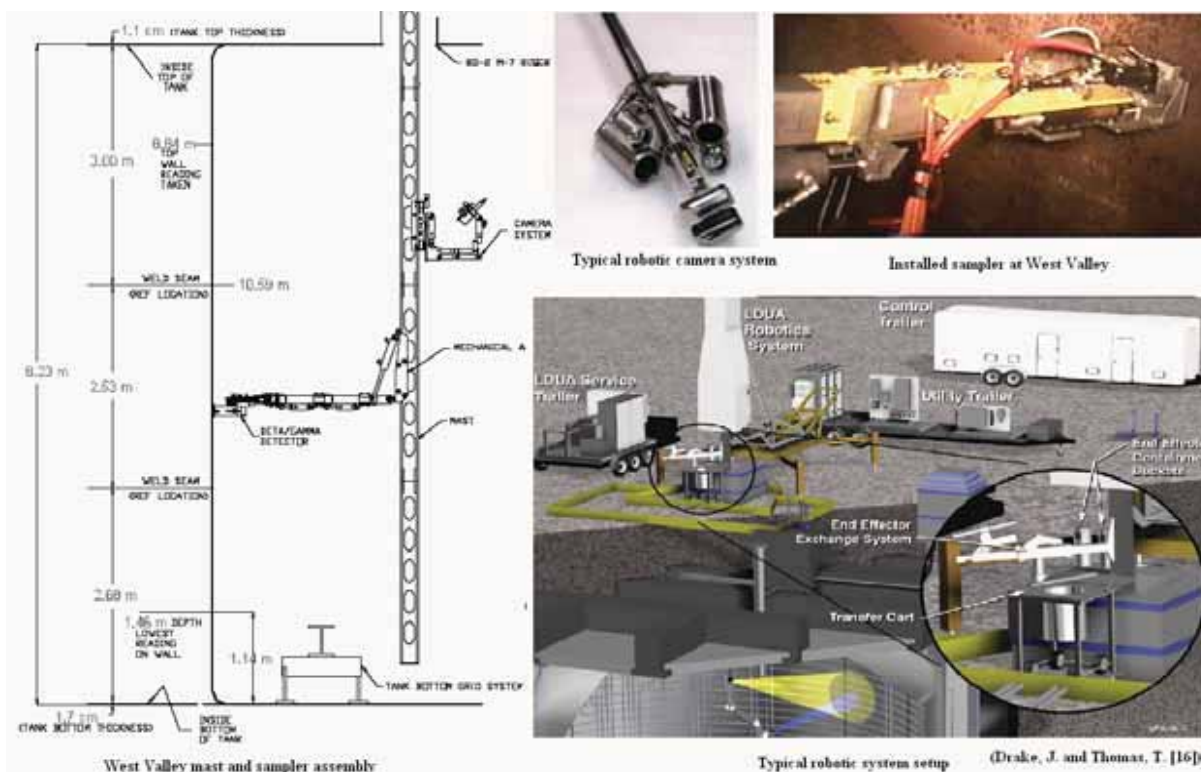


Figure 92: Oak Ridge and West Valley Wall Sampler Design

6.5 SUMMARY OF TANK 18 AND TANK 19 WALL SAMPLING

The FTF sample collection results are summarized in Table 4, Figure 66 and Figure 67. Several conclusions may be drawn:

For Tank 18:

1. Drill site characteristics varied at different locations, i.e., no evidence of drilling; small chips were removed from the waste on the wall; or shallow holes were drilled. In one case a shallow hole was drilled down to the wall surface as evidenced by black material in the bottom of the hole, where the material characteristics changed from waste attached on the wall to corrosion at the surface.
2. In some cases, the sampler was pushed from the wall when the drill bit was advanced.
3. Initial sampling attempts failed to drill down to steel, but a sample of the scale material was obtained for analysis, during the first sampling attempt.
4. The second sampling attempt collected negligible material.
5. In Tank 18, a sample was successfully machined at both required elevations. Shiny steel was observed for one location for both the upper and lower samples.
6. The Tank 18 sample surface areas were ill defined since the samples were ground from the wall, rather than drilled. Surface area determination therefore required additional calculation.
7. The materials were visually different at different sample locations in Tank 18.

8. Radiation rates were expected to be negligible but were as high as 4000 milliRem extremity, measured within two inches of the sampled materials on the filters. Rates were measured for a disassembled sampler.

For Tank 19:

9. In Tank 19 final sampling results, two holes were drilled at each required elevation, and the holes were similar to those drilled during testing.
10. The surface areas of the Tank 19 samples were well defined by the diameter of the drilled holes.
11. Radiation rates were less than 37 mRem extremity, measured on the filters.

General observations:

12. Sampling was successful.
13. Thick waste coatings, or scale, on walls diminishes sampler performance.
14. Salt liquefaction effects on efficiency were not investigated for other than test conditions, and efficiency of corrosion alone was not investigated.
15. Drill bit chattering was reduced, but not eliminated. Novel techniques were developed to evaluate chattering with respect to resonance.
16. Resonance was not previously identified as a principle design flaw of the sampler, although both West Valley and ORNL recognized that the drill bit chattered, and numerous changes were investigated and implemented in the final West Valley design.
17. Additional SRS research and experience furthered the understanding of wall sampling in waste tanks. Of particular interest, the West Valley sampler apparently did not drill into the tank wall corrosion layer, but only collected a sample down to the corrosion layer. According to the West Valley report (Drake, J. [13]), the researchers assumed that the black circles at the bottom of the holes were exposed steel. SRS sampling clearly showed that exposed steel is bright and shiny as expected. The black circles were the corrosion layer on the wall surface.
18. How can corrosion sampling be improved on waste coated walls? One recommendation is to locally clean the area to be sampled. Only a few hundred gallons of water would be required to pressure wash the areas to be tested, and the design issues for drilling through waste would not need to be resolved. As noted, electromagnets can be increased in size somewhat. Increasing the stiffness of the mast may, or may not, improve sampler performance.

7.0 CONCLUSIONS

7.1 Tank 18 and 19 Wall Samples

Wall samples were successfully obtained from FTF Tanks 18 and 19. An SRNL provided sampler was attached to a cantilevered arm, and lowered by cable from an SRR built mast assembly to drill samples from the tank walls at two different elevation ranges in each tank. SRR mounted the sampler and mast assembly by crane on the steel structure on top of Tank 18. After samples were collected, the sampler and mast were moved by crane to the top of Tank 19. To collect samples at different tank levels, the mast and sampler were raised and lowered by crane and pinned or clamped in place while sampling was performed.

7.1.1 Wall Sampler Design

The ORNL designed sampler required several modifications before successful operation could be demonstrated. Electromagnets held the sampler to the wall, and the sampler's drilling components were mounted to a guide rail and were forced against the wall by a pair of springs. A ½ inch diameter drill bit with a slightly tapered point was driven by a drill motor to drill a sample of material from the tank wall, which was expected to include, steel, rust, and salt. Controls advanced the drill 1/16 of an inch, or less, into the wall surface and coatings until stops on the sampler prevented further drill travel. During drilling, all material was collected by a vacuum system, where air flowed through a collar surrounding the drill bit. Particles were extracted from the drill site and transported to a filter section for collection. The drill bit, collar, and filter section assembly are referred to as a sampler head. These removable sampler heads were transported from FTF to SRNL for disassembly and further processing, after radioactive samples were machined from the tank walls.

7.1.1.1 Wall Sampler Improvements

SRNL design modifications prevented certain failure of the previous sampler design. At SRS, multiple ½ inch diameter by 1/16 inch deep sample holes were required. The sampler frequently jammed at completion of the first hole, and system controls were modified as required. The filters sheared when installed in the sampler heads. More importantly, the initial design had an inherent flaw, which was evident only under certain conditions. Specifically, rust or thick wall coatings like those found in waste tanks caused resonant vibrations of the spring due to drill bit chattering, which induced resonant vibrations. SRNL identified the resonance problem, and changed the spring design to reduce chattering. Without these changes performed during testing, the sampler would have failed to collect samples in either tank, since the sampler was required to machine down to bare steel.

The Oak Ridge and West Valley design was an essential step toward SRS success. Without their foundation design, SRS costs could have reached additional millions of dollars. SRS was able to improve the design through additional experience. Even so, SRS design improvements ensured success to overcome inherent design flaws in the equipment.

7.1.1.2 EDL Sampler Operation

At EDL, a curved steel plate was used to validate sampler operation. The sampler was shown to drill as many as 12 holes using a single drill bit without dulling the bit.

7.1.1.3 T-Area Sampler Operation

Testing in the T-Area, Full Scale Tank Facility provided an opportunity to completely investigate the sampler before installing it in the waste tanks. Without this crucial testing, the sampler would have failed when installed. At the Full Scale Tank, initially only a single hole was drilled per drill bit before the drill bits became dull, and even a single sample hole was not assured. The replacement spring design reduced resonance effects and increased the number of drilled holes per drill bit to six before the drill bit dulled. Further improvements were possible, but spring changes were considered adequate to obtain two holes in Tanks 18 and 19. The sampler and mast were demonstrated and ready for tank installation.

7.1.2 EDL Sample Results

Sample coupons were attached to a curved test plate at EDL to evaluate the collection efficiency of the sampler. Several tests were performed on one inch square test coupons. The before and after masses of the coupons and sampler heads were compared to determine the percentage of material collected in the sampler from the coupons. All material was collected at the wall surface, but some material escaped through the filters. Evaluated material conditions included: polished steel coupons with machined surfaces to evaluate steel removal by the sampler; steel coupons with a salt layer to evaluate the removal of salt only; and rusted steel coupons with a salt layer to evaluate machining all three materials in discrete samples.

Collection efficiencies were markedly affected by material properties. For the steel samples, the collection efficiency was above 97.4 % at expected operating conditions. For the salt samples, the measured collection efficiency was above 57.2 %, and testing was not performed to evaluate efficiencies for different salt thicknesses. Tests for the rusted, salt coated coupons were also not investigated for different salt thicknesses or for corrosion by itself. Given this limitation for the rusted, salt coupon results, the collection efficiency was above 95.6 %.

7.1.3 FTF Sample Results

Sampler results were also affected by the residual waste on the tank walls. The assumption that the wall was coated with salt was shown to be incorrect for Tank 18. An important aspect on the application of EDL testing relates to Tanks 18 and 19 conditions. Tank 19 was pressure washed, and Tank 18 was not. In Tank 18 a layer of waste coated the wall, and the waste thickness appeared to vary between 1/32 inches and 3/8 of an inch throughout the tank. In Tank 19, waste was removed from the walls, and corrosion seemed to be the principal coating on the walls, with perhaps a thin, transparent salt film.

7.1.3.1 Tank 18 Sampler Operation

The sampler was held to the wall by electromagnets, which were selected to operate within 0.030 inches of the wall. At this distance, the magnetic force of 750 pounds per magnet reduces to 75 pounds per magnet, which is opposed by the 37 pound maximum force of each spring. In Tank 18, the excessive waste thickness prevented the sampler from attaining proper attachment to the wall. As the drill bit advanced, the sampler released from the wall, and holes could not be effectively drilled. Even though holes could not be drilled into the wall, samples were successfully collected when the drill bit acted as a grinder to scrape samples from the wall at the two required elevations.

7.1.3.2 Tank 18 Sample Results

Sufficient material was collected for analysis, material was removed down to an exposed steel surface, and sampling was considered successful by FTF Engineering. All that was required for this report was an estimate of the surface area of exposed steel. Even though more than one hole was attempted, and the drill bit scraped along the wall in one case, the use of the exposed steel surface as a basis for radioactive contamination provides a conservative estimate for radiation per unit area. The contents of the sampler will be used to find the total radioactivity (Curies), and dividing this quantity by the steel surface area will provide a significantly higher value for activity per unit area. Subjectively, the calculated radiation level per unit area may actually be 75 % more than actual. The surface areas were found to conservatively equal 0.196 in² at the upper sample area in Tank 18 and 0.063 in² at the lower sample area in Tank 18

7.1.3.3 Tank 19 Sampler Operation and Results

In the absence of significant waste on the tank wall, the sampler drilled holes in the wall as designed. Consequently, the surface area was determined from two drilled holes collected by each sampler. The minimum possible hole size was used to establish a conservative value for the surface area of collected material. For samples at both the upper and lower sample areas, the area equaled 0.393 in². Samples were successfully collected from both tanks.

8.0 REFERENCES

1. D. Thaxton, Technical Assistance Request, 2009-LWOFT-004, "Tank 18 and 19 Wall Sampler", FTF, SRR.
2. R. Leishear, R. Minichan, and T. Steeper, EES Job Folder 23230, 2009, Engineering Drawings and Sketches for the Tank 18 / 19 Wall Sampler, SRNL.
3. R. Leishear, M. Fowley, e-HAP, SRNL-L3100-2009-00139, "Hazards Assessment Plan for Tank 18 / 19 Wall Sampler".
4. M. Fowley, Work Instructions, ITS-WI-0037, 2009, "Tank 18 / 19 Wall Sampler".
5. R. Leishear and M. Fowley, Lab Notebooks, SRNL-NB-2009-00068 and SRNL-NB-2009-00097, "Tank 18 / 19 Wall Sampler".
6. T. France, 2009, "Tanks 18 and 19 Wall Sampler Assembly and Controls", VPF22872, SRR.
7. W163941, W230907, 1956, "85 Foot Diameter, Steel Tank, Plan and Details", SRR.
8. M. Jackson, 2009, "Tank 18 and Tank 19 Videos: 1707, 2001, 2003, 2004, 2005, 2011, 2017", HTF, SRR.
9. T. France, 2009, "Tank 18 Wall Sampling", FTF Work Order – 942321-03, SRR.
10. T. France, 2009, "Tank 19 Wall Sampling", FTF Work Order – 942319-05, SRR.
11. B. Wiersma, X-CLC-F-00440, 2007, "Estimate of the Corrosion Product on the Walls of Tank 18, SRNL"
12. B. Wiersma, C-ESR-F-00043, 2007, "Estimate of the Corrosion Product on the Walls of Tank 19", SRNL
13. J. Drake, C. McMahon, 2002, "High Level Waste Tank Cleaning and Field Characterization at the West Valley Demonstration Project", Waste Management Conference.
14. T. R. Thomas, 2002, "Review of Analytes of Concern and Sample Methods for Closure of DOE High Level Waste Storage Tanks", Idaho National Engineering and Environmental Laboratory.
15. H. Coleman and W. Steele, 1989, "Experimentation and Uncertainty Analysis for Engineers", John Wiley, New York.
16. Taylor, B. N., Kuyatt, C. E, 1994, 1297 Edition, "Guidelines for Evaluating and Expressing the Uncertainty of NIST Measurement Results", NIST Technical Note.

APPENDIX A. OAK RIDGE NATIONAL LABORATORY, INITIAL DESIGN OF WALL SAMPLER

A SAMPLING END EFFECTOR FOR STEEL WASTE TANK WALLS*

Stephen Killough
Oak Ridge National Laboratory
P. O. Box 2008
Oak Ridge, TN 37831
killoughsm@ornl.gov
(865) 574-4537

ABSTRACT

As part of a remediation project of underground waste tanks at the West Valley Demonstration Project (WVDP), Oak Ridge National Laboratory (ORNL) has developed a sampling device to characterize the cleanup efforts of the West Valley tanks. This device will take a representative scrape sample from inside the tank. From this sample, the per-square-inch contamination of the tanks and an estimate of the total contamination inside the tank can be determined.

The goals for the sampler were to take an accurate sample and yet minimize any damage to the tank walls. Furthermore, the device had to be compatible with the high-radiation tank environment and must not add any undesirable oils into the tank. Since the sampler will be highly radioactive after a sample is taken, the sampler must be small, lightweight, and quick to retrieve to minimize exposure to personnel.

The sampler takes a scrape from the tank walls using an end-mill-type milling machine bit. The bit makes an essentially flat cut 0.5-in. in diameter and 0.030 in. deep. This shallow penetration collects all of the surface contamination while still being a near non-destructive test. A vacuum and filter system is used to collect all of the scraped shavings and a collar around the bit is used to collect any shavings that are flung out. The bit and filter are in a small housing assembly, which can be detached from the sampler base such that the sample will fit in a small lead container for shielding. The assembly is designed to be easily detachable from the sampler base using long-handle tools.

1. INTRODUCTION

The remediation activities at the WVDP high-level waste (HLW) tanks and the Gunite and Associated Tanks at ORNL are similar in that both efforts needed a measurement of the remaining contamination in the tanks after the cleanup process was completed. ORNL

*Oak Ridge National Laboratory, managed by UT-Battelle, LLC, for the U.S. Department of Energy under contract DE-AC05-00OR-22725

developed a device for sampling its tanks and offered its expertise to the WVDP to help characterize the West Valley tanks. The two situations are different in that the ORNL tanks are concrete and the WVDP tanks are carbon steel; also the WVDP tests were to be mostly non-destructive as compared to the ORNL tests. In late 1999, the two facilities began collaborating on a design for a sampling system for the steel tanks, with ORNL concentrating on the sampler device itself and WVDP concentrating on the deployment robot.

Unlike the concrete tanks at ORNL, it is assumed that the waste materials in the West Valley tanks have not permeated into the steel walls; therefore, only a surface scrape is necessary to characterize the tank. The new device takes this surface scrape with a plunge-cutting type end-mill bit and collects the scraped material in a filter for delivery to a laboratory for analysis. The area to be scraped is a 0.5-in. diameter circle, and the average weight of the collected sample is 0.5 g.

The development of such a sampler was an engineering exercise that took into account the accuracy needed, cost, compatibility with the chemicals and radioactivity in the tank, reliability, and simple, safe, low-exposure operation for personnel.

2. OVERALL CONCEPT

The heart of the sampler is the milling bit, which is mounted in a tube similar to a vacuum cleaner nozzle so that the vacuum will collect any material scraped up by the bit. The vacuum draws the material into a filter, which retains it for delivery to a laboratory. Because of the expected radioactivity of the sample, the filter system must be small enough to fit inside a lead-shielded container. Furthermore, to prevent cross contamination, a new milling bit and filter will be used for each sample. The system is modularized such that the disposable bit and filter section (also known as the sample housing) is compact and easily detachable from the system's base unit.

The base unit consists of hardware, which drives the sample housing. The base unit contains the drill motor for turning the drill bit, a linear slide to axially advance the bit, a motor to drive the slide, a spring system to limit the axial drive force, and a vacuum generator. The motors are lightweight, pneumatic units, and the vacuum generator is an air-driven venturi unit.

3. DESIGN DETAILS

The complete sampler device is shown in Fig. 1. The base attaches to a robotic arm, which will deploy the device into the tank and up to the tank walls. This arm is a water-hydraulic unit, which is provided by West Valley Nuclear Services (WVNS). Mounted to the base is a linear slide table, which is driven by an ACME screw and a small pneumatic bi-directional motor to advance the sampler to contact the wall. A second slide on the table connects with a force-limiting spring mechanism to limit the forces that the sampler can press on the wall. This force limit is presently 22 lb, although this value could easily be changed with different springs. The drill motor is a 0.5-hp pneumatic unit, which spins at 225 rpm and the

venturi vacuum pump generates up to 30-ft³/minute flow. The pneumatic systems are driven by 100-psi air and all of the custom parts are made of anodized aluminum.

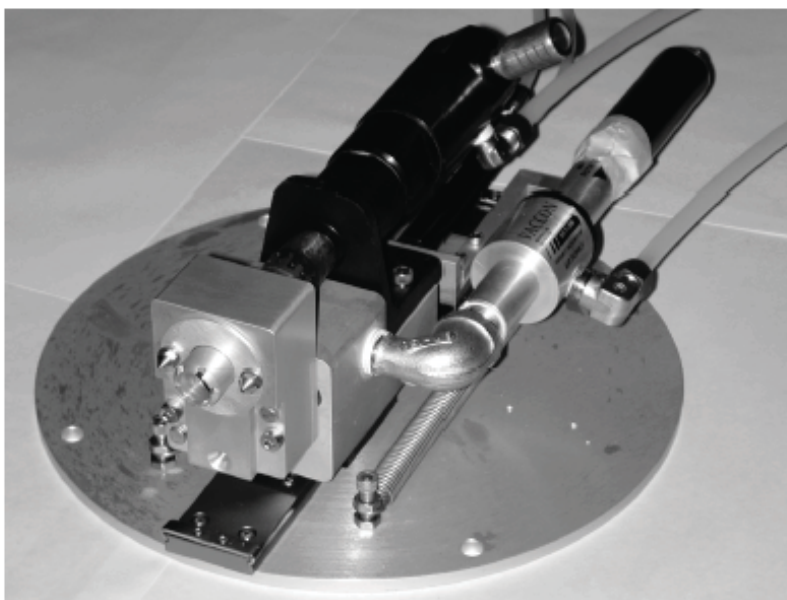


Fig. 1. Complete grab sampler system.

To minimize the size of the equipment that transports the sample to the laboratory, the bit, filter, and sample housing were made compact and easily detachable from the base, as is illustrated in Fig. 2. The sample housing is held to the base by two captive screws, a simple mechanical coupler engages the drill shaft, and an O-ring gasket is used to seal the vacuum connection. A threaded hole is also provided to allow the screwing in a temporary handle so that the device can be grasped with long-handle tools. The overall size of the housing is 3.5 x 3.4 x 2.3 in., and the weight is about 500 g.

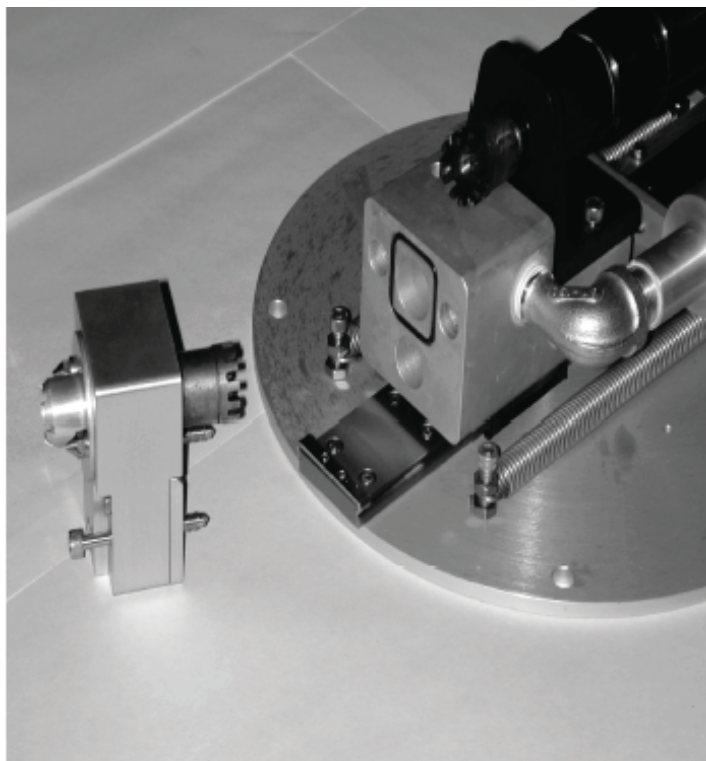


Fig. 2. Sample housing detached from base.

During the design process, components were selected that would survive the radioactive and corrosive environment inside the tank. Stainless steel and anodized aluminum parts were selected where possible, and the pneumatic motors were studied to identify any internal radiation-sensitive parts. The drill motor is carbon steel and will need to be painted, and radiation-tolerant air hoses will eventually be selected by WVNS.

A direct view of the milling bit is shown in Fig. 3. The bit is a standard 0.5-in. diameter, two-flute unit with a 3/8-in. shaft. Other standard bits could be used without changing the housing design. Unlike conventional drilling, no lubricants are permitted in the tank, so the drill is run dry.

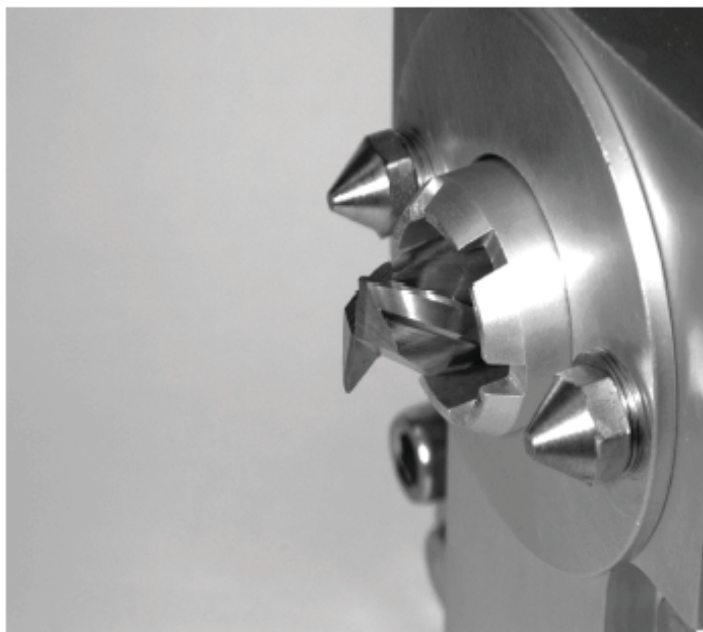


Fig. 3. View of the milling bit.

The sampler has other features that support the drilling operation. The collar around the bit is telescoping and spring-loaded in order to surround the bit until it is pressed against the wall during drilling. Air vents on the end of the collar permit suction air to flow in while catching any particles that are flung from the bit. To prevent the bit from drilling too deeply into the wall, cone-shaped bolts, which are 0.030-in. behind the end of the bit, are mounted on the housing. These bolts could also be adjusted for special cases, such as for drilling into columns and other non-flat surfaces. Since the 0.030-in. depth limit is for the steel wall and not for any scale that may be present, sharpening the bolt cone tips may be necessary to penetrate the scale.

The filter is in a milled out pocket in the lower half of the sample housing, as is shown in Fig. 4. The volume of this cavity is 0.8 in.³, and the surface area of the filter is 1.5 in.². Although this may seem large for shaving only 0.030 in. of material, experience has shown that the shaved sample is fluffed up and occupies a larger volume than expected; also, scales of significant thickness may also be encountered.

The filter media is based on a fiberglass high-efficiency particulate air (HEPA) element. Paper-based elements were also tried; however, the paper was degraded by wet sampling surfaces, and the dust particle capture performance was not as good as that of the HEPA elements. The WVDP also had concerns about the cellulose in the paper degrading its analysis results.

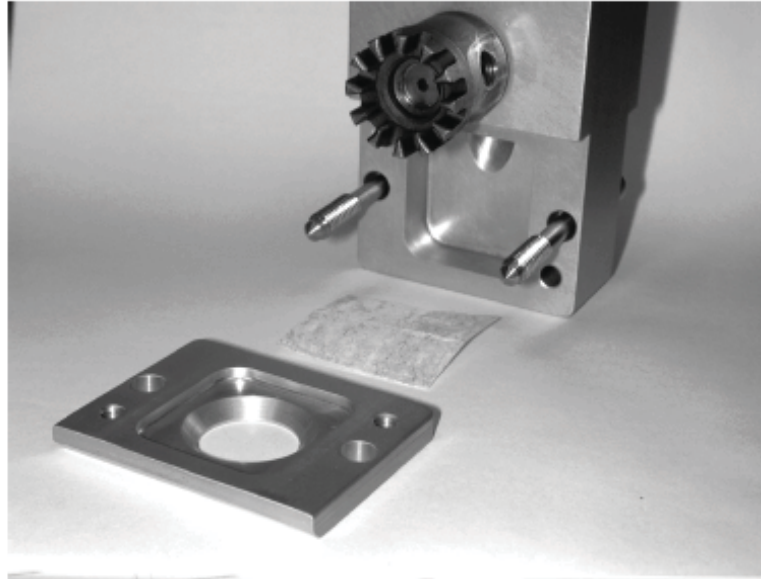


Fig. 4. Filter cavity area.

4. TEST RESULTS

The test arrangement consisted of the sampler base, which was clamped to a tabletop, and a test piece of steel, which was clamped to an adjoining table. Two tables were used to simulate compliance effects between the wall and the robot arm. Other tests were conducted to make sure that the sampler housings could be swapped using long-handle tools. Example operations with these tools showed that these operations could be performed without difficulty.

An operations concern is whether the operators will be able to adequately view the device through television cameras well enough so as to operate it correctly. To make sure the sampler is pressed perpendicular to the wall, WVNS added a compliant wrist to its robot. This wrist presses struts against the wall to ensure perpendicular operation. Since the operators cannot see well enough so as to advance the bit into the steel at the same rate as the actual steel milling, the technique was changed to allow the operators to instead rely on the force-limiting mechanism to apply a constant force with the bit. Since the depth-limiting bolts will prevent the sampler from cutting too deeply, the operators only need to advance the sampler onto the wall and wait a few minutes until the milling is finished.

The key test of the system was to precisely weigh the sampler housing and a test piece of steel and measure them again after a sample was taken from the steel. Ideally, all of the weight that disappeared from the test steel would appear in the sample housing. For tests on dry painted steel, the results were very good—with all of the weight that disappeared from the steel.

appearing in the sampler. Since we are near the accuracy limit (0.01 g) on our scale, we are claiming the recovery to be 99+%. Weights collected for these samples were about 0.5 g.

Other tests were conducted to simulate performance for walls covered with thick scales. WVDP expects up to 0.25 in. of sodium hydroxide scales, and bars of hand soap 0.25 in. thick were used to simulate these tests. The sampler appeared to collect the simulated scale very well; however, weight measurements showed only 80 to 85% collection efficiency because of compounds evaporating from the soap. Tests were also conducted with the soap wetted down to simulate wet conditions; however, the vacuum system evaporated the water such that the efficiency appeared to be only 50%. However, the main consideration for the wet tests is whether the sticky and wet soap gums up the sampler and prevents it from collecting its sample. Tests have shown that the sampler will still collect the gummy soap; however, the material becomes stuck throughout the inside of the sampler instead of only on the filter paper. This material is still retrievable in the analysis lab although it will need to be scraped out of the sampler head. The weights of materials collected for these tests are 2 to 3 g.

Another consideration is the efficiency of extracting the material from the sample head and getting it into the containers in the analytical laboratory. Tests in this area show an efficiency of 85 to 90%, although this efficiency requires manually scraping the material out of the sampler head if the material is sticky.

5. DEPLOYMENT PLANS

Present plans are to deploy the sampler in one of the West Valley HLW tanks in early 2001. The sampler itself is operational although further testing will be required to achieve NQA-1 certification for the device. Further tests with the full robot and sampler system will need to be conducted to verify that the robot is stiff enough to hold the sampler steady during the milling operation. In the future, new versions of the sampler may be considered for tank-floor sampling where the floor is under a few inches of water.

6. CONCLUSIONS

The West Valley Grab Sampler has been a very successful design activity and is anticipated to be an accurate, a reliable, and a robust device for samples at the WVDP tanks. Experience gained from designing and operating this device in an actual waste environment will be valuable for future work in waste-tank remediation at other U.S. Department of Energy and industrial sites.

APPENDIX B. Uncertainty Analysis for Test Data

Table 2 shows collection efficiencies and corresponding uncertainties (Coleman, H., Taylor, B. [15 and 16]). There is a collection efficiency for each test and an average collection efficiency for each set of tests (three tests for each set). There is also an uncertainty associated with each test and an uncertainty associated with the average. The efficiencies and uncertainties are further broken down into those corresponding to material captured on the filter only and those corresponding to material captured in the entire head. The derivation of the uncertainties is described in the following sections.

Uncertainty of the Average

The uncertainty associated with the average (σ_{CEA}) is based on the standard deviation of the three collection efficiencies in the set of samples. σ_{CEA} also included an uncertainty associated with the test σ_{CET} (maximum of the three values). It should be noted that σ_{CEA} was typically much greater than σ_{CET} . σ_{CEA} was therefore a Root-Sum-Square (RSS) combination of the standards deviation (at 95% confidence level) and σ_{CET} , as follows:

$$\sigma_{CEA} = +/- [(T \cdot SD)^2 + \max \sigma_{CET}^2]^{1/2} \quad (B0)$$

where, T is the Student T-Factor to provide a 95% confidence level, and
 SD is the standard deviation of the three test results that make up a set.

Uncertainty of the Test

The uncertainty associated with the collection efficiency for each test (σ_{CET}) consists of the combined uncertainty of the masses used to derive the efficiency. Included in σ_{CET} is the uncertainty due to hygroscopic effects.

The uncertainty of the masses that were used in determining the collection efficiency (CE) was determined using Equation 1 (Section 4.1) and the concept of the Law of Propagation of Uncertainty (Taylor, B. [15 and 16]). Note that the resulting equation is analogous to the Root-Sum-Square (RSS) method of combining uncertainties.

$$\sigma_{CET} = +/- 100 \cdot [(\sigma_{MS} \cdot (\partial CE / \partial M_S))^2 + (\sigma_{MC} \cdot (\partial CE / \partial M_C))^2]^{1/2} \quad (B1)$$

where, σ_{CET} is the uncertainty of the collection efficiency for each test, expressed as a percentage.

σ_{MS} is the uncertainty in the mass of material collected by the sampler head.

$\partial CE / \partial M_S$ is the sensitivity coefficient for the mass of material collected by the sampler head.

σ_{MC} is the uncertainty mass of material removed from the coupons.

$\partial CE / \partial M_C$ is the sensitivity coefficient for the mass of material removed from the coupons.

Simply stated, the sensitivity coefficient relates an incremental change (i.e. uncertainty) in the collection efficiency (\mathcal{CE}) to an incremental change in the variables (mass collected by the sampler head, \mathcal{M}_S , or removed from the coupon, \mathcal{M}_C). Note that the higher order terms from the Law of Propagation of Uncertainty equation are assumed to be negligible.

Solving the partial differential equations in Equation B1 and using Equation 1, yields the following:

$$\sigma_{CET} = +/- 100 \cdot [(\sigma_{MS}/M_C)^2 + (-\sigma_{MC} \cdot M_S/M_C^2)^2]^{1/2} \quad (B2)$$

Uncertainty of the Mass of Material Collected by the Sampler Head (σ_{MS})

As stated before, two collection efficiencies are reported; that of the filter only and that of the entire head. Several different masses are used for each case and the uncertainty of each mass was considered.

Filter Only

Using the Law of Propagation of Uncertainties for Equation 4 (Section 4.2.3) and solving the partial differential equations, the uncertainty of the material collected by the filter only yields the following;

$$\sigma_{MSF} = +/- (\sigma_{mSF2}^2 + \sigma_{mSF1}^2)^{1/2} \quad (\text{filter only}) \quad (B3)$$

where, σ_{MSF} is the uncertainty of the mass of material from the filter only,
 σ_{mSF2} is the uncertainty of the post-test filter mass, and
 σ_{mSF1} is the uncertainty of the pre-test filter mass.

The post-test filter was weighed in a weighing tray since the filter contained loose material from the sample. The post-test filter mass was determined by subtracting the tray mass from the overall mass. Therefore, equation B3 becomes;

$$\sigma_{MSF} = +/- (\sigma_{mSF2}^2 + \sigma_{mFT}^2 + \sigma_{mSF1}^2)^{1/2} \quad (\text{filter only}) \quad (B3A)$$

where, σ_{mFT} is the uncertainty of the weighing tray mass.

All associated filter masses were measured by the same analytical balance (M&TE # WP-1007), the tolerance of which was +/- (0.01 % of reading + 0.3 mg). To simplify the calculation of the uncertainty of the filter masses the tolerance of WP-1007 was stated as +/- 0.75 mg [+/- (0.01% of 4.5 g + 0.3 mg), where 4.5 g is a conservative representation of the filter mass for all testing]. The uncertainty of the tolerance of WP-1007 was stated as +/- 0.5 mg [+/- (0.01% of 2 g + 0.3 mg), where 2 g is a conservative representation of the tray mass for all testing]. The uncertainty of the filter only mass becomes;

$$\sigma_{MSF} = +/- (0.75^2 + 0.5^2 + 0.75^2)^{1/2} = +/- 1.17 \text{ mg} \quad (\text{filter only})$$

Entire Head

Using the Law of Propagation of Uncertainties for Equation 5 (Section 4.2.4) and solving the partial differential equations, the uncertainty of the material collected by the entire head simplifies to;

$$\sigma_{MSH} = +/- (\sigma_{mH2}^2 + \sigma_{mH1}^2 + \sigma_{MSF}^2)^{1/2} \quad (\text{entire head}) \quad (\text{B4})$$

where, σ_{MSH} is the uncertainty of the mass of material from the entire head,

σ_{mH2} is the uncertainty of the post-test head mass,

σ_{mH1} is the uncertainty of the pre-test head mass, and

σ_{MSF} is the uncertainty of the mass of material from the filter only.

Both the pre-test and post-test head masses were measured by the same analytical balance (M&TE # SL-1004). The tolerance of SL-1004 used for this uncertainty calculation was derived from calibration data before and after use, and was determined to be +/- 1.2 mg in the range measured (~500 g). The uncertainty of the entire head mass becomes;

$$\sigma_{MSH} = +/- (1.2^2 + 1.2^2 + 1.17^2)^{1/2} = +/- 2.06 \text{ mg} \quad (\text{entire head})$$

Uncertainty of the Mass of Material Removed from the Coupons (σ_{MC})

Using the Law of Propagation of Uncertainties for Equation 6 (Section 4.2.4) and solving the partial differential equations, the uncertainty of the material removed from the polished coupons simplifies to;

$$\sigma_{MCP} = +/- (\sigma_{mCa1}^2 + \sigma_{mCb1}^2 + \sigma_{mCa2}^2 + \sigma_{mCb2}^2)^{1/2} \quad (\text{polished coupons}) \quad (\text{B5})$$

where, σ_{MC1} is the uncertainty of the mass of material from polished coupons,

σ_{mCa1} is the uncertainty of the pre-test mass of the first coupon,

σ_{mCb1} is the uncertainty of the pre-test mass of the second coupon,

σ_{mCa2} is the uncertainty of the post-test mass of the first coupon,

σ_{mCb2} is the uncertainty of the post-test mass of the second coupon,

Using the Law of Propagation of Uncertainties for Equation 7 and solving the partial differential equations, the uncertainty of the material removed from the salt coupons simplifies to;

$$\sigma_{MCR} = +/- (\sigma_{mCa1}^2 + \sigma_{mCb1}^2 + \sigma_{mCT1}^2 + \sigma_{mCa2}^2 + \sigma_{mCb2}^2 + \sigma_{mCT2}^2)^{1/2} \quad (\text{coupons with salt residue}) \quad (\text{B5A})$$

where, σ_{MC2} is the uncertainty of the mass of material from coupons with salt,

σ_{mCT1} is the uncertainty of the pre-test mass of the collection tray.

σ_{mCT2} is the uncertainty of the pos-test mass of the collection tray.

All of the above masses were measured by the same analytical balance (M&TE # WP-1007). To simplify the calculation of the uncertainty of the masses associated with the coupons, the tolerance of WP-1007 was stated as ± 2.1 mg [$\pm (0.01\%$ of 18 g $+ 0.3$ mg)], where 18 g is a conservative representation of pre- and post-test coupon masses for all testing]. The uncertainty of the mass associated with the coupons becomes;

$$\sigma_{MCP} = \pm (2.1^2 + 2.1^2 + 2.1^2 + 2.1^2)^{1/2} = \pm 4.20 \text{ mg} \quad (\text{polished coupons})$$

In the case of test with coupons with salt, the tolerance of WP-1007 for the collection tray was stated as ± 0.45 mg [$\pm (0.01\%$ of 1.5 g $+ 0.3$ mg)], where 1.5 g is a conservative representation of pre- and post-test tray masses for all testing], and uncertainty of the mass associated with the coupons becomes;

$$\sigma_{MCR} = \pm (2.1^2 + 2.1^2 + 0.45^2 + 2.1^2 + 2.1^2 + 0.45^2)^{1/2} = \pm 4.25 \text{ mg} \quad (\text{coupons with salt residue})$$

Uncertainty Due to Hygroscopic Effect

To quantify hygroscopic effects, multiple masses were recorded for items having salt. The items with salt were kept in a desiccator when not used and trays of desiccant were placed in the enclosure of the analytical balance to establish and maintain a consistent moisture level of the salt. However, even with these measures the masses fluctuated for repeated measurements. From the repeated measurements an uncertainty of the mass of each item was determined. The multiple uncertainties were compared and a conservative estimate was chosen to represent the uncertainty of all items with salt due to hygroscopic effects. The representative uncertainty was ± 15 mg.

Example of Uncertainty Calculation

The following is an example of the process for determining a collection efficiency and the uncertainty of that collection efficiency.

The pre-test and post-test masses of a filter and polished coupon are shown in the table below. Two sets of coupon masses are shown to represent the pair of coupons sampled per test.

Filter Mass Pre-test (m_{F1}) (g)	Filter Mass Post-test (m_{F2}) (g)	Coupon Mass Pre-test (m_{C1}) (g)	Coupon Mass Post-test (m_{C2}) (g)
0.63428	-	16.39022	15.34034
-	2.70924	16.44033	15.37953

Using Equations 3 and 6 (Section 4.2.3 – 4.2.4) respectively the quantity of material collected on the filter and the quantity of material removed from the coupons is found.

$$M_{SF} = M_{SF2} - M_{SF1} = 2.70924 - 0.63428 = 2.07496 \text{ g}$$

$$M_{CP} = M_{Cal} + M_{Cb1} - (M_{Ca2} + M_{Cb2}) = 16.39022 + 16.44033 - 15.34034 - 15.37953 = 2.11068 \text{ g}$$

Using Equation 1 the filter only collection efficiency is found (M_S would be M_{SA} in this case since it is for the filter only).

$$CE = 100 \cdot M_S / M_C = 100 \cdot 2.07496 / 2.11068 = 98.3 \%$$

Using equation B2 the filter only instrument uncertainty is found (σ_{MS} would be +/- 1.17 mg in this case since it is for the filter only, and σ_{MC} would be +/- 4.2 mg in this case since it is for polished coupons).

$$\sigma_{CET} = 100 \cdot [(\sigma_{MS} / M_C)^2 + (-\sigma_{MC} \cdot M_S / M_C^2)^2]^{1/2} = 100 \cdot [(0.00117/2.11068)^2 + (0.0042 \cdot 2.07496/2.11068^2)^2]^{1/2} = 0.203 \%$$

Material Mass Collected on Filter (M_{SA}) (g)	Material Mass Removed from Coupon (M_C) (g)	Collection Efficiency (CE) (filter only) (%)	Instrument Unc. (σ_{CET}) (filter only) (%)
2.07496	2.11068	98.3	+/- 0.20

The pre-test and post-test masses of the sampler head are shown in the table below. Using Equation 5 the mass of the material in the head can be found.

$$M_{SH} = M_{SH2} - M_{SH1} + M_{SF} = 517.2313 - 517.1978 + 2.07496 = 2.10846 \text{ g}$$

Using Equation 1 the collection efficiency for the head plus the filter plus the sample is found (M_S would be M_{SB} in this case since it is calculated for the head plus filter).

$$CE = 100 \cdot M_S / M_C = 100 \cdot 2.10846 / 2.11068 = 99.9 \%$$

Using equation B2 the entire head instrument uncertainty is found (σ_{MS} would be +/- 2.06 mg in this case since it is for the entire head, and σ_{MC} would be +/- 4.2 mg in this case since in is for polished coupons).

$$\sigma_{CET} = +/- 100 \cdot [(\sigma_{MS}/M_C)^2 + (-\sigma_{MC} \cdot M_S/M_C^2)^2]^{1/2} = +/- 100 \cdot [(0.00206/2.11068)^2 + (0.0042 \cdot 2.07496/2.11068^2)^2]^{1/2} = +/- 0.218 \%$$

Head Mass Pre-Test (M_{H1}) (g)	Head Mass Post-test (M_{H2}) (g)	Mass of Material in Head (M_{SB}) (g)	Collection Efficiency (CE) (entire head) (%)	Instrument Unc. (σ_{CE}) (entire head) (%)
517.1978	517.2313	2.10846	99.9	+/- 0.22

The table below shows three typical, filter only, collection efficiencies for a test series. The average efficiency is simply $(98.3+99.0+97.5)/3 = 98.3 \%$. The uncertainty of the average is the standard deviation of the three values, $Std Dev = 0.734 \%$. The student T-factor to produce a 95% confidence level for three data points is 4.303. Using equation B0 the uncertainty of the average is found.

$$\sigma_{CEA} = +/- [(T \cdot SD)^2 + \max \sigma_{CET}^2]^{1/2} = +/- [(4.303 \cdot 0.734)^2 + 0.22^2]^{1/2} = +/- 3.16 \%$$

CE test 1 (filter only) (%)	CE test 3 (filter only) (%)	CE test 3 (filter only) (%)	Average CE (filter only) (%)	Uncertainty Of Average (%)
98.3	99.0	97.5	98.3	+/- 3.2

Test Instrumentation

Table 5 describes the instrumentation used for the SRNL sampler tests. The only instruments that measured critical data were the two analytical balances. The tolerances of these instruments were verified by calibrations (or calibration checks) before and after usage.

Table 5: Test Instrumentation

Item	Designation	M&TE #	Manufacture	Model	Range	Tolerance
Analytical Balance	N/A	WP-1007	Mettler	AX205	0 – 200 g	+/- (0.01 %RDG + 0.3 mg)
Analytical Balance	N/A	SL-1004	Mettler	PR2004	0 – 2000 g	+/- 0.0012 g ¹
Linear Motor Flow Rate	LM FLOW	TR-00138	Cole-Parmer	10A6132N	1.5 – 21 gph ² liq., sg 1, 1 cps	+/- 2 %FS
Linear Motor Pressure	P _{LM}	TR-03949	WIKA	N/A	0 – 160 psig	+/- 3 %FS
Drill Motor Flow Rate	DM FLOW	N/A	Brooks	1305EJ19CL	1 – 10 scfm air 14.7 psia, 70°F	N/A
Drill Motor Pressure	P _{DM}	TR-03950	WIKA	N/A	0 – 160 psig	+/- 3 %FS
Eductor Supply Flow Rate	V1 FLOW	N/A	N/A	N/A	1 – 15 scfm air STP	N/A
Eductor Supply Pressure	P _V	TR-03951	SPAN	N/A	0 – 160 psig	+/- 3 %FS
Eductor Outlet Flow Rate	V2 FLOW	N/A	Blue & White	F-410	2 – 20 gpm ² sg 1	N/A
Eductor Vacuum	V	TR-03952	N/A	N/A	-30 in Hg to 60 psig	+/- 3 %FS
Drill Motor RPM	N/A	TR-03817	Cole-Parmer	8199-41	2.5-100,000 rpm	+/- 2 %RDG
Barometer	N/A	TR-01503	Sensotec	EB/125-01/060	26 – 32 in Hg	+/- 0.12 %RDG
Room Temperature	N/A	TR-03667 TR-03769	Barnart Cole-Parmer	600-1075 EW93210-50	-40 to 125°C	+/- 0.2°C
Hole depth	N/A	TR-00499	Starrett	No. 445 (1" rod)	0 – 1 in	+/- 0.001 in
Hole Width	N/A	N/A	Starrett	No. 120	0 – 6 in	N/A

1. This tolerance was calculated from Before and After Use calibration data. The stated instrument tolerance was +/- (0.01 % rdg + 0.3 mg), which would be too detrimental at the measurement mass of 520 grams. Therefore, a less restrictive tolerance was calculated for data at and around 500 grams and assigned to this instrument.
2. These instruments display units of liquid flow rate. Using Appendix F, the output was converted to units of air flow rate.

APPENDIX C. Salt Sample Processing



SRNL-L7400-2009-00008

September 10, 2009

TO: R. A. Leishear, 786-5A

FROM: P. E. Zapp, 773-A *PEZ*
Charles Hoffman
 Technical Reviewer

Kurtine E. Zeigler
 Manager, Materials Performance and Corrosion Technology
Preparation of Wall Sampler Test Specimens**Summary**

Materials Science & Technology provided specimens of ASTM A285 carbon steel to Engineering Development Laboratory personnel for use in evaluating the collection efficiency of the waste tank wall sampler. Specimens were provided as requested with four surface conditions: 1) corroded, mill-scale surface, (2) machined surface (electro-discharge machined), (3) salt-coated mill-scale surface, and (4) salt-coated machined surface. Most salt-coated specimens were prepared by evaporating a solution of sodium carbonate, sodium nitrate, and sodium nitrite; a few were prepared with sodium carbonate only. The thicknesses of the mixed sodium salt coating ranged from 0.005 to 0.130 inches.

Report

Materials Science & Technology provided specimens of ASTM A285 carbon steel to Engineering Development Laboratory personnel for use in evaluating the collection efficiency of the waste tank wall sampler. The specimens, ASTM A285 carbon steel provided by MS&T, were machined by the Robotics, Remote and Specialty Equipment machine shop according to a drawing provided by EDL personnel. One-eighth-inch-thick sheet stock was cut from the A285 plate by wire electro-discharge machining (EDM). Sheet stock was prepared with the existing corroded, mill-scale surface of the A285 plate or with the EDM surface. The approximately 1-inch-square test specimens were EDM-cut from the sheet stock.

Test specimens were provided as requested with four surface conditions: 1) corroded, mill-scale surface, (2) machined surface (electro-discharge machined), and (3) salt-coated mill-scale surface

We Put Science To Work™

The Savannah River National Laboratory is managed and operated for the U.S. Department of Energy by

SAVANNAH RIVER NUCLEAR SOLUTIONS, LLC
 Aiken, SC USA 29808 • SRNL.DOE.GOV

(specimens 1R – 9R), and (4) salt-coated machined surface (specimens 1E – 11E). Figure 1 is a photograph of a corroded, mill-scale surface specimen and an EDM surface specimen.

The salt-coated specimens were prepared by evaporating a sodium salt solution on heated test specimens. The majority of salt-coated specimens were prepared with a solution of 0.27 M sodium carbonate, 1.71 M sodium nitrate, and 1.62 M sodium nitrite. These concentrations were taken from the Tank 19 composition dated June, 1990. Residual salt, if any, on the tank wall is expected to have derived from this liquid composition. (Salt derived from a solution that contained sodium hydroxide redissolved in room air.) The salt was built up on the selected test specimens by warming the specimens on a hot plate to less than 100°C (to avoid boiling the solution) and applying drop wise the salt solution. Salt was built up in this manner in about 30 minutes to a target thickness of about 0.06 inches (60 mils). Figure 2 is a photograph of the typical salt-coated specimens. Actual salt thicknesses were variable as seen in Table 1. The listed thicknesses were measured with an optical microscope equipped with a digital micrometer, and represent data from six approximately equally spaced locations on the deposited salt.

Specimens were also prepared with an evaporated solution of sodium carbonate. Salt thicknesses were not measured for these specimens, and the sodium carbonate salt proved to be less adherent than that derived from the solution of sodium carbonate with sodium nitrate and sodium nitrite.



Figure 1. Mill-scale specimen (left) and EDM-cut specimen (right).

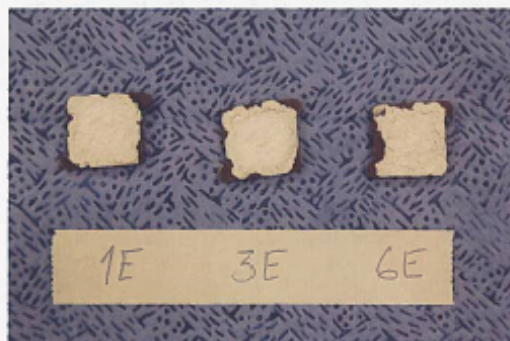


Figure 2. Salt-coated, machine-surface specimens.

Table 1. Measure Thicknesses of Deposited Salt

Mill-Scale Surface		EDM Surface	
Specimen Number	Thickness in mils	Specimen Number	Thickness in mils
1R	15	1E	70
	18		55
	27		72
	14		55
	27		50
2R	34		64
	9	3E	47
	7		60
	9		57
	10		53
	13		52
3R	5		44
	20	6E	48
	26		45
	20		70
	14		71
4R	21		63
	25		45
	41	2E	55
	33		54
	46		54
5R	57		30
	43		47
	36		56
	30	4E	57
	46		43
6R	56		40
	39		73
	54		53
	73		56
	96	5E	60
7R	108		106
	78		130
	70		110
	72		110
	45		77
8R	44	7E	65
	50		46
	51		56
	50		46
	50		49
9R	39		51
	42	8E	40
	33		44
	54		47
	45		51
	45		46
	43		45
	38	9E	57
	35		67
	44		65
	44		39
	67		45
			49
		10E	50
			66
			52
			66
			56
		11E	100
			57
			50
			42
			50
			46
			55

APPENDIX D: Vibration Data for Sampler Assembly

Virginia Vaughn/SRR/Srs

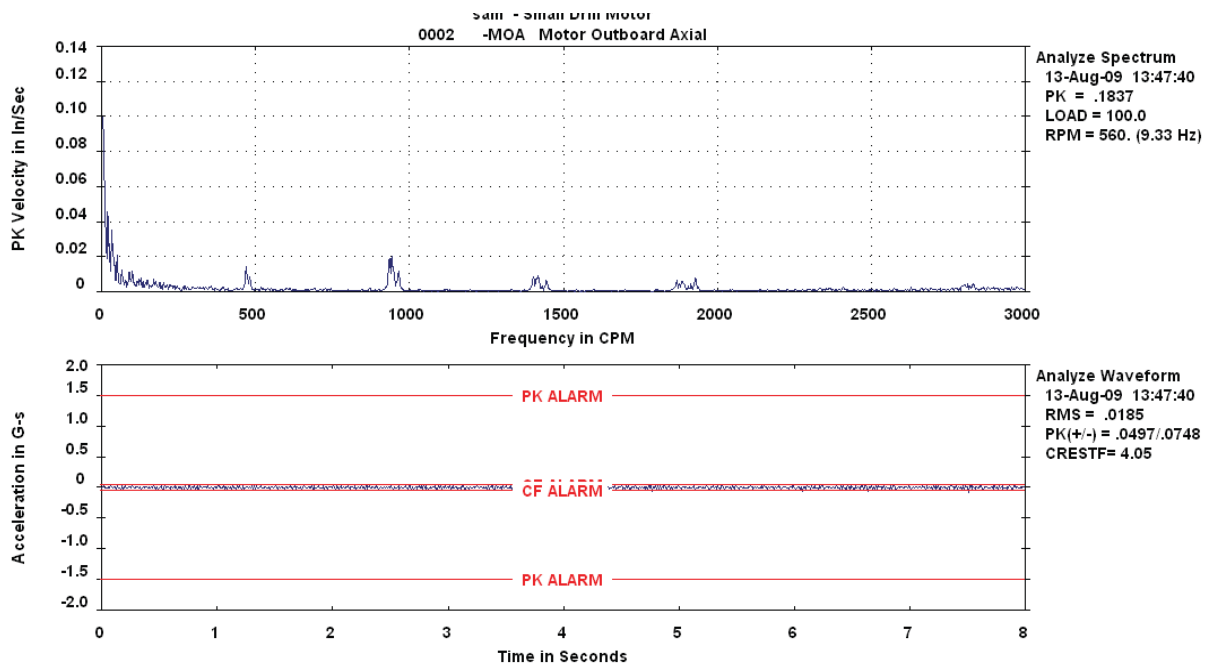
08/13/2009 03:17 PM

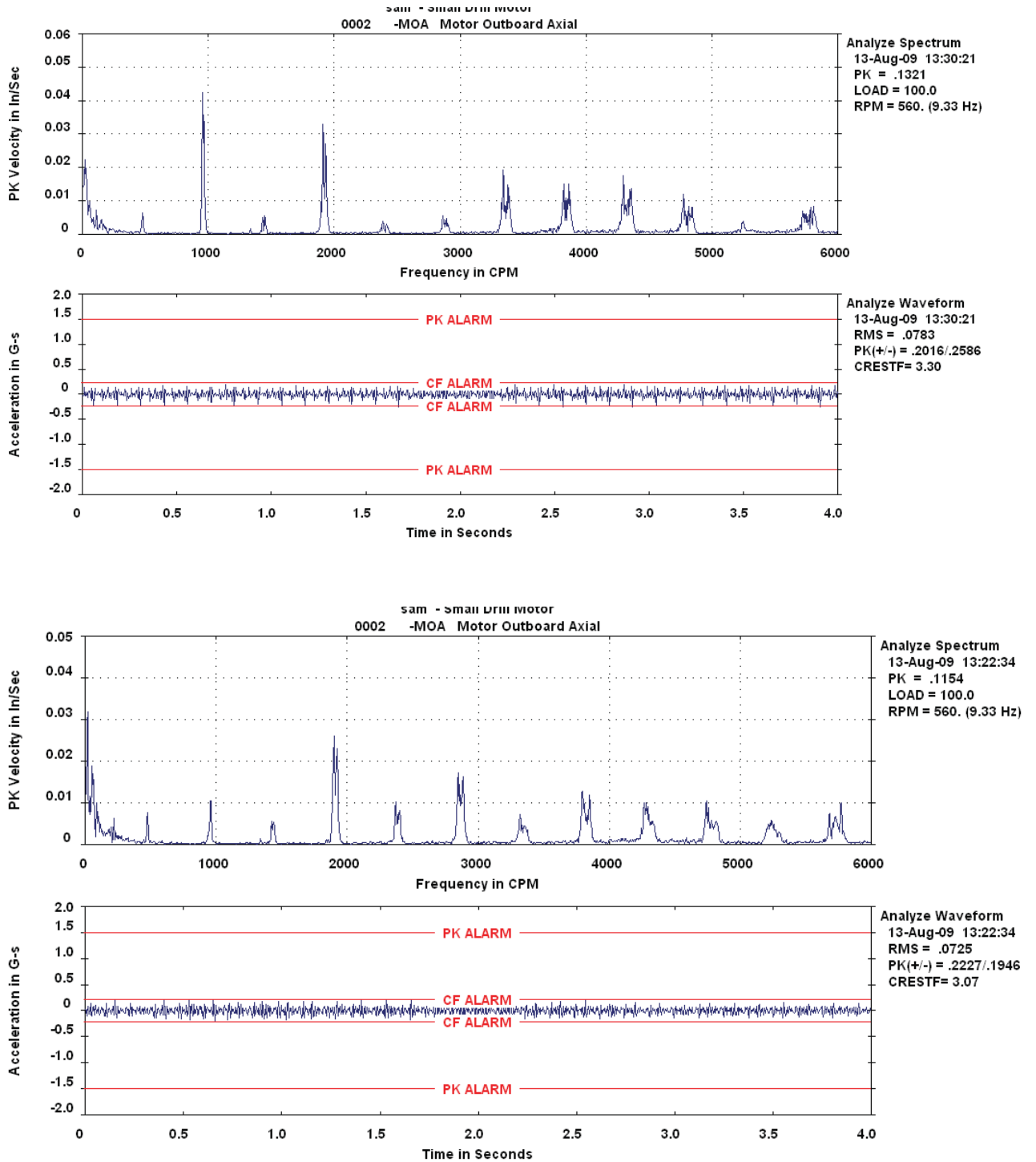
To Robert Leishear/SRNL/Srs@Srs

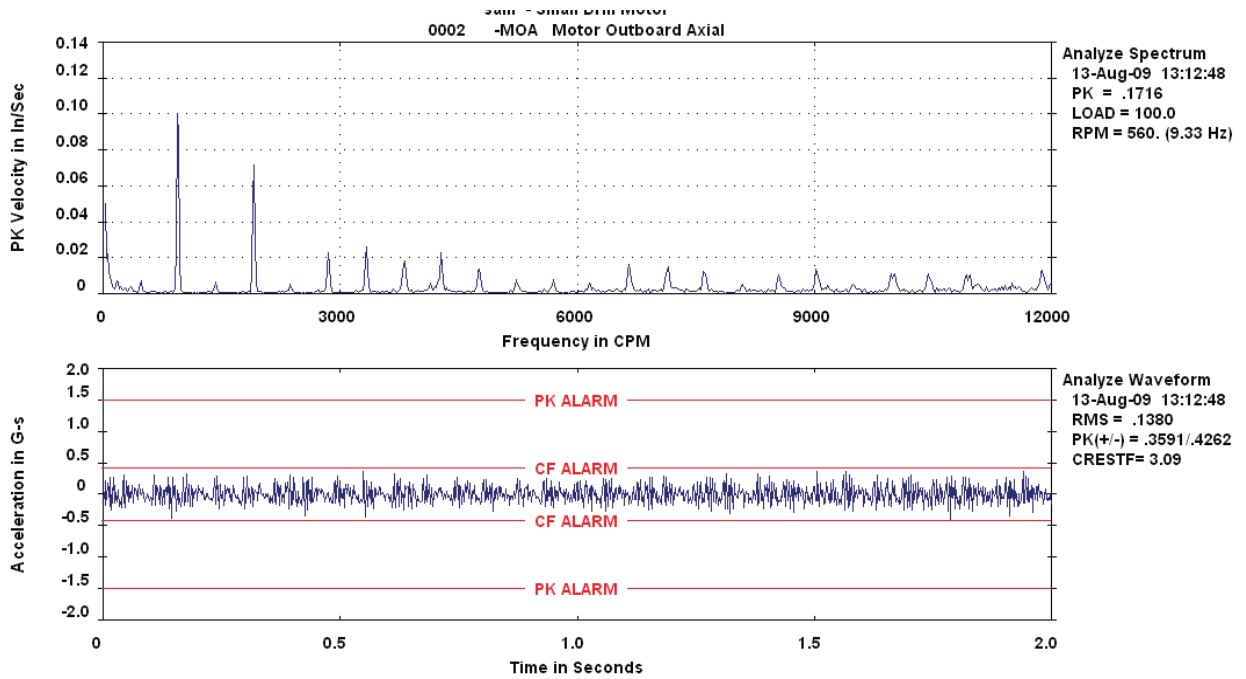
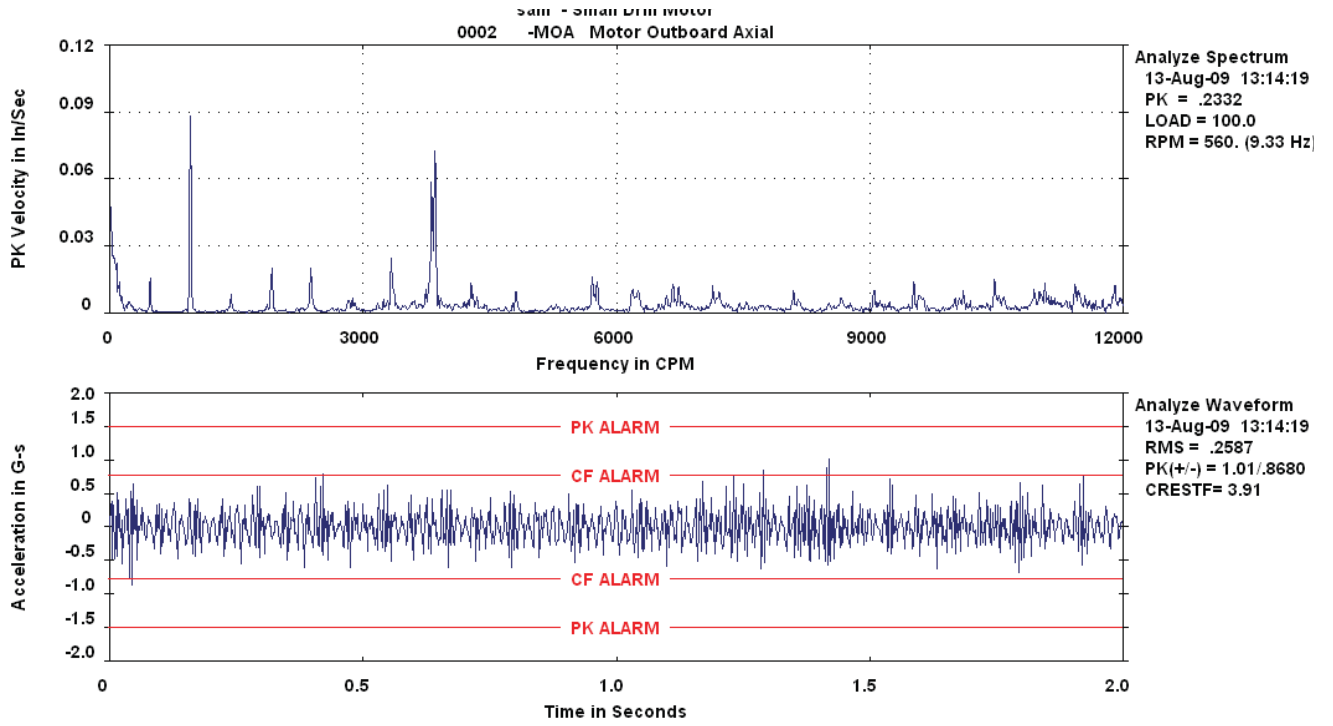
cc Anthony Wells/SRR/Srs@Srs, David
Gleaton/WSRC/Srs@Srs, Albert Tanner/SRR/Srs@Srs
Fw: Small Drill Motor

Bob,

Below are the readings that were taken on the Drill Motor: Note: Data was taken at different frequencies.







APPENDIX E: Resonance in Structures

Proceedings of the ASME 2010 Pressure Vessels & Piping Division / K-PVP Conference
PVP2010
July 18-22, 2010, Bellevue, Washington, USA

PVP2010-25266

Higher Mode Frequency Effects on Resonance in Structures

Robert A. Leishear
Savannah River National Laboratory
Aiken, South Carolina, 29803
803-725-2832
Robert.Leishear@SRNL.DOE.gov

ABSTRACT

The complexities of resonance in multi-degree of freedom systems (multi-DOF) may be clarified using graphic presentations. Multi-DOF systems represent actual systems, such as beams or springs, where multiple, higher order, natural frequencies occur. Resonance occurs when a cyclic force is applied to a structure, and the frequency of the applied force equals one of the natural frequencies. Both equations and graphic presentations are available in the literature for single degree of freedom (SDOF) systems, which describe the response of spring-mass-damper systems to harmonically applied, or cyclic, loads. Loads may be either forces or forced displacements applied to one end of the spring. Multi-DOF systems are typically described only by equations in the literature, and while equations certainly permit a case by case analysis for specific conditions, graphs provide an overall comprehension not gleaned from single equations. In fact, this collection of graphed equations provides novel results, which describe the interactions between multiple natural frequencies, as well as a comprehensive description of increased vibrations near resonance.

KEYWORDS

Resonance, multi degree of freedom, single degree of freedom, transmissibility, dynamic stress, bending of beams, critical speeds.

SYMBOLS

C	damping coefficient, Newtons/ meter/second
d	diameter, meters
$C_{critical}$	critical damping coefficient, Newtons/ meter/second
DOF	degree of freedom
E	modulus of elasticity, Newtons/ meter ²
f	forcing frequency, cycles / second
f_n	natural frequency, cycles / second

F_0	force, Newtons
I	moment of inertia, meters ⁴
j	constant
k	spring constant, Newtons / meter
L	length, meters
m	mass, kilogram
N_c	number of coils
p	period, seconds
r	radius, meters
St	static stress, Newtons / meters ²
t	time, seconds
TR	transmissibility
x	variable displacement of a mass, meters
x_0	constant vibration amplitude of a forcing function, meters
x_i	initial displacement from equilibrium, meters
x_{max}	maximum vibration amplitude for a mass, meters
y	variable displacement of a support, meters
y_0	constant vibration amplitude of a displacement function, meters
y_{max}	maximum vibration amplitude for a support, meters
z	distance, meters
ω	excitation force frequency, radian / second
ω_n	natural frequency, radian / second
ω_i	modal frequencies: $\omega_1, \omega_2, \dots, \omega_{\infty}$ radian / second
ϕ	phase angle for steady state vibration, radians
ρ	mass density, kg / meter ³
σ_{max}	maximum dynamic stress, Newtons / meters ²
θ	phase angle for free vibration, radians
ζ	damping factor

INTRODUCTION

To simplify this discussion of resonance, the maximum values of harmonic vibrations will be considered for linear, elastic structures. The structural material is assumed to be elastic

and linear, where elastic materials will not permanently deform, and linear materials have a constant stiffness. When a structure vibrates due to a varying applied load, the structure vibrates at multiple frequencies. These natural frequencies are known for many simple structures, such as axially loaded rods and helical springs; and transversely loaded beams with different support conditions, such as fixed or free ends. The vibration at any point in a structure is simply the sum of the vibrations acting at that point due to each of the vibrations, or responses, of each modal frequency caused by the forcing function, or excitation force, which may be either a changing force applied to the structure, or a changing position, or displacement, of the structural supports. For the examples considered here, the applied forces and displacements are assumed to act as steady state sinusoidal functions.

When the frequency of the forcing function equals a natural frequency of a structure, resonance exists, and in the absence of damping the structure vibrates with an infinite magnitude. However, all real structures have some damping and the maximum vibration is limited. Even so, the response of the structure is magnified. For example, common helical springs frequently have transmissibilities (TR) exceeding 100 (Thomson [1]), where the transmissibility equals the transmitted force divided by the applied force. For the case of a spring with $TR = 100$, a weight slowly added to the end of a spring will stretch the spring to a specific length at rest, or static equilibrium. If that same weight is applied using a sinusoidal forcing function at resonance, the maximum length of the spring equals 100 times the length of the spring at rest.

Although this example is drastic, a typical implication is that acceptable vibrations may be greatly magnified and cause equipment damage if resonant conditions exist. Resonance will first be considered here for simple systems with a single natural frequency, followed by consideration of systems with multiple natural, or modal, frequencies, i.e., first mode, second mode, etc.

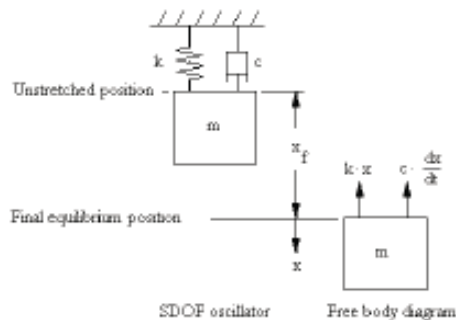


Figure 1: Free Vibration (Thomson [1])

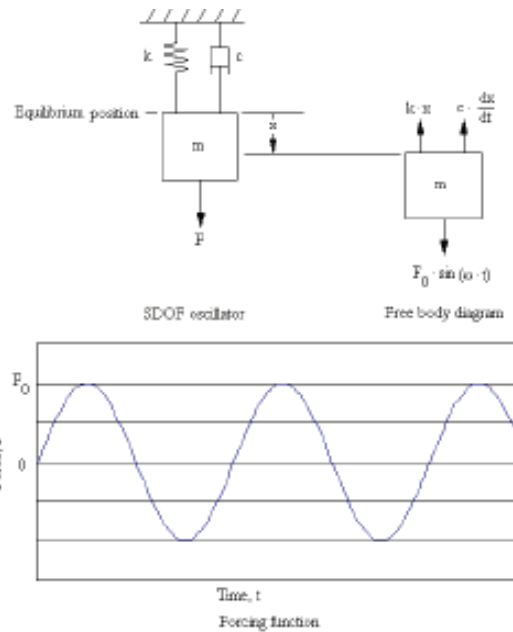


Figure 2: Load Controlled SDOF Oscillator (Thomson [1])

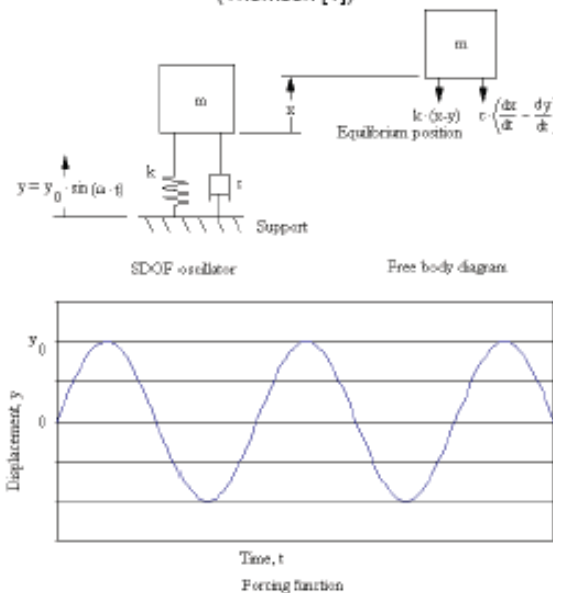


Figure 3: Displacement Controlled SDOF Oscillator (Thomson [1])

SDOF SYSTEMS

To introduce resonance, single degree of freedom (SDOF) systems are used as examples. Even though these examples are presented in detail in the literature (Thomson [1]), they are summarized here to lead into a discussion of multi-DOF systems. Structures are simplified as SDOF oscillators, consisting of a spring, a mass, and a damper, as shown in Figs. 1 & 2. The oscillator is assumed to vibrate in response to an excitation force: which can be a changing force (load control), a changing displacement of the supports (displacement control), or a free vibration, which represents stretching the spring to its equilibrium position and releasing the mass.

SDOF Equation of Motion

The dynamic response of an oscillator is described in terms of Newton's equation of motion.

$$m \cdot \frac{d^2x}{dt^2} + c \cdot \frac{dx}{dt} + k \cdot x = f(t) \quad (1)$$

where m is the mass of the object; k is the spring constant; c is a constant, linear damping coefficient; $f(t)$ describes the excitation force as a function of time, t ; and

$$\frac{d^2x}{dt^2} \quad (2)$$

equals the instantaneous acceleration of the mass, and

$$\frac{dx}{dt} \quad (3)$$

equals the instantaneous velocity of the mass. For constant, linear damping coefficients, Eq. 1 yields

$$m \cdot \frac{d^2x}{dt^2} + 2 \cdot \zeta \cdot \omega_n \cdot \frac{dx}{dt} + \omega_n^2 \cdot x = f(t) \quad (4)$$

$$\zeta = \frac{c}{2 \cdot m \cdot \omega_n} = \frac{c}{c_{critical}} \quad (5)$$

$$\omega_n = \sqrt{\frac{k}{m}} = 2 \cdot \pi \cdot f_n \quad (6)$$

$$p_n = \frac{1}{f_n} = \frac{2\pi}{\omega_n} \quad (7)$$

where ω_n is the natural frequency in radians / second; f_n is the natural frequency in cycles per second; p_n equals the period of the natural frequency which is the time between successive peaks of vibration; $c_{critical}$ is the critical damping factor; and ζ is the damping factor. Damping and frequency effects can be described using a free vibration equation.

SDOF Free Vibration

To evaluate free vibration, assume that the spring has an initial displacement, x_f , such that $x = x_f = \text{constant}$ at $t = 0$. Equation 4 yields

$$m \cdot \frac{d^2x}{dt^2} + 2 \cdot \zeta \cdot \omega_n \cdot \frac{dx}{dt} + \omega_n^2 \cdot x = 0 \quad (8)$$

$$x = x_f \cdot e^{-\zeta \cdot \omega_n \cdot t} \cdot \sin\left(\sqrt{1 - \zeta^2} \cdot \omega_n \cdot t + \phi\right) \quad (9)$$

$$\omega_d = \omega_n \cdot \sqrt{1 - \zeta^2} \quad (10)$$

$$p_d = \frac{1}{f_d} = \frac{2\pi}{\omega_d} \quad (11)$$

where ω_d , f_d , p_d are the circular frequency, frequency, and period for damped vibration, respectively; and ϕ is the phase angle.

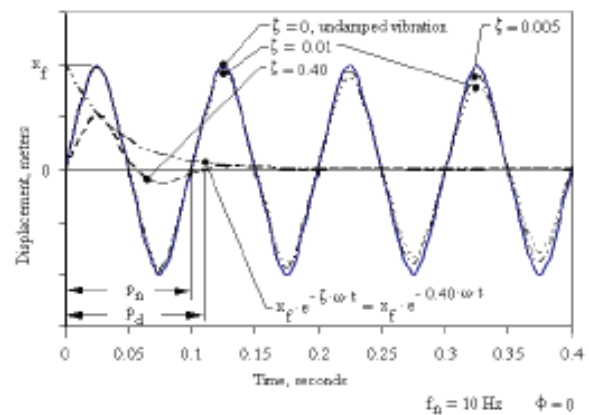


Figure 4: Example of Damped and Undamped Free Vibrations, Eq. 9

Damping effects. Free vibrations are graphed in Fig. 4 to demonstrate the effects of damping and clarify nomenclature. In the figure, p_d is shown for 40% damping, since p_d for 1% damping is near the undamped period, p_n , of the natural frequency. Different damping values are presented, where 0.5 - 6.0% damping is the range of damping values for steel structures, 7 - 14% is the range for concrete structures, 15 - 40 % is the range for masonry structures (Pilkey [2]), and damping for helical springs drops below 0.005% (Harris and Piersol [3]).

Note that $e^{-\zeta \cdot \omega_n \cdot t}$ bounds each sinusoidal response, and varies with the damping ratio, ζ . The exponential function is only shown for the 40% damping case.

Damping ratio. Vibrations in structures occur for positive damping ratios, $1 > \zeta > 0$. Vibrations are critically damped when $c = c_{critical}$, $\zeta = 1$, and vibrations do not occur. Below $\zeta = 1$, nonoscillatory motion occurs and the system returns to equilibrium. Between $\zeta = 0$ and $\zeta = 1$, vibrations decay to

equilibrium in the absence of a forcing function. For $\zeta = 0$, the system is undamped and constant amplitude, natural frequency vibrations theoretically continue unabated even in the absence of a forcing function. For $\zeta < 0$, the system is unstable, and once initiated, vibrations increase without limit in the absence of a forcing function. Although numerous damping models are available, constant damping used here provides many simplifications to approximate structural behavior.

Phase angle effects. The relationship of phase angle to vibration is shown in Fig. 5. As a special case, a spring is stretched to a length, x_f , and then released. Then $\phi = \pi/2$, and the response is shown in the figure. An arbitrarily selected phase angle of $\phi = \pi/4$ is also shown in the figure.

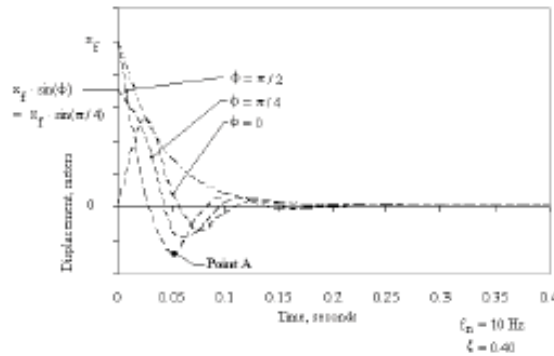


Figure 5: Phase Angle Effects on Vibration Amplitude, Eq. 9

Having defined nomenclature, Eq. 4 provides the basis for load or displacement controlled equations of motion. The above mathematical relationships for periods, frequencies, and damping ratios are, of course, the same for all vibrations considered here.

SDOF Load Control

Load control is shown in Fig. 1, and to describe the oscillator motion assume that

$$m \cdot \frac{d^2 x}{dt^2} + 2 \cdot \zeta \cdot \omega_n \cdot \frac{dx}{dt} + \omega_n^2 \cdot x = F_0 \cdot \sin(\omega \cdot t) \quad (12)$$

To solve this differential equation, a particular solution for the displacement is assumed to be

$$x = x_0 \cdot \sin(\omega \cdot t - \theta) \quad (13)$$

where ω is the circular frequency of the applied force, x_0 is the amplitude of the impressed vibration, and θ is the phase of the displacement vibration with respect to the phase of the excitation force. Note that θ and ϕ may be the same, but need not be

equal, depending on the boundary conditions. Equations 12 and 13 can be solved to yield the displacement at any time, t , to yield

$$x = \frac{F_0 \cdot \sin(\omega \cdot t - \theta)}{k \cdot \sqrt{\left(1 - \left(\frac{\omega}{\omega_n}\right)^2\right)^2 + \left(\frac{2 \cdot \zeta \cdot \omega}{\omega_n}\right)^2}} + x_f \cdot e^{-\zeta \cdot \omega_n \cdot t} \cdot \sin\left(\sqrt{1 - \zeta^2} \cdot \omega_n \cdot t + \phi\right) \quad (14)$$

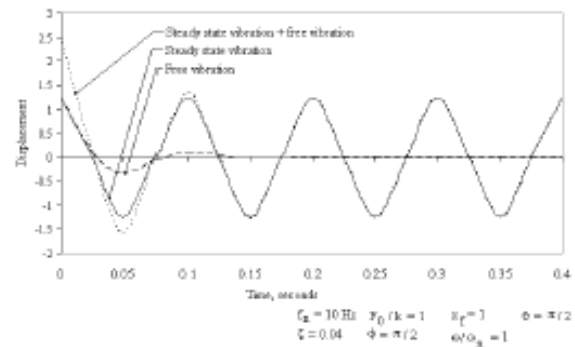


Figure 6: SDOF Load Controlled Vibrations, Free Vibration and Steady State Vibration, Eq. 14

An example of load control (Eq. 14) is shown in Fig. 6. This example displays the vibration when a spring is stretched, and the applied load is in phase with the free vibration, where the total initial force is applied at time, $t = 0$. Terms were arbitrarily selected: where the force / displacement ratio is expressed as a unit displacement ($x_0 = F_0 / k = 1$), the initial position is expressed as a unit displacement, $x_f = 1$, and the frequency was arbitrarily selected.

Compare the steady state vibration to the cumulative vibration shown in the figure to justify neglecting the transient free vibration. Note that the free vibration (for $\phi = \pi/2$) has a decreasing effect on vibrations, and the transient vibration reduces x_{max} , which is the length that the spring is initially stretched. That is, the transient and steady state vibrations are additive from Eq. 14, and the negative transient vibration subtracts from the amplitude. In successive periods, the transient approaches zero. The damped transient affects vibration for only the initial vibration cycles, and for this example the damped vibration serves to increase the maximum amplitude. If θ and ϕ are equal and the vibrations are in phase, the free and steady state vibrations add, and the total vibration is higher during the initial cycles. In other words, the free vibration is typically neglected, but free vibration has an effect on vibration during the initial vibration cycles. For many cases, x_f equals zero and so does the free vibration.

Steady state, load controlled vibration. Considering only the steady state, forced vibration, the transient free vibration term may be neglected. To do so, assume that the system is initially at rest, and the spring is stretched to the equilibrium position, where $t = 0$, $x = x_s = 0$, and $dx/dt = 0$. Load controlled vibrations are then described, using

$$x = \frac{F_0 \cdot \sin(\omega \cdot t - \theta)}{k \cdot \sqrt{\left(1 - \left(\frac{\omega}{\omega_n}\right)^2\right)^2 + \left(\frac{2 \cdot \zeta \cdot \omega}{\omega_n}\right)^2}} \quad (15)$$

$$\phi = \tan^{-1} \left(\frac{2 \cdot \zeta \cdot \omega_n}{1 - \left(\frac{\omega}{\omega_n}\right)^2} \right) \quad (16)$$

From Eq. 15, the maximum amplitude at resonance equals

$$x_{\max} = \frac{F_0}{2 \cdot \zeta \cdot k} \quad (17)$$

Figure 7 provides examples for the effects of forcing frequency. Vibrations with damping values of 1% are displayed for values of $\omega / \omega_n = 0.5$ and $\omega / \omega_n \approx 1.0$. A unit displacement, $1 = k / F_0$, is used to simplify Fig. 7, although unit displacement is atypical for most systems. Effects on both amplitude and phase are readily observed, since only the frequency of the impressed force is altered for the figure.

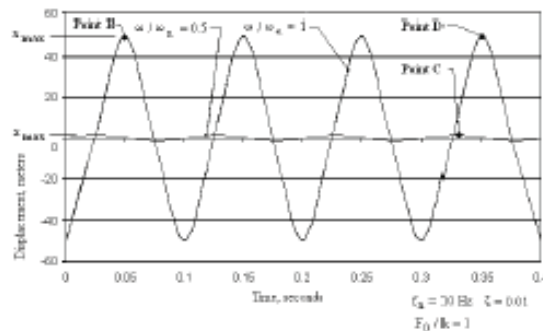


Figure 7: Example of Steady State, Load Controlled Vibrations, Eq. 15

Damping and frequency effects on transmissibility during load controlled vibration. Since a unit displacement was used in Fig. 7, transmissibility simply equals $TR = x_{\max} = k \cdot x_{\max} / F_0$, where transmissibility is defined as the maximum vibration amplitude divided by the static impressed force. When $\omega / \omega_n = 0$, the applied force is constant, the load is

static, and $TR = 1$. For the examples in Fig. 6, the amplitude, x_{\max} , increases from $TR = 1.3$ at point C to $TR = 50$ at point D for 1% damping when ω / ω_n is doubled from 0.5 to 1.0. This large increase in amplitude clearly shows the effects at resonance.

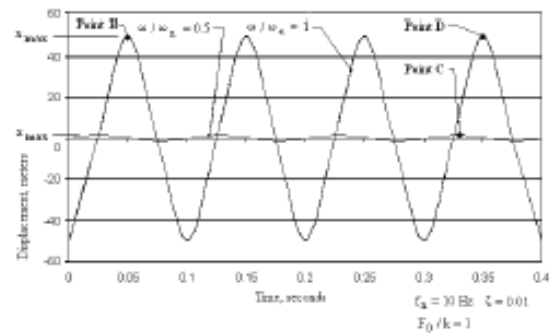


Figure 7: Example of Steady State, Load Controlled Vibrations, Eq. 15

Transmissibility for load control. To visualize transmissibility over a range of frequencies, non-dimensional transmissibility is typically presented in the literature. An expression for transmissibility is derived from Eq. 15, such that

$$TR = \frac{x_{\max} \cdot k}{F_0} = \frac{1}{\sqrt{\left(1 - \left(\frac{\omega}{\omega_n}\right)^2\right)^2 + \left(\frac{2 \cdot \zeta \cdot \omega}{\omega_n}\right)^2}} \quad (18)$$

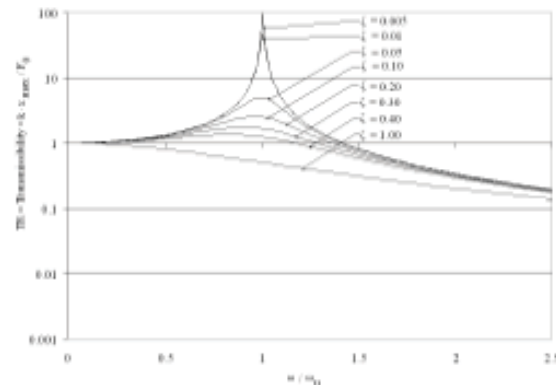


Figure 8: Transmissibility for Steady State Load Control, (Log Scale), Eq. 18 (Thomson [1])

Figure 8 logarithmically shows the effects of damping and transmissibilities which approach zero with increasing non-dimensional frequencies, ω / ω_n . Figure 9 shows the same data to scale.

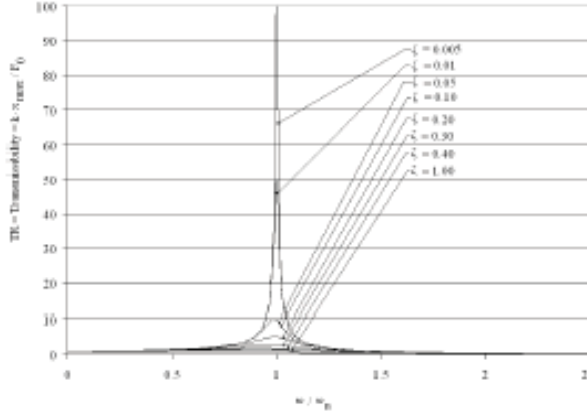


Figure 9: Transmissibility for Steady State Load Control, (Linear Scale), Eq. 18 (Thomson [1])

SDOF Displacement Control, Support Motion

For displacement control, consider Fig. 3. Assuming, $y = y_0 \cdot \sin(\omega \cdot t)$, the equation of motion is expressed as

$$m \cdot \frac{d^2(x-y)}{dt^2} + 2 \cdot \zeta \cdot \omega_n \cdot \frac{d(x-y)}{dt} + \omega_n^2 \cdot (x-y) = m \cdot \frac{d^2(y_0 \cdot \sin(\omega \cdot t))}{dt^2} = m \cdot \omega^2 \cdot y_0 \cdot \sin(\omega \cdot t) \quad (19)$$

where y_0 is the vibration amplitude of the support, and x and y are the local coordinates for the mass and the support respectively. Neglecting free vibration,

$$x - y = \frac{m \cdot \omega^2 \cdot y_0 \cdot \sin(\omega \cdot t - \phi)}{\sqrt{\left(1 - \left(\frac{\omega}{\omega_n}\right)^2\right)^2 + \left(\frac{2 \cdot \zeta \cdot \omega}{\omega_n}\right)^2}} \quad (20)$$

Then the steady state transmissibility is shown in Figure 10 and is expressed by Eq. 21, which closes this discussion on SDOF systems. There are other SDOF systems described in the literature, but consideration is limited here to load and displacement controlled vibrations as they are related to higher order vibrations.

$$TR = \frac{|x_{\max}|}{y_0} = \frac{\sqrt{1 + \left(\frac{2 \cdot \zeta \cdot \omega}{\omega_n}\right)^2}}{\sqrt{\left(1 - \left(\frac{\omega}{\omega_n}\right)^2\right)^2 + \left(\frac{2 \cdot \zeta \cdot \omega}{\omega_n}\right)^2}} \quad (21)$$

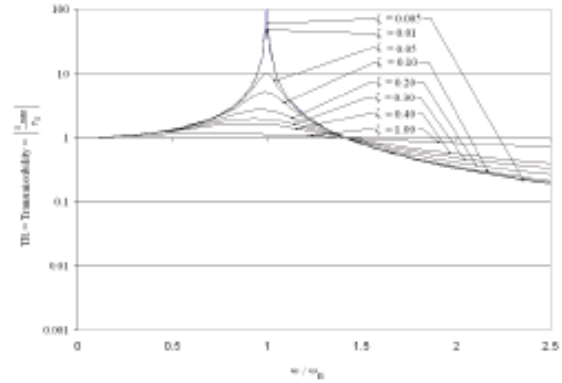


Figure 10: Transmissibility for Displacement Controlled Vibration (Support Motion), Eq. 21 (Thomson [1])

VIBRATIONS AND HIGHER ORDER FREQUENCIES

Structures are multi-DOF systems, where the degrees of freedom are a series of natural frequencies, $\omega_1 = \omega_1, \omega_2, \dots, \omega_{\infty}$ at which a structure vibrates. For the case of linear damping, the equations of motion are uncoupled. That is, each higher mode frequency of a system may be considered independently. For this discussion, equations to describe higher mode vibration equations are developed here for both load and displacement controlled vibrations, and these equations are combined with available frequency equations for some structures to investigate modal effects on structural response.

Multi-DOF Load Control

For load controlled vibrations, some cases may be described by assuming that each frequency is described by a sin response, where

$$m \cdot \frac{d^2 x_i}{dt^2} + 2 \cdot \zeta_i \cdot \omega_i \cdot \frac{dx_i}{dt} + \omega_i^2 \cdot x_i = F_0 \cdot \sin(\omega \cdot t) \quad (22)$$

$$x_i = \frac{F_0 \cdot \sin(\omega \cdot t - \theta)}{k_i \cdot \sqrt{\left(1 - \left(\frac{\omega}{\omega_i}\right)^2\right)^2 + \left(\frac{2 \cdot \zeta_i \cdot \omega}{\omega_i}\right)^2}} \quad (23)$$

$$\omega_i^2 = \frac{k_i}{m} \Rightarrow k_i = \frac{\omega_i^2 \cdot m}{1} \quad (24)$$

where x_i and k_i are displacements and frequencies associated with each mode, i . These equations are used here to describe the maximum response of springs, axially loaded rods, and simply supported beams.

As shown in Fig. 11, the discrete modal vibration magnitudes add to yield the total vibration. Participation factors

approximate the contribution of each mode to the vibration, our participation factors are available for only a few cases in the literature.

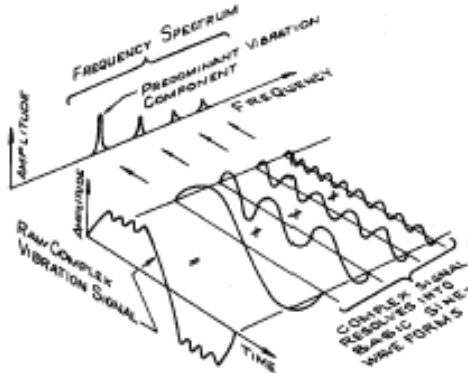


Figure 11: Vibration Frequencies (Karrassik [4])

Load Controlled Vibrations for Springs

Spring displacements can be described in terms of higher mode frequencies, where the frequencies for common steel springs are expressed as

$$\omega_i = \frac{i \cdot 22.05 \cdot d}{r^2 \cdot N_c} \quad (25)$$

where d is the diameter of the spring wire, r is the mean radius of the helix, and N_c is the number of active coils

Modal Contributions for Spring Vibrations. Figure 12 shows the contribution of other vibration frequencies to a fundamental mode, in this case the first mode. This contribution to the overall vibration is sometimes referred to as a participation factor, where each of the modal frequencies is affected by vibrations from other modes.

To consider these effects due to other modes on a primary mode of vibration for springs, first substitute Eq. 24 into Eq. 23 to yield

$$x_i = \frac{\omega_1^2 \cdot F_0 \cdot \sin(\omega \cdot t - \theta)}{\omega_i^2 \cdot k_1 \cdot \sqrt{1 - \left(\frac{\omega}{\omega_i}\right)^2 + \left(\frac{2 \cdot \zeta \cdot \omega}{\omega_i}\right)^2}} \quad (26)$$

Set $F_0/k_1 = x_0 = 1$, and from Eq. 25 for a spring note that

$$\frac{\omega_1^2}{\omega_i^2} = \frac{1}{i^2} \quad (27)$$

Then, vibration is described for each mode as

$$x = \sum_{i=1}^{\infty} x_i \approx \sum_{i=1}^j x_i = \sum_{i=1}^j \frac{\sin(\omega \cdot t - \theta)}{i^2 \cdot \sqrt{1 - \left(\frac{\omega}{\omega_i}\right)^2 + \left(\frac{2 \cdot \zeta \cdot \omega}{\omega_i}\right)^2}} \quad (28)$$

where j is selected to provide reasonable accuracy. In the example of Fig. 12, j equals 25. In this figure, the first four vibration modes are shown, along with the total vibration for the first 25 modes of vibration.

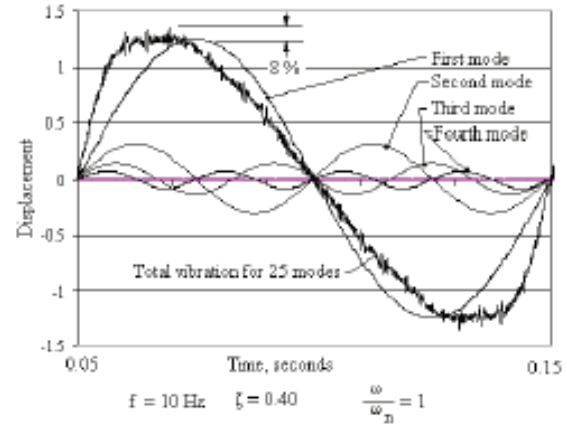


Figure 12: Participation of Higher Mode Frequencies for the First Mode for Springs, Eq. 28

Resonance occurs for each mode, and each higher mode is treated similarly when the system is excited at that modal frequency. For example, when the second mode is excited, ω_2 is treated as the fundamental natural frequency, and ω_1 is half of ω_2 , such that

$$\frac{\omega_1^2}{\omega_2^2} = \frac{1}{2^2} \quad (29)$$

and

$$x = \sum_{i=1}^{\infty} x_i \approx \sum_{i=1}^j x_i = \sum_{i=1}^j \frac{\sin(\omega \cdot t - \theta)}{2^2 \cdot \sqrt{1 - \left(\frac{\omega}{\omega_i}\right)^2 + \left(\frac{2 \cdot \zeta \cdot \omega}{\omega_i}\right)^2}} + \sum_{i=2}^j \frac{\sin(\omega \cdot t - \theta)}{i^2 \cdot \sqrt{1 - \left(\frac{\omega}{\omega_i}\right)^2 + \left(\frac{2 \cdot \zeta \cdot \omega}{\omega_i}\right)^2}} \quad (30)$$

Participation factors for the second mode are comparable to the first mode factors shown in Fig. 12. The approximate 8 % contribution of higher modes to the total vibration shown in the

figure is typical for springs. This higher mode effect can be calculated for each point on a transmissibility curve, but for the purposes of this paper the 8 % value is neglected when considering transmissibility.

Transmissibility Calculations for Vibrations of Springs. The example shown in Figs. 13 and 14 highlights a method to calculate transmissibilities due to higher mode frequencies. To explain the figures, each of the resonant frequencies is first plotted in Fig. 13, where Eq.18 is rewritten as

$$TR = \frac{x_{i,max} \cdot k_i}{F_0} = \frac{1}{\sqrt{\left(1 - \left(\frac{\omega}{\omega_i}\right)^2\right)^2 + \left(\frac{2 \cdot \zeta \cdot \omega}{\omega_i}\right)^2}} \quad (31)$$

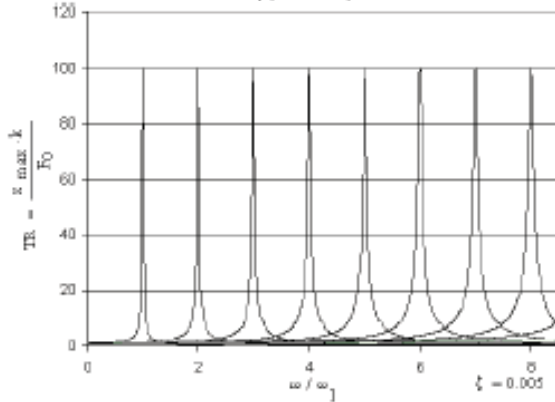


Figure 13: Example of Modal Frequencies for Load Control of a Spring, Eq. 31

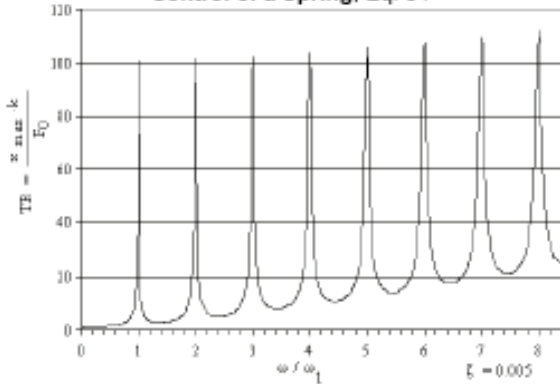


Figure 14: Transmissibility Example for Load Control of a Spring, Eqs. 32 and 33

Then, to relate transmissibilities for multiple modes, the vibration needs to be reconsidered. Each of the resonant vibrations acts separately, and the vibrations are therefore additive. However, Fig. 13 shows only the maximum

transmissibility for each modal frequency. To add the frequencies, the fact must be recognized that the transmissibilities are referenced to static equilibrium, where $TR = 1$, and only the transmissibility magnitudes with respect to $TR = 1$ are additive. Then the transmissibilities (Eq. 31) may be related by

$$\sum_{i=1}^{75} \frac{x_{i,max} \cdot k_i}{F_0} \approx TR = 1 + \sum_{i=1}^{\infty} \left(\frac{1}{\sqrt{\left(1 - \left(\frac{\omega}{\omega_i}\right)^2\right)^2 + \left(\frac{2 \cdot \zeta \cdot \omega}{\omega_i}\right)^2}} - 1 \right) \quad (32)$$

For this example, the first 75 modes were used in the calculation to ensure reasonable accuracy for highly damped vibrations ($\zeta = 0.40$), although only 8 modes are displayed in the figures. Then,

$$\sum_{i=1}^{75} \frac{x_{i,max} \cdot k_i}{F_0} \approx TR = 1 + \sum_{i=1}^{\infty} \left(\frac{1}{\sqrt{\left(1 - \left(\frac{\omega}{\omega_i}\right)^2\right)^2 + \left(\frac{2 \cdot \zeta \cdot \omega}{\omega_i}\right)^2}} - 1 \right) \quad (33)$$

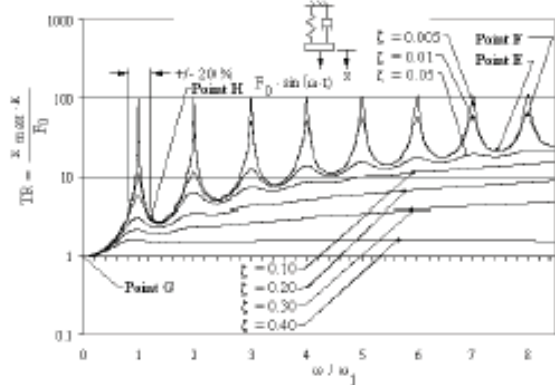


Figure 15: Multi-DOF Transmissibility for Load Control of Springs, Eqs. 32 and 33

Total Transmissibility for Vibrations of Springs. Transmissibilities are shown for different values of damping in Fig. 15. Substitution of different damping values into Eq. 33 yielded the figure. Comparing Fig. 8 to Fig. 15, the results are markedly different following the first mode vibration, with respect to increasing ω .

For example, resonance in machinery occurs at the critical speed, which is the speed, where the motor speed $= \omega = \omega_n$. Common misconceptions are that operating between resonant frequencies always corrects vibration problems, and that operating at least 10 – 20 % away from resonance always corrects vibration problems. Assume that a motor applies a force

to a spring and consider point E, where the transmissibility equals 21. If equipment is operated under these conditions at $\zeta = 1\%$ between the seventh and eighth mode frequency, the best that can be done to minimize vibrations without added damping is to operate at point E. Then TR is reduced from 62 for resonance at point F to 21 at point E. In other words, any equipment vibration is still significantly amplified for lightly damped structures, such as machinery, piping, or steel buildings. Vibrations can be reduced by operating at point E, but vibration magnitudes are still significant. The problem may, or may not, be corrected by operating between frequencies. Point H presents the first mode frequency and operating at least 20% away from resonance. The $TR = 3.4$, which again may, or may not be acceptable, depending on design and reliability requirements for the system of concern where point G represents static design.

Load Controlled Vibrations for Rods. Vibrations are similar for axially loaded rods which are fixed at one end and free to move at the other end. To calculate TR, Eq. 32 was used except that

$$\omega_i = \frac{(2 \cdot i - 1) \cdot \pi}{2 \cdot L} \cdot \sqrt{\frac{E}{\rho}} \quad (34)$$

$$\sum_{i=1}^{75} \frac{x_{i,max} \cdot k_i}{F_0} \approx TR - 1 + \sum_{i=1}^{\infty} \left(\frac{1}{\sqrt{1 - \left(\frac{1}{(2 \cdot i - 1)} \right)^2 + \left(\frac{2 \cdot \zeta \cdot i - 1}{(2 \cdot i - 1)} \right)^2}} - 1 \right) \quad (35)$$

where L is the length of the rod, E is the modulus of elasticity, ρ is the mass density, and 75 modes were used to ensure calculation accuracy.

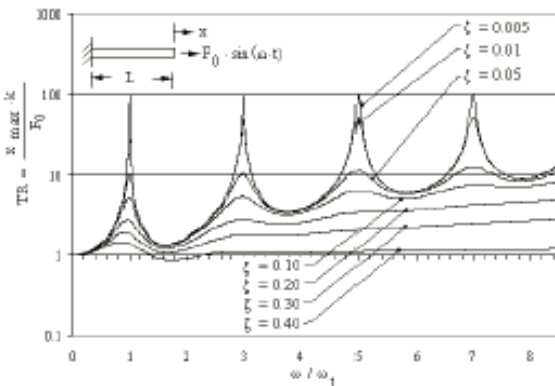


Figure 16: Transmissibility for Axially Loaded Rods, Eqs. 33 and 34

Figure 16 shows transmissibility for axially loaded rods, and Fig. 17 shows the effects of additional higher mode frequencies (Eq. 28), which are neglected here. However, note that the

overall vibrations are reduced, while the vibrations were increased for a spring.

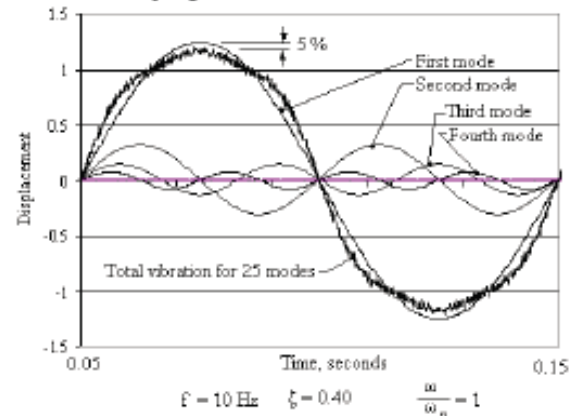


Figure 17: Participation of Higher Mode Frequencies for First Mode Response of a Loaded Rod, Eq. 28

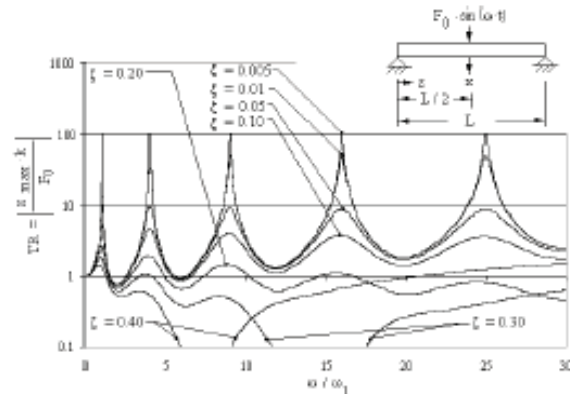


Figure 18: Transmissibility for a Simply Supported Beam, Eq. 38

Load Controlled Vibrations for Transversely Loaded Uniform Beams. The response for beams with different types of end supports can be evaluated using the techniques presented here, but this discussion is limited to the case of a beam with pinned, or hinged, supports. For this case the mode shape and frequencies are listed by (Pilekey [2]), such that

$$\text{beam_deflection_mode_shape} = \sin\left(\frac{i \cdot \pi \cdot z}{L}\right) \quad (36)$$

$$\omega_i = \frac{(i \cdot \pi)^2}{L^2} \cdot \sqrt{\frac{E \cdot I}{\rho}} \quad (37)$$

$$\sum_{i=1}^{\infty} \frac{75}{F_0} \frac{x_{i,\max} \cdot k_i}{F_0} \approx TR = 1 + \sum_{i=1}^{\infty} \left[\frac{1}{\sqrt{1 - \left(\frac{1}{i^2}\right)^2 + \left(\frac{2-\zeta \cdot i}{i^2}\right)^2}} \right] - 1 \quad (38)$$

where I is the moment of inertia, L is the length of the beam, and x is the distance along the beam from a support. The absolute value was used, since vibrations may be negative with respect to static equilibrium, but structural vibration motion is always a positive quantity.

To evaluate beam deflections with respect to resonance, assume that the vibration is sinusoidal, and that the maximum deflection occurs at the center of the beam. Both of these assumptions are consistent with Eq. 36. Then the equations presented for a spring are applicable, and all that is required is to substitute the appropriate frequencies into Eq. 32 to obtain Fig. 8. Note that as damping increases, the effects of resonance diminish significantly, due to structural stiffness.

Multi-DOF Displacement Control

An example of displacement control is provided in Fig. 19. Derivations comparable to those above are performed to describe support motion with respect to multi-DOF resonance, where

$$m \frac{d^2(x_i - y_i)}{dt^2} + 2 \cdot \zeta \cdot \omega_i \cdot \frac{d(x_i - y_i)}{dt} + \omega_i^2 \cdot (x_i - y_i) = m \cdot \omega^2 \cdot y_0 \cdot \sin(\omega \cdot t) \quad (39)$$

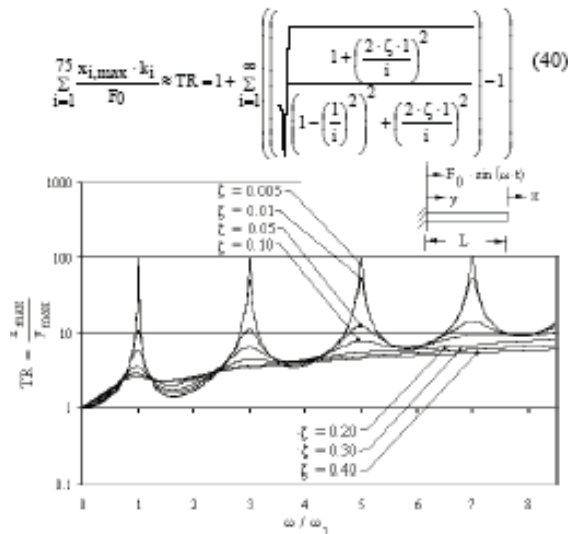


Figure 19: Support Motion for an Axially Loaded Rod, Eq. 40

Compare support motion (Fig. 19) and load control (Fig. 16) to note the similarities for light damping and differences for higher damping.

CONCLUSIONS

Resonance was considered for the components, such as vibrating springs, rods, and simply supported beams to better understand the effects of higher mode frequencies. Transmissibility was defined as the maximum value of the magnification of deflection when compared to the deflection for statically loaded components. Transmissibility was used to explain resonance along with critical speeds. Transmissibilities varied. A critical speed is defined as a resonant condition where the speed of the motor equals one of the natural frequencies of the system.

For most applications, operating above the first mode frequency results in magnified displacement, and potential equipment damage. Operating midway between critical speeds decreases the vibration, but significant vibration may still be present. For a few cases of high damping, resonance effects can be nearly eliminated. Single mode, single degree of freedom approximations were shown to be incorrect.

In short, the first comprehensive explanation of the physics associated with resonance in real structures is presented to better understand machinery, piping, vehicle, and building failures due to vibration. Novel graphic presentations provide a level of understanding for this common failure mechanism not previously available, and this advancement of vibration theory is widely applicable to safer and more reliable equipment designs and applications.

REFERENCES

- [1] Thomson, W. T., 1993, "Theory of Vibrations with Applications", Prentice hall, Englewood cliffs, New Jersey, pp. 31-80.
 - [2] Pilkey, W. D., 1994, "Stress Strain and Structural Matrices", John Wiley and Sons, New York, pp. 564, 574.
 - [3] Harris, C. M., Piersol, A. G., 2002, "Harris' Shock and Vibration Handbook", McGraw Hill, New York, pp. 2.15, 7.17, 32.9.
 - [4] Karrasik, I. J., Messina, J. P., Cooper, P., Heald, C.H., 2001, "Pump Handbook", McGraw Hill, New York, p. 2.420.
- This manuscript has been authored by Savannah River Nuclear Solutions, LLC under Contract No. DE-AC09-08SR22470 with the U.S. Department of Energy. The United States Government retains and publisher, by accepting this article for publication, acknowledges that the United States Government retains a non-exclusive, paid-up, irrevocable, worldwide license to publish or reproduce the published form of this work, or allow others to do so, for United States Government purposes.

APPENDIX F: Flow Rate Conversion Factors

Gas Service

Sizing Data

How to determine air equivalent

1. Start with your desired maximum flow. Then,
2. From Table 1, determine Gas Molecular Weight Correction Factor (F_1).
3. From Table 2, determine Pressure Correction Factor (F_2) using operating pressure in psig.

4. From Table 3, determine Temperature Correction Factor (F_3) using operating temperature in °F.
5. Multiply all: (Desired Maximum Flow) \times (F_1) \times (F_2) \times (F_3) = Air Equivalent.

Example:

Find air equivalent of 25 scfm CO₂ metered at 35 psig and 150°F.

Step 1, your flow is 25

Step 2, from Table 1, (F_1) = 1.238Step 3, from Table 2, (F_2) = 0.544Step 4, from Table 3, (F_3) = 1.073Step 5, multiply: (25) \times (1.238) \times (0.544) \times (1.073) = 18.07Table 1 — Gas Molecular Weight Correction Factor (F_1) $\sqrt{\frac{\text{Sp. Gr.}}{29}}$ or $\sqrt{\frac{\text{Mol. Wgt.}}{29}}$

Gas	Correction Factor	Gas	Correction Factor	Gas	Correction Factor
Acetylene	0.906	Ethane	1.024	Natural Gas	.775
Air	1.0	Ethylene	.988	Neon	.695
Ammonia (ANH.)	.77	Helium	.372	Nitrogen	.982
Ammonia (DISS.)	.54	Hydrogen	.264	Nitrous Oxide	1.24
Argon	1.175	Hydrogen Chloride	1.26	Oxygen	1.05
Carbon Monoxide	.982	Hydrogen Sulfide	1.18	Propane	1.25
Carbon Dioxide	1.238	Methane	.745	Sulfur Dioxide	1.504
Chlorine	1.576	Methyl Oxide	1.59		

Table 2 — Pressure Correction Factors (F_2) $\sqrt{\frac{14.7}{\text{psig} + 14.7}}$

PSIG Tens	UNITS									
	0	1	2	3	4	5	6	7	8	9
0	1.00	.966	.938	.910	.885	.863	.842	.823	.804	.787
10	.771	.756	.742	.728	.716	.704	.692	.681	.670	.660
20	.651	.642	.633	.624	.616	.609	.601	.594	.587	.580
30	.573	.567	.561	.555	.549	.544	.538	.533	.528	.523
40	.518	.514	.509	.505	.500	.496	.492	.488	.484	.480
50	.477	.473	.469	.466	.463	.459	.456	.453	.450	.447
60	.444	.441	.438	.435	.432	.429	.427	.424	.422	.419
70	.417	.414	.412	.409	.407	.405	.403	.400	.398	.396
80	.394	.392	.390	.388	.386	.384	.382	.380	.378	.377
90	.375	.373	.371	.369	.368	.366	.364	.363	.361	.360

PSIG Hundreds	TENS									
	0	10	20	30	40	50	60	70	80	90
100	0.358	.343	.3303	.3187	.3083	.2988	.2901	.2821	.2748	.2680
200	.262	.256	.2503	.2451	.2402	.2357	.2313	.2272	.2233	.2196
300	.216	.213	.2096	.2065	.2036	.2008	.1981	.1955	.1930	.1906
400	.186	.186	.1839	.1818	.1798	.1779	.1760	.1741	.1724	.1707
500	.169	.167	.1658	.1643	.1628	.1613	.1599	.1586	.1572	.1559
600	.155	.152	.1522	.1510	.1498	.1487	.1476	.1465	.1455	.1444
700	.142	.142	.1414	.1405	.1396	.1386	.1377	.1369	.1360	.1352
800	.134	.1325	.1327	.1319	.1311	.1304	.1296	.1289	.1282	.1275
900	.127	.1261	.1254	.1247	.1241	.1234	.1228	.1222	.1216	.1210
1000	.120	.1198	.1192	.1186	.1181	.1175	.1170	.1164	.1159	.1154

Table 3 — Temperature Correction Factors (F_3) $\sqrt{\frac{F + 460}{530}}$

°F Hundreds	TENS									
	0	10	20	30	40	50	60	70	80	90
0	.932	.942	.952	.962	.971	.981	.991	1.00	1.009	1.019
100	1.028	1.037	1.046	1.055	1.064	1.073	1.082	1.090	1.099	1.107
200	1.116	1.124	1.133	1.141	1.149	1.157	1.166	1.174	1.182	1.189
300	1.197	1.205	1.213	1.221	1.229	1.236	1.244	1.251	1.259	1.266
400	1.274	1.281	1.289	1.296	1.303	1.310	1.318	1.325	1.332	1.339

NOTE: Formulas are those used in derivation of factors

Liquid Service

Sizing Data

How To Determine Water Equivalent

1. Start with your desired maximum flow.
Then,
2. Using your liquid density in grams/milliliter (g/mL), enter Table 4 from the left (for the units and tenths), and then from the top (for the hundredths). You will find the correction factor at the intersection of the appropriate row and column.
3. Multiply: (Desired Maximum Flow) \times (Correction Factor) = Water Equivalent

Example:

Find water equivalent of 5 gpm of liquid with a density of 0.86 grams/milliliter:

Step 1—your flow is 5

Step 2—In the table below find 0.8. In the top row find .06. Follow the two (column and row) until they intersect. Correction factor is .918.

Step 3—multiply (5) \times (.918) = 4.59 gpm water equivalent.

Table 4—Liquid Density Correction Factors

$$\sqrt{\frac{(8.02-1.0) e}{(8.02-e) 1.0}}$$

SP. GR.	HUNDREDTHS									
	.00	.01	.02	.03	.04	.05	.06	.07	.08	.09
0.4	.607	.615	.623	.631	.639	.646	.654	.661	.669	.676
0.5	.684	.691	.698	.705	.712	.719	.726	.733	.740	.747
0.6	.754	.760	.767	.774	.780	.787	.794	.800	.807	.814
0.7	.820	.826	.832	.839	.845	.851	.857	.864	.870	.876
0.8	.882	.889	.895	.900	.906	.912	.918	.924	.930	.936
0.9	.942	.948	.954	.960	.966	.971	.977	.983	.989	.995
1.0	1.000	1.006	1.012	1.018	1.023	1.029	1.034	1.040	1.046	1.051
1.1	1.056	1.061	1.068	1.073	1.079	1.084	1.090	1.095	1.100	1.106
1.2	1.111	1.117	1.122	1.128	1.133	1.139	1.144	1.150	1.155	1.160
1.3	1.165	1.171	1.177	1.182	1.188	1.193	1.198	1.203	1.209	1.213
1.4	1.219	1.223	1.229	1.234	1.240	1.245	1.250	1.255	1.260	1.265
1.5	1.270	1.275	1.280	1.285	1.289	1.294	1.298	1.303	1.309	1.318
1.6	1.322	1.327	1.332	1.337	1.343	1.348	1.352	1.357	1.362	1.369
1.7	1.373	1.378	1.384	1.389	1.395	1.400	1.405	1.411	1.416	1.421
1.8	1.426	1.431	1.436	1.441	1.447	1.452	1.457	1.462	1.467	1.472
1.9	1.477	1.483	1.489	1.494	1.499	1.504	1.509	1.514	1.519	1.523
2.0	1.528	1.533	1.538	1.543	1.549	1.553	1.559	1.563	1.569	1.573

This table is only for meters with stainless steel floats. If floats are of other materials, determine the water equivalent as above, and then multiply to compensate for float density (Pf) as follows:

$$\left(\frac{\text{Desired Maximum Flow Rate}}{\text{Flow Rate}} \right) \times \left(\frac{\text{Liquid Density}}{\text{Correction Factor}} \right) \times \sqrt{\frac{8.02}{Pf}} = \text{Water Equivalent}$$

Steam Service

How to determine air equivalent

1. Start with desired maximum in units of lbs./hr. then,
2. Using Steam Tables determine specific volume of steam, cubic feet per pound.
3. Multiply: (desired maximum flow) $\times \sqrt{\text{specific volume}} \times 0.06 = \text{SCFM air equivalent}$

Example:

Find air equivalent of 1000 lb./hr. steam at 100 PSIA and 350°F

1. Flow is 1000 lb./hr.
2. Specific volume is 4.592 cubic ft./lb.
3. Multiply:
 $1000 \times \sqrt{4.592} \times 0.06 = 128.6 \text{ SCFM air equivalent}$

Correction Factors**Liquid Service****Gas Service**

For correcting flowmeter readings when fluid density varies from the value for which the scale is calibrated.

(Applicable only when viscosities are below the Viscosity Immunity Ceiling [VIC] and only on volume units)

$$\text{Corrected Flow Rate} = \frac{\text{Scale Reading}}{\text{Correction factor for scale sp gr}} \times \frac{\text{Correction factor for new sp gr}}{\text{Correction factor for new sp gr}}$$

Example: Determine flow rate when metering liquid sp gr 1.52 when scale reads 16 gpm on meter calibrated for sp gr 0.86.

From p. 37

$$\text{Correction factor for sp gr } 0.86 = 0.918$$

$$\text{Correction factor for sp gr } 1.52 = 1.28$$

$$\text{Correct flow} = 16 \times \frac{0.918}{1.28} = 11.5 \text{ gpm}$$

(Applicable on standard volume units such as scfm, scfh, std. liters per minute, etc.)

$$\text{Corrected Flow Rate} = \frac{\text{Scale Reading}}{\text{Reading}} \times \frac{F_{g1} \times F_{p1} \times F_{t1}}{F_{g2} \times F_{p2} \times F_{t2}}$$

Where: F_{g1} = Scale specific gravity correction factor

F_{g2} = New specific gravity correction factor

F_{p1} = Scale pressure correction factor

F_{p2} = New pressure correction factor

F_{t1} = Scale temperature correction factor

F_{t2} = New Temperature correction factor

(All factors from page 36)

Example: Determine the flow rate, when metering propane at 50 psig and 80°F when scale reading is 100 scfh on meter calibrated for natural gas metered at 10 psig and 60°F

From p. 36

$$F_{g1} = 0.775, F_{g2} = 1.25, F_{p1} = 0.771, F_{p2} = 0.477, F_{t1} = 0.991, F_{t2} = 1.009$$

Correct Flow =

$$100 \times \frac{0.775}{1.25} \times \frac{0.771}{0.477} \times \frac{0.991}{1.009} = 98.4 \text{ scfh}$$

Useful Factor

GPM Water $\times 4.12$ = SCFM Air (Metered @ 14 PSIA & 70°F)

APPENDIX G: EDL Work Instructions

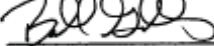
SAVANNAH RIVER NATIONAL LABORATORY
E&CPT RESEARCH PROGRAMS SECTION

Tank 18 & 19 Wall Sampler Test in 786-A(U)

Procedure Type: Work Instruction
Instruction Number: ITS-WI-0037
Revision: 1
Issue Date: 1-6-2010

Page: 1 of 10

APPROVED BY:



Manager, ERPS-EDL

1/6/10

Date



Preparer, ERPS-EDL

1/6/10

Date

1.0 PURPOSE/SCOPE

The purpose of this task is to demonstrate the F-area Tank 18 & 19 wall sampler and to quantify the efficiency of the sampler at removing and capturing material from the tank wall surface. The sampler will be tested in the Engineering Development laboratory (EDL, building 786-A) located in the Savannah River National Laboratory (SRNL).

The test will use a 3"x4"x3/8" thick steel plate to represent the tank wall and steel coupons, coated with a film (salt residue, corrosion layer, both or none) and attached to the wall, to represent the scaling on the walls of Tank 18 & 19. The sampler will be attached to the wall with electromagnets where it will take a sample of the coupons by milling to a depth of 0.030". A vacuum system will capture the removed film and deposit it on a HEPA filter. Using an analytical balance the weight loss of the coupon will be compared to the weight gain of the filter to determine the efficiency of removal and capture.

2.0 PERFORMANCE

This Work Instruction consists of the following Performance Sections:

- 2.1 Acquire a Sample
- 2.2 Test Matrix
- 2.3 Weighing Procedure
- 2.4 Attach and Detach the Coupon
- 2.5 Assembly and Disassembly of the Sampler Head
- 2.6 Positioning the Sampler on the Wall

Section 2.1 is the primary performance section and references the other sections for greater detail of a specific activity.

The following Attachments are located after the Performance Section:

- 1, Safety Information
- 2, Control Apparatus
- 3, Coupon Detail
- 4, Sampler head Assembly

Laboratory Notebook SRNL-NB-2009-00068 will be used for this task to capture all relevant information concerning the test.

2.1 Acquire a Sample

- 2.1.1 **Ensure** that the stops (cone head machine screws) are positioned appropriately for the sample to be taken (shim washers will be required under the stops for coupons with salt or corrosion films).
- 2.1.2 **Weigh** the coupon and the filter prior to testing with the sampler (reference section 2.3, Weighing Procedure). **Record** the weights in the laboratory notebook.
- 2.1.3 **Attach** the coupon to the steel plate (reference section 2.4, Attach and Detach the Coupon). **Use** proper PPE while handling a coupon with the salt film (reference Attachment 1 – Safety Information). Gloves (nitrile) shall be worn to prevent oils from the fingers transferring to the coupon and for personnel safety when salt coupons are tested.
- 2.1.4 **Assemble** the sampler head with the (reference section 2.5, Assembly and Disassembly of the Sampler Head). **Use** gloves (nitrile) while handling the filter to avoid transferring oil from your fingers to the filter and for protection from salts.
- 2.1.5 **Attach** the head to the sampler (ref section 2.5).

SAVANNAH RIVER NATIONAL LABORATORY
E&CPT RESEARCH PROGRAMS SECTION

Tank 18 & 19 Wall Sampler Test in 786-A(U)

Procedure Type: Work Instruction

Instruction Number: ITS-WI-0037

Revision: 1

Issue Date: 1-6-2010

Page: 2 of 10

- 2.1.6 Place the sampler assembly on the hydraulic lift table and ensure that it is stable.

NOTE: The sampler assembly may weigh as much as 50 lbs. If necessary, use two people to move the sampler and use proper lifting techniques?

- 2.1.7 Position the lift table in the desired location on the plate and energize the electromagnets per section 2.6, Positioning the Sampler on the Wall.
- 2.1.8 Perform an initial service leak test per ASME B31.3 (category D fluid), during the first operation of this equipment. Verify that the house air supply is ~ 90 psig. Document the ten minute leak test for both the advance and retract positions in the Lab notebook. (complete 6/8/9, SRNL-NB-2009-00068, p. 35)
- 2.1.9 Position the cameras (there may be a hand held digital camera, a high-speed camera and a digital camera mounted to the sampler) as necessary to capture the sampler in operation. Synchronize the time and date on the cameras, if applicable. Position lighting equipment as necessary.
- 2.1.10 Ensure that valves V1, V2, V3 are closed and that valve V4 is set in the ADVANCE position then apply house air to the system by opening valve V0 (reference Attachment 2 – Control Apparatus).
- 2.1.11 Apply air to the vacuum eductor by opening valve V3 (ref. Attachment 2). Set the pressure to 50 psig using valve V3 as displayed by pressure gauge PV.

NOTE: Industrial Hygiene will measure the noise level of the air driven equipment when it is initially used to determine the need for hearing protection. (complete 6/4/09, SRNL-NB-2009-00068, p. 37)

NOTE: A flow meter will be used to measure the flow from the sampler head to the vacuum eductor to verify proper operation. The flow meter will be removed after operation has been verified.

- 2.1.12 Apply air to the drill by opening valve V1 (ref. Attachment 2). Set the pressure to 100 psig using valve V1.
- 2.1.13 Verify that valve V4 is in the ADVANCE position and verify that the pressure regulator is set for 70 psig as displayed by pressure gauge PLM. If timing the sampler operations, start stop watch.
- 2.1.14 Start the sample operation by opening valve V2. Start the stopwatch if timing the advance event.
- 2.1.15 During the sampler operation observe, verify, and record the following:
- 2.1.15.1 Operating pressures (PDM, PLM, PV, and V) and flows (DM FLOW, LM FLOW, FLOW V1 and FLOW V2). Valve adjustments may be necessary to maintain constant flow and pressure.
 - 2.1.15.2 Time required for advance.
 - 2.1.15.3 Effectiveness of the vacuum system.
 - 2.1.15.4 System anomalies.
 - 2.1.15.5 Note the time when the MAXIMUM EXTENSION limit switch is activated.
- 2.1.16 Take pictures of the operation as necessary.

NOTE: A face shield is required while observing the operation in close proximity of the sampler when using coupons with salt residue (ref. Attachment 1).

NOTE: The drill will continue to drill into the metal after the linear motor has stopped advancing due to the force of the springs.

- 2.1.17 When the drill head is no longer advancing stop the stopwatch and record the time required to drill the hole in the lab notebook. The drill will advance after the LM stops.
- 2.1.18 Start the retract operation by turning the 4-way valve V4 to the RETRACT position (ref. Attachment 2) and restart the stopwatch to time the retract event.
- 2.1.19 At the end of the retract event verify that the linear actuator has triggered the stop switch and has stopped retracting then close valve V2.
- 2.1.20 Stop the air supply to the drill by closing valve V1 (ref. Attachment 2).
- 2.1.21 Stop the vacuum eductor by closing valve V3.

SAVANNAH RIVER NATIONAL LABORATORY
E&CPT RESEARCH PROGRAMS SECTION

Tank 18 & 19 Wall Sampler Test in 788-A(U)

Procedure Type: Work Instruction

Instruction Number: ITS-WI-0037

Revision: 1

Issue Date: 1-6-2010

Page: 3 of 10

- 2.1.22 If desired, stop the supply of house air to the system by closing valve V0.
- 2.1.23 Verify that the lift table is in position to accept the sampler when the electromagnets are de-energized.
- 2.1.24 De-energize the electromagnets and ensure that the sampler is safely resting on the lift table.
- 2.1.25 Stop the digital cameras.
- 2.1.26 Inspect the sampler and take pictures as necessary. Record any observations in the laboratory notebook.
- 2.1.27 Carefully remove the sampler head per section 2.5. Take pictures of the head as necessary. Record any observations in the laboratory notebook.
- 2.1.28 Carefully remove the coupon from the steel plate per section 2.4. Take pictures of the coupon as necessary. Record any observations in the laboratory notebook.

NOTE: The sampler head and coupon will be placed in a suitable container for transportation to the lab containing the analytical balance (the balance may be located in a separate lab that has temperature control and a stable base). Reference sections 2.4 and 2.5.

- 2.1.29 Repeat section 2.1 for each coupon listed in the test matrix (ref. section 2.2, Test Matrix).

2.2 Test Matrix

The required tests are listed in the table below. However, there are spare coupons available to practice the technique prior to actual testing. In addition to the spare coupons, sampler operation can be verified on a section of the wall away from the coupon. During the trial sampler operations ensure the following:

- The integrity of the hold on the plate by the electromagnets.
- The depth and diameter of the hole.
- The ease or complexity of positioning the sampler.

Test Number	Coupon Coating
1	None
2	None
3	None
4	Corrosion + Salt (0.006" layer)
5	Corrosion + Salt (0.006" layer)
6	Corrosion + Salt (0.006" layer)
7	Salt (0.030" layer)
8	Salt (0.030" layer)
9	Salt (0.030" layer)
10	None
11	None
12	None

2.3 Weighing Procedure

Use an analytical balance with the accuracy necessary to achieve the desired results (~99% accuracy at removing and capturing wall scale). A typical balance to use is a Mettler-Toledo model AX205 (or equal) with a capacity of ~200 grams and resolution of 0.0001 grams or better.

- 2.3.1 Don proper PPE for handling items with salt residue. Gloves (nitrile or cotton for coupons without salt) shall be worn to prevent oils from the fingers transferring to the item.
- 2.3.2 Remove the item to be weighed from the transport container.

SAVANNAH RIVER NATIONAL LABORATORY
E&CPT RESEARCH PROGRAMS SECTION

Tank 18 & 19 Wall Sampler Test in 786-A(U)

Procedure Type: Work Instruction

Instruction Number: ITS-WI-0037

Revision: 1

Issue Date: 1-6-2010

Page: 4 of 10

NOTE: Reference section 2.5 for disassembly of the sampler head to remove the filter.

- 2.3.3 Allow sufficient time (~30 minutes) for the items to be weighed to stabilize to the room temperature where the analytical balance is located.
- 2.3.4 Record the item to be weighed and other pertinent information in the laboratory notebook.
- 2.3.5 Carefully handle the coupons and filter with nitrile or cotton gloves to avoid transferring oils from the fingers to these items.

NOTE: Extreme care must be taken to ensure that the film on the coupon or the residue on the filter is not disturbed while handling.

- 2.3.6 Ensure that the doors are closed on the balance and tare the balance, if necessary.
- 2.3.7 Open the door on the balance, place the item to be measured on the platen and close the door.
- 2.3.8 Allow weight displayed on the balance to stabilize. If the weight does not stabilize then contact the PI.
- 2.3.9 Record the weight in the laboratory notebook.
- 2.3.10 Open the door of the balance, remove the weighed item and close the door.
- 2.3.11 Place the weighed item in plastic bag for protection during storage. Place the plastic bag in the container for transportation back to the EDL.

2.4 Attach and Detach the Coupon (ref. Attachment 3, Coupon Detail)

- 2.4.1 Don proper PPE for handling items with salt residue. Gloves (nitrile or cotton for coupons without salt) shall be worn to prevent oils from the fingers transferring to the coupon.

2.4.2 Attaching coupons.

- 2.4.2.1 Ensure that the mounting tabs of the coupons and about an 1/8 inch perimeter around the edge of the coupon are free of salts to permit installation without loss of salt.
- 2.4.2.2 Ensure that the coupon has been pre-weighed.
- 2.4.2.3 Ensure that the jack screw is retracted so as not to interfere with the coupon.
- 2.4.2.4 Remove the retaining screws.
- 2.4.2.5 Place the coupon in the steel plate recess. **DO NOT DISTURB THE SALT LAYER WHILE INSTALLING THE COUPON.**
- 2.4.2.6 Keep a finger on one of the tabs to prevent the coupon from falling while re-installing the retaining screws.

2.4.3 Detaching coupons.

- 2.4.3.1 Remove one of the retaining screws. **DO NOT DISTURB THE SALT LAYER WHILE REMOVING THE COUPON.**
- 2.4.3.2 Place a finger on the exposed tab and remove the other retaining screw.
- 2.4.3.3 Carefully remove the coupon. If necessary, advance the jack screw to push the coupon out of the recess.
- 2.4.3.4 Place the coupon in its transport container (film up) in preparation for post test weighing.

NOTE: Use a suitable container to transport the sampler head and coupon to the analytical balance to prevent jarring or any other action that may disturb sample material.

- 2.4.3.5 Transport the container to the location of the analytical balance. Use extreme care during transportation to prevent jarring.
- 2.4.3.6 Weigh the coupon per section 2.3.

2.5 Assembly and Disassembly of the Sampler Head (ref. Attachment 4, Sampler Head Assembly)

- 2.5.1 Don proper PPE for handling items with salt residue.
- 2.5.2 Removing the sampler head.

SAVANNAH RIVER NATIONAL LABORATORY
E&CPT RESEARCH PROGRAMS SECTION

Tank 18 & 19 Wall Sampler Test in 788-A(U)

Procedure Type: Work Instruction
Instruction Number: ITS-WI-0037
Revision: 1
Issue Date: 1-6-2010

Page: 5 of 10

- 2.5.2.1 Back the lift table away from the steel plate to gain access to the sampler head. Ensure that the air lines to the sampler do not become entangled or kink.
- 2.5.2.2 Remove the sampler head by loosening the sampler head attachment screws (they will remain with the head).
- 2.5.2.3 Place the sampler head in a suitable container (kit up) for transport to the analytical balance.

NOTE: Use a suitable container to transport the sampler head and coupon to the analytical balance to prevent jarring or any other action that may disturb sample material.

- 2.5.2.4 Transport the container to the location of the analytical balance. Use extreme care during transportation to prevent jarring.
- 2.5.2.5 Carefully remove the sampler head from the container and place the head (kit up) on the work table.
- 2.5.2.6 Remove the filter by loosening the four filter plate attachment screws and lifting off the filter plate.

NOTE: Use gloves (nitrile) when handling the filter to prevent oils from the fingers transferring to the items.

- 2.5.2.7 Inspect sampler head passages upstream of the filter cavity for residue. Contact the PI if residue is observed in the passages.
- 2.5.2.8 Weigh the filter per section 2.3.
- 2.5.3 Assembling the sampler head.
- 2.5.3.1 Weigh the filter per section 2.3.

NOTE: Use gloves (nitrile or cotton) when handling the filter to prevent oils from the fingers transferring to the items.

- 2.5.3.2 With the sampler head in the kit down position, place the filter on top of the filter cavity in the head (the filter may sensitive to flow direction, place the upstream side of the filter face down). The filter should fit between the two sampler head attachment screws and be flush with the top of the filter plate recess.
- 2.5.3.3 Attach the filter plate using the four filter plate attachment screws. The will be held between the filter plate and the sampler head body.

- 2.5.4 Attach the sampler head to the sampler using the two sampler head attachment screws.

2.6 Positioning the Sampler on the Wall

- 2.6.1 Carefully set the sampler assembly on the lift table so that the drill bit extends past the edge of the table by about 5 inches. If necessary, secure the sample assembly to the table with C-clamps.
- 2.6.2 Verify that the electromagnets are de-energized.
- 2.6.3 Position the lift table so that the electromagnets are about 2 inches away from the steel plate.
- 2.6.4 Carefully position the drill bit by moving/actuating the lift table so that the center of the bit is positioned at the center of the coupon.
- 2.6.5 Carefully push the lift table to the steel plate until the electro magnets touch the steel plate.
- 2.6.6 Verify that the center of the drill bit is still at the center of the coupon.
- 2.6.7 Energize the electromagnets.

NOTE: The electromagnets present a pinch point hazard. Wear leather gloves when working with and around the electromagnets.

- 2.6.8 Slowly lower the lift table about 1/4" to 1/2" to verify that the electromagnets are firmly attached to the steel plate and that the sampler remains perpendicular to the wall surface.

SAVANNAH RIVER NATIONAL LABORATORY
E&CPT RESEARCH PROGRAMS SECTION

Tank 18 & 19 Wall Sampler Test in 788-A(U)

Procedure Type: Work Instruction
Instruction Number: ITS-WI-0037
Revision: 1
Issue Date: 1-6-2010
Page: 6 of 10

2.6.9 Verify that the center of the drill bit is still over the center of the coupon.

NOTE: If necessary, mark the steel plate, or otherwise provide a positioning aid, at the location of the electromagnets to aid future positioning.

SAVANNAH RIVER NATIONAL LABORATORY
E&CPT RESEARCH PROGRAMS SECTION

Tank 18 & 19 Wall Sampler Test in 788-A(U)

Procedure Type: Work Instruction

Instruction Number: ITS-WI-0037

Revision: 1

Issue Date: 1-6-2010

Page: 7 of 10

Attachment 1

Safety Information

EHAP# SRNL-L3100-2009-00139

EEC# TC-A-2009-041

MSDS Numbers

The following are the MSDS numbers of the sodium salts that make up the salt film on the coupons.

Chemical	MSDS#	Health	<u>Hazard Rating</u>		Reactivity
			Flammability		
Sodium Nitrate	6909-1	1	0		3
Sodium Nitrite	5973-1	2	0		3
Sodium Carbonate	10370-1	2	0		0

PPE

PPE required for handling items with salt residue:

Lab coat, safety glasses, chemical resistant gloves (nitrile), safety shoes.

PPE required while in close proximity of sampler during operation with salt residue:

Lab coat, safety glasses, face shield, chemical resistant gloves (nitrile), safety shoes.

PPE required for using hand tools

Leather gloves in addition to the PPE listed above.

Hazard Response

It is unlikely that the small quantities of chemicals in the salt film will cause problems, however in general for:

INGESTION	Call a Physician immediately. Do not induce vomiting.
INHALATION	Remove to fresh air. Give oxygen if breathing is difficult.
SKIN CONTACT	Flush with water for 15 minutes
EYE CONTACT	Flush with water for 15 minutes.

Contacts

IH Contact: Charles Stoyke; 5-5277, 13396
Sherolyn Bishop; 5-6862, 17132
ECA Contact: Jim Gillam; 5-5827, 14829
PI: Bob Leishear; 5-2832, 19107
Test Engr: Mark Fowley; 5-1492, 17676

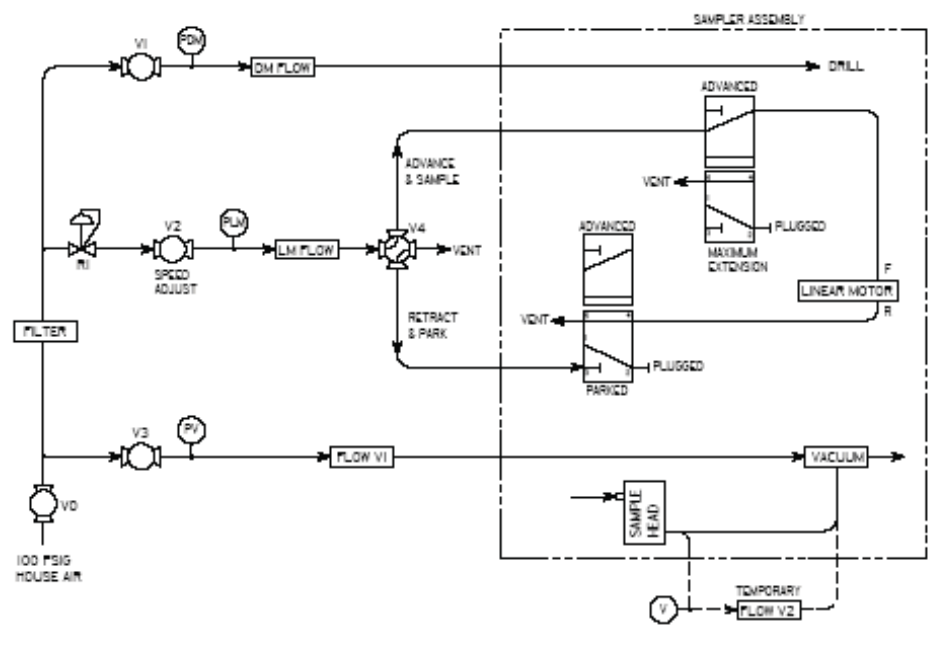
SAVANNAH RIVER NATIONAL LABORATORY
E&CPT RESEARCH PROGRAMS SECTION

Tank 18 & 19 Wall Sampler Test in 788-A(U)

Procedure Type: Work Instruction
Instruction Number: ITS-WI-0037
Revision: 1
Issue Date: 1-6-2010

Page: 8 of 10

Attachment 2
Control Apparatus



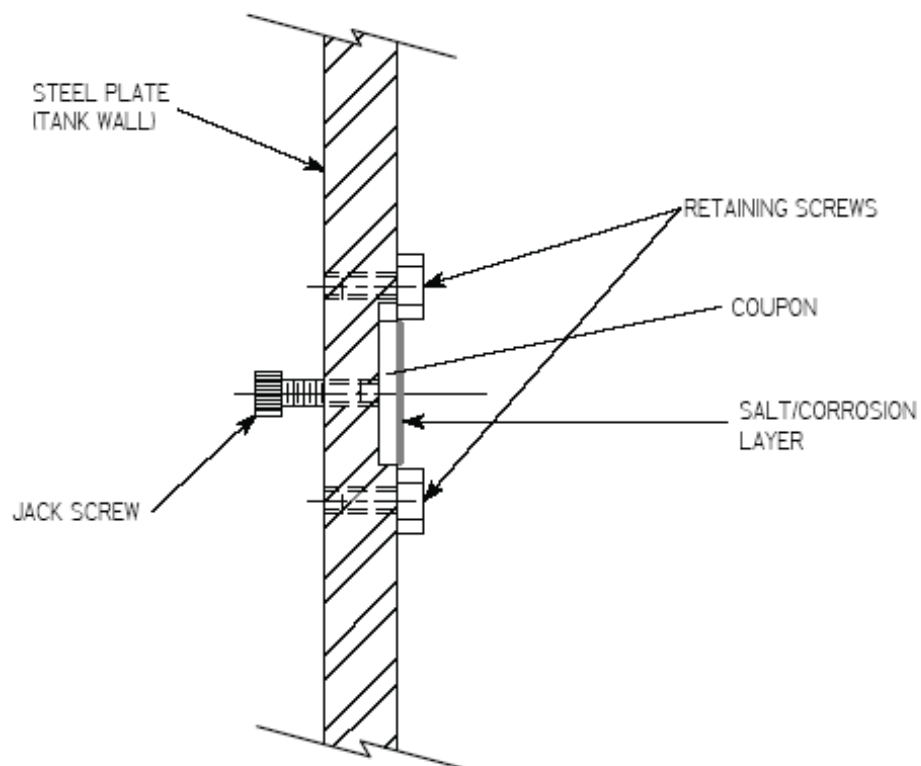
SAVANNAH RIVER NATIONAL LABORATORY
E&CPT RESEARCH PROGRAMS SECTION

Tank 18 & 19 Wall Sampler Test in 786-A(U)

Procedure Type: Work Instruction
Instruction Number: ITS-WI-0037
Revision: 1
Issue Date: 1-6-2010

Page: 9 of 10

Attachment 3
Coupon Detail



SAVANNAH RIVER NATIONAL LABORATORY
E&CPT RESEARCH PROGRAMS SECTION

Tank 18 & 19 Wall Sampler Test in 788-A(U)

Procedure Type: Work Instruction

Instruction Number: ITS-WI-0037

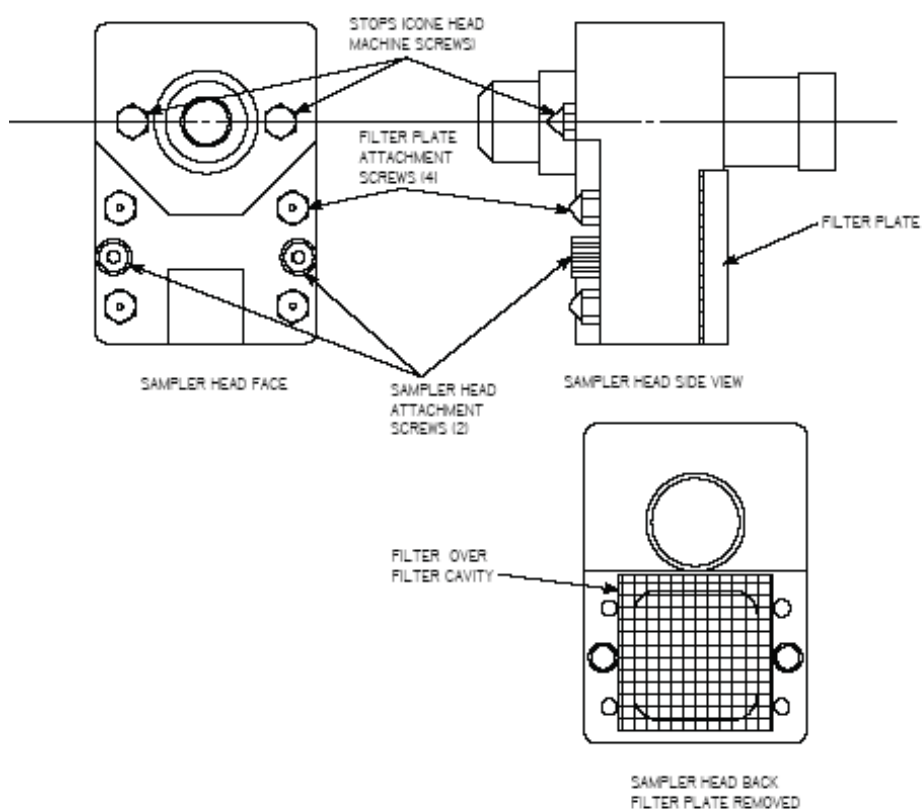
Revision: 1

Issue Date: 1-6-2010

Page: 10 of 10

Attachment 4

Sampler Head Assembly



APPENDIX H: SRR Sampler Controls

